

Removal of Pharmaceuticals from Human Waste by Adsorption Process for Nutrient Recovery and Reuse

by Abdulaziz Yousef Almontashiri

Thesis submitted in fulfilment of the requirements for
the degree of

Doctor of Philosophy

under the supervision of Associate Professor Sherub Phuntsho
and Professor Ho Kyong Shon

University of Technology Sydney
Faculty of Faculty of Engineering and Information Technology

March 2024

CERTIFICATE OF ORIGINAL AUTHORSHIP

I, **Abdulaziz Almontashiri**, declare that this thesis, is submitted in fulfilment of the requirements for the award of **Doctor of Philosophy, in the School of Civil and Environmental Engineering/Faculty of Engineering and Information Technology** at the University of Technology Sydney.

This thesis is wholly my own work unless otherwise referenced or acknowledged. In addition, I certify that all information sources and literature used are indicated in the thesis.

This document has not been submitted for qualifications at any other academic institution.

This research is supported by the Australian Government Research Training Program.

Production Note:

Signature: Signature removed prior to publication.

Date: 28th March 2024

ACKNOWLEDGMENT

I would want to convey my deepest appreciation to everyone who have graciously contributed their advice and support, and whose contributions have enabled me to complete my dissertation.

First and foremost, I want to thank to my Principal Supervisor, Associate Prof. Sherub Phuntsho, whose consistent advice, support and encouragement, understanding enabled me to complete my thesis. He exposed me to the realm of study and established in me a desire to investigate novel ideas while exercising critical thinking. I am appreciative for his contributions to my professional development as a researcher, and I am excited about the prospect of continuing to collaborate in the future.

I also wish to express my deepest gratitude to my co-supervisor, Prof. Ho Kyong Shon, who provided me with invaluable guidance and support during my studies. His knowledge and views were crucial in defining and leading my study. I appreciate his contributions to this thesis.

I would like to express my heartfelt appreciation to Dr. Mohamad Johir and Dr. Nirenkumar Pathak for their excellent support in the laboratory. Their knowledge and assistance were invaluable in carrying out my study. Moreover, I am thankful to all of my friends and colleagues at UTS who have played a significant part in my academic path and whose unwavering support has made me feel at home since the day I arrived.

I would like to take this opportunity to offer my deepest appreciation to my loving parents, my dad (Eng. Yousef), and my mom (Allowh), for their unending support and prayers during my period of study. Their advice has instilled in me the fortitude to overcome challenges and stand strong, even in the face of adversity.

I am eternally thankful to my lovely wife Sahlah, whose love and inspiration have provided me with ongoing strength and motivation. I am thrilled to celebrate this accomplishment with her and want to thank her for her unfailing support, and faith in my skills. Her emotional support in both good and bad times, as well as her incredible tolerance over the years, have all contributed to my achievement. Thank you for being my inspiration and companion, my love.

Malk, my beloved daughter, I am overwhelmed with appreciation for your love and support during my study journey. Your unfailing tolerance over the long hours of studying was a huge source of comfort for me, and I am grateful for your willingness to share my efforts with me. Your contagious humour was continual motivators and sources of inspiration. Thank you for being such a wonderful source of light and strength in my life, my lovely daughter.

I wish to convey my heartfelt appreciation to my sisters, Najllaa, Halimah, Sahlah, Tamadur, Rawan, and Lama, as well as my father and mother-in-law (Yahya and Hamidah), for their steadfast support and sacrifices on my behalf. Their existence in my life has provided me with strength and inspiration, for which I will be eternally grateful. They have been there for me through the ups and downs of life, and their kindness have made all the difference. Thank you for their contributions to completing this thesis.

I would like to convey my heartfelt appreciation to Umm Al-Qura University for funding my PhD study. I am grateful for the chance to do research and to be associated with such a prestigious university, University of Technology Sydney. I would like to thank both Umm Al-Qura University and the University of Technology, Sydney for their contributions to my academic and personal development. Their advice and support have been essential, and I will be eternally thankful for the possibilities and experiences they have provided me.

LIST OF PUBLICATIONS

1. **Almuntashiri, A.**, Hosseinzadeh, A., Badeti, U., Shon, H.K, Freguia, S., Dorji, U., Phuntsho, S. 2022. Removal of pharmaceutical compounds from synthetic hydrolysed urine using granular activated carbon: Column study and predictive modelling. *Journal of Water Process Engineering*, 45, 102480.
2. **Almuntashiri, A.**, Hosseinzadeh, A., Volpin, F., Ali, S.M., Dorji, U., Shon, H.K, Phuntsho, S. 2021. Removal of pharmaceuticals from nitrified urine. *Chemosphere*, 130870
3. Badeti, U., Jiang, J., **Almuntashiri, A.**, Pathak, N., Dorji, U., Volpin, F., Freguia, S., Ang, W.L., Chanan, A., Kumarasingham, S. Shon, H.K, Phuntsho, S. 2022. Impact of source-separation of urine on treatment capacity, process design, and capital expenditure of a decentralised wastewater treatment plant. *Chemosphere*, 300, 134489.
4. Jiang, J., **Almuntashiri, A.**, Sohn, W., Phuntsho, S., Wang, Q., Freguia, S., El-Saliby, I., Shon, H.K. 2022. Feasibility study of powdered activated carbon membrane bioreactor (PAC-MBR) for source-separated urine treatment: a comparison with MBR. *Desalination*.
5. **Almuntashiri, A.**, Jiang, J., Hosseinzadeh, A., Badeti, U., Shon, H.K., Navidpour, A., Dorji, P., Phuntsho, S. Removal of antibiotics from a biologically nitrified real human urine using granular activated carbon adsorption. (Ready for submission to *Chemosphere*).
6. **Almuntashiri, A.**, Shon, H.K., Phuntsho, S. Assessing the potential for chemical regeneration of pharmaceuticals-exhausted GAC: efficiency and reusability experiments. (Ready for submission).

CONFERENCE PRESENTATIONS

1. **Almuntashiri, A.** Removal of pharmaceuticals from nitrified urine by GAC adsorption. Oral presentation in 2021 International Conference on the “*Challenges in Environmental Science and Engineering*” (CESE-2021) 6 – 7 Nov, 2021.
2. **Almuntashiri, A.** Removal of pharmaceuticals from nitrified urine. Oral presentation in (*School of CEE Research Showcase in 2021*) 23 Sep, 2021.
3. **Almuntashiri, A.** Removal of antibiotics form a biologically urine using granular activated carbon. Oral presentation in (*Rich Earth Summit in 2022*) 01 Nov., 2022.

LIST OF ABBREVIATIONS

APAP	Acetaminophen
AOPs	Advanced Oxidation Processes
ANN	Artificial Neural Network
CBZ	Carbamazepine
DOC	Dissolved Organic Carbon
DS	Draw Solution
EBCT	Empty Bed Contact Time
FS	Feed Solution
FO-RO	Forward And Reverse Osmosis
FBU	Fraction Of Bed Utilisation
GAC	Granular Activated Carbon
h_{MTZ}	Height Of Mass Transfer Zone
HSZ	High-Silica Zeolite
H_2O_2	Hydrogen Peroxide
IBP	Ibuprofen
C_0	Initial Concentrations
C_t	Instantaneous Concentrations
LCMS	Liquid Chromatography With Mass Spectrometry

LP	Low-Pressure
MSE	Mean Square Error
MBR	Membrane Bioreactor
MD	Membrane Distillation
MTZ	Metronidazole
NF	Nano-Filtration
NAP	Naproxen
pH_{pzc}	Point Of A Zero-Charge
PAC	Powdered Activated Carbon
RO	Reverse Osmosis
SDZ	Sulfadiazine
SMZ	Sulfamethazine
SMX	Sulfamethoxazole
TOC	Total Organic Carbon
UV	Ultraviolet
Ur	Usage Rate
WWTPs	Wastewater Treatment Plants

LIST OF SYMBOLS

Ca^{2+}	Calcium
Cl^-	Chloride
K^+	Potassium
KCl	Potassium chloride
KHCO_3	Potassium hydrogencarbonate
HCl	Hydrochloric acid
HCO_3^-	Hydrogencarbonate
K_{ow}	Octanol-Water Partition Coefficient
K_{yn}	Yoon-Nelson Rate Constant
K_{th}	Thomas Model Rate Constant
Mg^{2+}	Magnesium
MeOH	Methanol
MgSO_4	Magnesium Sulphate
Na^+	Sodium
NaCl	Sodium Chloride
NaOH	Sodium Hydroxide
Na_2SO_4	Disodium Sulfate
NaH_2PO_4	Sodium dihydrogen Phosphate

NH_3	Ammonia
$\text{NH}_3\text{-N}$	Ammonia Nitrogen
$\text{NH}_4^+ \text{-N}$	Ammonium Nitrogen
$\text{NH}_4\text{-Acetate}$	Ammonium Ethanoate
NH_4HCO_3	Ammonium Hydrogen Carbonate
NH_4NO_3	Ammonium Nitrate
$\text{NO}_2^- \text{-N}$	Nitrite
$\text{NO}_3^- \text{-N}$	Nitrate
pKa	Acidity Constant
PDS	Peroxydisulfate
$\text{PO}_4^{3-} \text{-P}$	Phosphate Phosphorus
q_b	Adsorption Capacity at The Breakthrough Point
q_t	Maximum Adsorption Capacity at Saturation
SO_4^{2-}	Sulfate
TiO_2	Titanium Dioxide
$t_{50\%}$	Time Required To Reach 50% Of Micropollutant Breakthrough

TABLE OF CONTENTS

CERTIFICATE OF ORIGINAL AUTHORSHIP	i
LIST OF PUBLICATIONS	iv
CONFERENCE PRESENTATIONS	v
LIST OF ABBREVIATIONS	vi
LIST OF SYMBOLS	viii
LIST OF TABLES	xv
LIST OF FIGURES	xvi
Abstract	xix
CHAPTER 1 Introduction	1
1.1 Background research.....	1
1.2 Research significance.....	2
1.3 Research aim	3
1.4 Research objective	3
1.5 Organisation thesis/outline.....	4
CHAPTER 2 Literature Review.....	7
2.1 Literature Review.....	7
2.2 Composition of fresh and hydrolysed urine	8
2.3 Water and nutrients recovery from urine matrix	9
2.3.1 Thermal driven processes.....	10
2.3.2 Struvite precipitation.....	10
2.3.3 Combined forward osmosis/ reverse osmosis	12
2.4 Types of micropollutants and their influence on the human and aquatic environment	14

2.5	Pharmaceutical concentrations in source-separated urine.....	16
2.6	Granular activated carbon adsorption process	21
2.6.1	Application of granular activated carbon adsorption process	21
2.6.2	Granular activated carbon regeneration and reuse	26
2.6.3	Artificial neural network modelling for pharmaceutical removal via adsorption	27
2.7	Alternatives treatment for pharmaceuticals removal	28
2.7.1	Ultraviolet and Ultraviolet /peroxide processes	29
2.7.3	Polymer resin adsorption.....	31
2.7.4	Biochar	31
2.7.5	Membrane Filtration.....	33
2.7.6	Membrane bioreactor	34
2.8	Conclusion.....	35
 CHAPTER 3 Pharmaceutical compounds removal from synthetic hydrolysed urine using GAC: Column study and predictive modelling.....		
3.1	Abstract.....	36
3.2	Introduction.....	37
3.3	Material and methods.....	40
3.3.1	Adsorbent and adsorbate.....	40
3.3.2	Fixed-bed column experiments	41
3.3.3	GAC column adsorption analysis	42
3.3.4	Data collection and ANN modelling.....	43
3.3.5	Breakthrough curve modelling.....	45
3.3.6	Pharmaceutical compounds analysis.....	46

3.4	Results and discussion	47
3.4.1	Influence of operational conditions on pharmaceuticals removal.....	47
3.4.2	Breakthrough curves modelling	54
3.4.3	Modelling of Pharmaceuticals removal using ANN	61
3.4.4	Adsorption of pharmaceuticals onto GAC.....	66
3.5	Conclusion	69
CHAPTER 4	Removal of pharmaceuticals from nitrified urine	70
4.1	Abstract.....	70
4.2	Introduction.....	71
4.3	Materials and methods	74
4.3.1	Pharmaceuticals and adsorbent	74
4.3.2	Batch adsorption experiments.....	75
4.3.3	ANN Modelling	76
4.3.4	Micropollutant compounds and nutrients analysis.....	78
4.3.5	Analyzing the zeta potential for GAC.....	79
4.4	Results and discussions.....	79
4.4.1	Micropollutant removal by GAC adsorption	79
4.4.2	Adsorption isotherms	82
4.4.3	Micropollutants removal modelling by ANN	84
4.4.4	Effect the GAC onto pharmaceuticals.....	89
4.4.5	Effect the GAC onto TN & PO ₄ -P	92
4.5	Conclusion	93
CHAPTER 5	Removal of antibiotics from a biologically nitrified real human urine using granular activated carbon adsorption	95

5.1	Abstract.....	95
5.2	Introduction.....	96
5.3	Materials and methods	99
5.3.1	Antibiotics and the reagents.....	99
5.3.2	Source separated nitrified urine	100
5.3.3	Fixed-bed GAC adsorption column and analysis.....	101
5.3.4	Mathematical breakthrough modelling	103
5.3.5	Data collection and ANN modelling.....	105
5.3.6	Sample analysis.....	106
5.4	Results and discussion	107
5.4.1	Influence of the volumetric flow rate.....	107
5.4.2	Influence of the bed heights	111
5.4.3	Influence of the particles sizes	112
5.4.4	Breakthrough curve modelling.....	113
5.4.5	Antibiotics removal via ANN modelling	118
5.4.6	Antibiotics adsorption on GAC.....	120
5.5	Conclusion	122
CHAPTER 6 Assessing chemical regeneration of GAC saturated with pharmaceuticals ..		123
6.1	Abstract.....	123
6.2	Introduction.....	124
6.3	Material and Methods	125
6.3.1	Pharmaceuticals and adsorbent	125
6.3.2	Adsorption experiments	127

6.3.3	Desorption experiments	128
6.3.4	Influence of contact time chemical regenerant concentrations	129
6.3.5	Regeneration and reusability experiments	129
6.3.6	Pharmaceuticals analysis.....	130
6.4	Results and discussions.....	130
6.4.1	Adsorption Isotherm	130
6.4.2	Desorption experiments	133
6.4.3	The Influence of MeOH concentration on desorption experiments	135
6.4.4	Influence of contact time and kinetics models	136
6.4.5	Reusability: Adsorption and desorption	139
6.5	Conclusion	142
CHAPTER 7	Conclusion and recommendations	143
7.1	Conclusion	143
7.2	Recommendations and Future Work.....	144
	Appendix.....	146
	References.....	170

LIST OF TABLES

Table 2-1 Properties and ionic fresh and hydrolysed urine composition	9
Table 2-2 Occurrence of pharmaceuticals detected in surface water, wastewater and urine.	15
Table 2-3 Concentrations of pharmaceuticals and antibiotics found in human urine	17
Table 3-1 The physicochemical pharmaceuticals properties.....	41
Table 3-2 Error functions equations.....	45
Table 3-3 Parameters of competence and mass transfer obtained from empirical breakthrough curves for pharmaceuticals adsorption by GAC on fixed-bed column.	50
Table 3-4 Thomas and Yoon-Nelson models parameters for pharmaceuticals adsorption by GAC on fixed-bed column.	58
Table 4-1 Removal of micropollutants by biological treatment.....	74
Table 4-2 Compositions of synthetic nitrified urine.	75
Table 5-1 The GAC characteristics in various particle sizes.....	100
Table 5-2 Properties and ionic composition of the nitrified urine before and after GAC	101
Table 5-3 Error functions equations.....	106
Table 5-4 provides specific details about the experimental parameters of competence and mass transfer obtained from empirical breakthrough curves for pharmaceuticals adsorption by GAC on fixed-bed column.	109
Table 5-5 Thomas, Yan and Yoon-Nelson models parameters acquired from breakthrough curves for antibiotics via GAC on the column.	116
Table 6-1 Physicochemical characteristics of the chosen pharmaceuticals.	127
Table 6-2 The parameters of Freundlich and Langmuir isotherm data on GAC.....	131

LIST OF FIGURES

Figure 1-1 Thesis structure.	6
Figure 2-1 Illustration of the diagram struvite precipitation process to produce a fertiliser from urine	12
Figure 2-2 Illustration of the diagram hybrid forward osmosis – reverse osmosis.....	14
Figure 2-3 Schematic diagram of the batch test procedure.....	22
Figure 2-4 Schematic diagram of granular activated carbon column.	23
Figure 2-5 Principles of FO and RO.	34
Figure 3-1 Breakthrough curves of pharmaceuticals adsorption onto GAC at various flow rates of (a) 1.15 L/d; (b) 2.59 L/d and (c) 4.32 L/d; $m = 4$ g and $C_0 = 0.2$ mM.....	49
Figure 3-2 Breakthrough curves of pharmaceuticals adsorption onto GAC at various mass of adsorbent of adsorbent column heights of (a) 4.0 g; (b) 6.0 g and (c) 12.0 g; $Q = 1.15$ L/d and $C_0 = 0.2$ mM.....	54
Figure 3-3 Modelling breakthrough curve for fixed- bed adsorption of pharmaceuticals onto GAC ($Q = 1.15$ L/d; $C_0 = 0.2$ mM and $m = 4.0$ g).	57
Figure 3-4 Elucidation the experimental and ANN predicted data for all three phases of (a) CBZ, (b) NAP, (c) IBP, (d) APAP and (e) MTZ removal models.....	62
Figure 3-5 Illustration the residual errors of the evolved ANN models for (a) CBZ, (b) NAP, (c) IBP, (d) APAP and (e) MTZ.	64
Figure 3-6 Elucidation the experimental and ANN predicted data for additional tests of (a) CBZ, (b) NAP, (c) IBP, (d) APAP and (e) MTZ removal models.....	66
Figure 4-1 Variations in the normalised effluent concentrations C_t/C_0 with adsorption time for different GAC doses of (a) 10 mg/L, (b) 80 mg/L and (c) 3,000 mg/L, and (d) mass of micropollutant adsorbed per unit GAC mass for 800 mg/L GAC dose.	81
Figure 4-2 Experimental data (dots) and linear Freundlich isotherm (line) for adsorption of naproxen (a), carbamazepine (b), acetaminophen (c) ibuprofen, (d) and metronidazole (e).	83
Figure 4-3 Scatter plots of the predicted and actual values of the (a) naproxen, (b) carbamazepine, (c) acetaminophen, (d) ibuprofen, and (e) metronidazole.....	86

Figure 4-4 The residual errors of the developed ANN models for (a) naproxen, (b) carbamazepine, (c) acetaminophen, (d) ibuprofen, and (e) metronidazole.....	88
Figure 4-5 Illustration the predicted data versus the experimental data of normalized removal from ANN for (a) naproxen, (b) carbamazepine, (c) acetaminophen, (d) ibuprofen, and (e) metronidazole.....	88
Figure 4-6 Total nitrogen concentrations upon completion of batch tests at 25-3000 mg /L doses in a nitrified urine.....	93
Figure 5-1 Breakthrough curves at various flow rates for antibiotics adsorption by GAC (a) 0.06; (b) 1.2 and (c) 1.8 L/hr; m = 0.5 g, particle size = 425 μ m and $C_0 = 10 \mu$ M.	111
Figure 5-2 Breakthrough curves at various adsorbent mass for antibiotics adsorption by GAC (a) 0.5 (b) 0.8 and, (c) 1.5 g; particle size= 425 μ m, $Q = 0.06$ L/hr, and $C_0 = 10 \mu$ M.	112
Figure 5-3 Breakthrough curves at various particle sizes for antibiotics adsorption by GAC (a) 425 μ m (b) 600 μ m and (c) 1,000 μ m; $Q = 0.06$ L/hr, m = 0.5 g and $C_0 = 10 \mu$ M.	113
Figure 5-4 Modelling breakthrough curves for antibiotics adsorption on GAC ($Q = 0.06$ L/hr; $C_0 = 10 \mu$ M; particle size= 425 μ m and m = 0.5 g).	115
Figure 5-5 Illustration the values of ANN predicted and actual for all stages of (a) SMZ, (b) SMX and (c) SDZ removal models.	118
Figure 5-6 The residual errors distribution of evolved ANN models for (a) SMZ, (b) SMX and (c) SDZ.	119
Figure 5-7 Illustration the experimental value versus predicted value of normalised removal from developed ANN models for (a) SMZ, (b) SMX and (c) SDZ.....	119
Figure 6-1 Depicts the results of empirical adsorption experiments for adsorption of CBZ (a), NAP (b), IBP (c) APAP, (d) and MTZ (e).	133
Figure 6-2 The impact of MeOH concentrations on desorption efficiency of CBZ, NAP, IBP, APAP, and MTZ.....	136
Figure 6-3 Kinetic modelling for pharmaceuticals desorption onto GAC of CBZ (a), NAP (b), IBP (c) APAP, (d) and MTZ (e).....	138

Figure 6-4 Adsorption/desorption cycles of pharamceuticls onto/from GAC of CBZ (a), NAP (b),
IBP (c) APAP, (d) and MTZ (e)..... 140

Abstract

Discharging wastewater effluent containing nutrients (nitrogen-N, potassium-K and phosphorous-P) can cause significant environmental problem. Most energy consumed at the conventional wastewater treatment plant using activated sludge process therefore goes towards removing nutrients mainly nitrogen from the wastewater by biological nitrification processes. N, K and P are essential nutrients for the plants and crops however, separation and recovery of nutrients from the wastewater effluent is not easy requiring expensive processes as nutrients are present in highly diluted form. Hence, source separation of urine is a novel strategy not only to reduce the nutrient load coming to the wastewater treatment plants but makes it easier for nutrient recovery and use it as a fertiliser for growing crops. However, the presence of a wide range of pharmaceutical compounds in the urine is one of the major concerns for fertiliser resource recovery from the urine as these micropollutants can persist within the food chain when used as fertiliser.

Investigations for GAC adsorption were conducted under both batch and lab-scale column adsorption experiments. Five mostly commonly found pharmaceutical compounds were used in this study and they include naproxen, carbamazepine, acetaminophen, ibuprofen, and metronidazole. The fundamental studies using batch tests were performed to study the adsorption kinetics involved in the pharmaceutical removal from nitrified urine, using various GAC doses (ranging from 10–3000 mg/L). At the maximum dosage, all pharmaceuticals exhibited removal rates exceeding 99% after 6 hours. The study also included fixed-bed GAC column tests to gain breakthrough curves and evaluate GAC efficacy in the pharmaceutical adsorption under various conditions. Based on the breakthrough curves, carbamazepine demonstrated the greatest capacity for adsorption onto GAC, with a value of (56.1 mg/g), while metronidazole had the lowest adsorption capacity of (32.2 mg/g), which may limit the effectiveness of column adsorption applications. In comparison to actual removal rates, the artificial neural network model demonstrated a 99% accuracy in predicting the pharmaceuticals removal.

On the other hand, a possible alternative strategy is to conduct chemical regeneration of GAC on-site, employing a suitable solution that can effectively desorb organic compounds. Methanol was discovered to be more efficient, with desorption efficiencies ranged from around 40% to 75%, depending on the contaminant.

Overall, it is expected that outcomes of this project will provide the credible information for the real-scale application of fixed-bed GAC column adsorption for the removal of pharmaceuticals from the processed urine thereby helping make urine-derived fertiliser safer and more valuable.

CHAPTER 1 Introduction

1.1 Background research

Considering today's serious issues of environmental degradation and depletion of resources, sustainability is essential for conserving and protecting our finite resources on the planet. One of the ways to facilitate a sustainable society is to treat wastewater in removing the pollutants, which contains including various types and concentrations of micropollutants present in the wastewater. The inability of current wastewater treatment processes to thoroughly remove micropollutants such as pharmaceuticals, results in them being released into the environment, and subsequently affect soil and land quality as well as marine ecosystems and aquatic life.

In 2012 alone, United States spent \$325.8 billion on pharmaceutical products and majority of these pharmaceuticals are excreted as metabolites/uncharged in urine and feces into sewage wastewater streams. Escher et al. (2006) and Lienert et al. (2007) estimated that 64% of pharmaceutical compounds are excreted through urine and 36% in feces. The majority of the existing wastewater treatment plants (WWTPs) are not capable of removing these micropollutants. Since most pharmaceuticals are excreted in urine, micropollutant removal from urine stream (for nutrient recovery) is essential to prevent plant uptake or release to the environment.

Source separation of urine from the wastewater stream for treatment is an opportunity to mobilize the concepts of the circular economy and recover nutrients for reuse as liquid fertiliser for food crops to support agricultural production. Reducing the load of pharmaceuticals and nutrients by WWTPs would improve the sustainability and efficiency of waste management (Badeti et al., 2021; Volpin et al., 2018). Several countries have been actively testing and applying various source separation processes and technologies. Progressive nations such as Denmark, Germany,

South Africa, Sweden, and Switzerland have been using source separation for years and applying liquid urine directly as fertiliser. Direct nutrient recovery from source-separated urine is more sustainable and potentially more economical than synthesizing virgin fertilisers from natural resources, most of which are depleting (Maurer et al., 2003). Biological and physio-chemical processes are generally adopted for the recovery of nutrients from the human urine such as nitrification-denitrification, integrated forward osmosis-membrane distillation systems, ammonia stripping, etc. Although these techniques can recover nutrients from urine, failure to remove pharmaceutical drugs remains a concern. A separate treatment process may be adopted targeting the removal of pharmaceuticals such as activated carbon adsorption (granular activated carbon or GAC and powdered activated carbon or PAC), membrane processes, advanced oxidation, etc. (Almuntashiri et al., 2022; Almuntashiri et al., 2021; Alturki et al., 2010; Kanakaraju et al., 2018; Kovalova et al., 2013; Nguyen et al., 2012).

1.2 Research significance

Interest in human urine is increasing for three important reasons. First, the greater part of human urine consists of nutrients such as K, P and N that could be recycled as fertilisers for agriculture or water recovered for washing or flushing purposes (Volpin et al., 2020b). Second, effective urine treatment could decrease residual micropollutants (pharmaceuticals) which are presently discharged through sewer overflows and by WWTPs, which currently do not effectively remove such pharmaceuticals. Third, the separation of urine streams from combined sewerage flows may reduce energy consumption of wastewater treatment plants, which currently incur significant cost for removing nitrogen from the wastewater (Badeti et al., 2022; Badeti et al., 2021). Many countries are now making efforts to promote sustainable buildings and the features of the sustainable buildings include reducing per capita water consumption, reducing and recycling wastes to enhance circular economy and improving their energy efficiencies including through greening. Per capita water consumption can be achieved through wastewater recycling and reuse (Massoud et al., 2009; Rawat et al., 2011) while nutrient circular economy can be achieved

through the recovery of nutrients via source separation of urine, treatment and reusing as fertiliser (Sohn et al., 2023; Volpin et al., 2020b).

However, the urine-derived fertilisers must be safe for reuse as nutrients and hence should also be free from harmful micropollutants such as pharmaceuticals. The existing literature on the removal of pharmaceuticals by GAC adsorption including their kinetics from the different forms of source separated urine is still limited highlighting the importance of this research in advancing our understanding of GAC adsorption kinetics and removal predictions for pharmaceutical compounds from the source separated human urine. Therefore, the studies conducted in this thesis makes significant contributions to the field of pharmaceutical removal by GAC adsorption from a source separated urine (hydrolysed urine or nitrified urine) in the form of enhanced understanding of their adsorption kinetics, isotherm, and breakthrough curves. Additionally, the study also explored the application of ANN modelling to predict the removal of pharmaceutical compounds from the urine.

1.3 Research aim

The aim of this research is to produce a clean and high value fertiliser from the source-separated urine free of micropollutants. Removal of micropollutants from source-separated urine, or even reducing their concentration would prevent from reaching to the environment and the food chain. Although such treatment has become more possible due to source separation, the process requires refinement, especially if treated urine is to be reused for agriculture where many safety regulations apply.

1.4 Research objective

The objective of this study is to evaluate the removal of pharmaceuticals by GAC adsorption from the source-separated urine through lab-scale experimental studies and understand their adsorption kinetics, isotherm, and breakthrough curves. This involves evaluation of GAC adsorption for

micropollutant removal from different stages of source-separated urine processing, to produce a micropollutant-free high quality fertiliser product suitable for agriculture food crops. Additionally, it explores the application of artificial neural network (ANN) predictive modelling to assess pharmaceutical compounds.

To fulfil this goal, several open research questions have been investigated:

- Q1: How effective is GAC adsorption in the removal of pharmaceuticals from the human urine subjected to various stages of urine treatment?
- Q2: What operating conditions impact the performances of the adsorption column for pharmaceutical removal from human urine?
- Q3: What are the adsorption kinetics, isotherm and mechanisms for removal of pharmaceuticals involved during the GAC adsorption treatment of urine?
- Q5: How efficient is chemical regeneration of the GAC?

The following are the specific objectives of this work:

- Investigate the performance of GAC for the removal of pharmaceuticals from hydrolysed urine.
- Evaluate the removal efficiency and mass transfer based on breakthrough curves for pharmaceutical adsorption by the GAC column.
- Removal of pharmaceuticals from the MBR effluent before further processing for resource recovery.
- Investigate the performance of chemical regeneration to desorb pharmaceuticals from GAC surface.

1.5 Organisation thesis/outline

This thesis is written in a “Thesis by compilation” format and comprises 7 chapters, with chapters 3 to 6 presenting the key experimental findings of this study. Some of these chapters have been

already published in the peer-reviewed journals while some are currently under peer review. The overall structure of this thesis is illustrated in Figure 1.1. and is summarised as below:

- Chapter 1 presents the background research, problem statement, research significance, and research aim and research objectives of this thesis.
- Chapter 2 provides a detailed literature review on urine treatment processes for water/nutrient recovery. The subsequent review describes micropollutants, their types, and their influence on the natural environment. Existing literature and scientific research on pharmaceutical removal is also presented to provide background to this research.
- Chapter 3 assesses pharmaceutical removal from hydrolysed urine (stored urine before any form of treatment). A detailed assessment of the pharmaceutical removal by GAC column (lab scale) to produce breakthrough curves for evaluating the performance of GAC adsorption of pharmaceuticals under various operating parameters. This data is then applied for ANN modelling to predict pharmaceutical removal. Mathematical models are used to recreate breakthrough curves and predict levels of pharmaceutical adsorption. A version of this chapter was published in *Journal of water process engineering* (Almuntashiri et al. 2022)
- Chapter 4 investigates pharmaceutical compound removal from synthetic nitrified urine (where hydrolysed urine is assumed to have been subjected to biological nitrification process) by GAC, batch adsorption. A detailed assessment of pharmaceutical removal to understand the adsorption kinetics, investigate the impact of GAC adsorbent doses on the adsorption capacity for removing pharmaceuticals, to affect of GAC onto the nutrients (e.g. total nitrogen and phosphorus) (TN & PO₄-P) removal, to apply the adsorption isotherm models for each micropollutant. This chapter was published in *Chemosphere Journal* (Almuntashiri et al. 2021)
- Chapter 5 evaluates sulfonamide antibiotic removal from the real nitrified urine (a real hydrolysed urine was treated by biological nitrification in the urine MBR process). A detailed assessment of column tests produced breakthrough curves for evaluating the performance of GAC to adsorb sulfonamide antibiotics under various operating parameters including particle

size, adsorbent mass, flow rates, adsorption/contact time and pH at 6.2.

- Chapter 6 investigates the effect of organic and inorganic solvents to regenerate the exhausted GAC.
- Chapter 7 summarizes the key findings of this study and provides recommendations for future research.

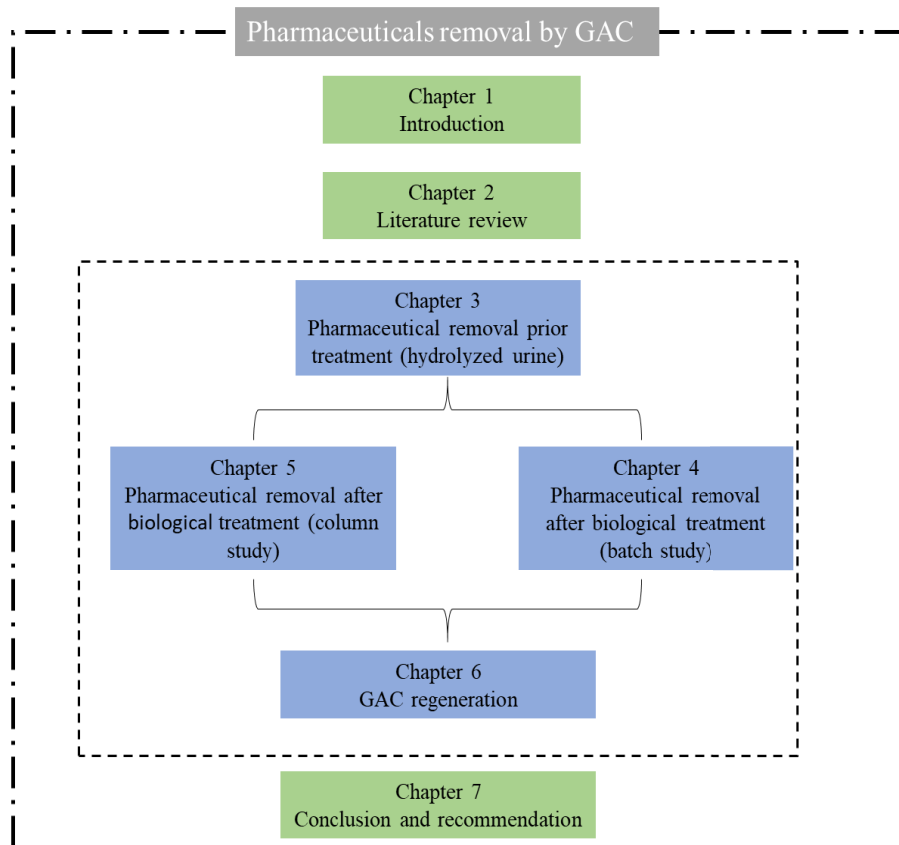


Figure 1-1 Thesis structure.

CHAPTER 2 Literature Review

2.1 Literature Review

This chapter serves as the cornerstone for the thesis, providing a comprehensive review of related literature that lays the groundwork for the research in this thesis. In essence, Chapter 2 encompasses the following key elements:

- Review of existing urine treatment processes by critically evaluating methodologies designed for the recovery of water and nutrients from human urine.
- A detailed examination of micropollutants prevalent in wastewater and human urine is presented, encompassing their various types and the potential environmental ramifications if released without adequate removal from urine or wastewater.
- Explores pertinent literature and scientific research related to the removal of micropollutants, particularly pharmaceuticals, utilizing GAC.
- Review practical applications of the GAC adsorption process, shedding light on its efficacy in removing contaminants from various sources, with a focus on pharmaceuticals.
- An in-depth exploration of literature pertaining to the utilisation of ANN modelling for the removal of pharmaceuticals via adsorption is undertaken, providing insights into this advanced methodology.
- Review existing body of knowledge regarding GAC regeneration and reuse methods, offering a comprehensive understanding of sustainable practices in this domain.
- Review alternative treatment methods reported in the literature for the removal of pharmaceuticals are presented, providing a comprehensive view of diverse methodologies beyond GAC adsorption.

By synthesising and analysing these critical components, Chapter 2 establishes a robust foundation for the subsequent research, ensuring a thorough understanding of the existing landscape and paving the way for the original contributions to follow in the thesis.

2.2 Composition of fresh and hydrolysed urine

Urine is produced by the kidneys whose sole purpose is to remove salts and toxins from blood. Therefore, it can contain high concentrations of nutrients and organic micropollutants. Fresh and stored urine have different characteristics including pH value and concentrations of heavy metals. Fresh urine matrix contains urea as the main form of nitrogen, which is rapidly hydrolysed to form ammonia (NH_3)/ammonium (NH_4^+) and bicarbonate (HCO_3^-) due to the action of urease enzyme. This hydrolysis process increases the urine's pH, leading to precipitation of calcium and magnesium based phosphates including struvite in the stored hydrolysed urine compared to fresh urine (Udert et al., 2006). As the pH of the hydrolysed urine is over 7.0, the nitrogen is mainly in the form of ammonia and hence ammonia volatilisation of urine when exposed to air, can result in significant nitrogen loss besides the unpleasant pungent smell associated with the hydrolysed urine. The basic properties of the urine such as electrical conductivity (EC), pH and concentrations values of macro and micronutrients in both fresh and hydrolysed urine are shown in Table 2-1 (Siegrist et al., 2013).

Table 2-1 Properties and ionic fresh and hydrolysed urine composition

	Fresh urine ^a	Hydrolysed urine ^b	Unit
EC	8.7–31	30	mS/cm
pH	5.5–7.0	9.1	NA
COD	6,300–18,000	10,000	mg/L
Urea	3,400–12,000	0	mg/L
NH ₄ ⁺ -N	130–730	3038 ± 271	mg/L
NO ₃ ⁻ -N	NA	NA	mg/L
NO ₂ ⁻ -N	NA	NA	mg/L
Na ⁺	1,800–5,800	1220 ± 258	mg/L
K ⁺	750–2,600	1023 ± 240	mg/L
Mg ²⁺	70–120	2 ± 5	mg/L
Ca ²⁺	32–230	51 ± 12	mg/L
SO ₄ ²⁻	600–1,300	780 ± 120	mg/L
PO ₄ ³⁻ -P	350–2,500	230 ± 51	mg/L
Cl ⁻	2,300–7,700	1410 ± 71	mg/L

^a (Larsen et al., 2021)

^b (Volpin et al., 2020b)

2.3 Water and nutrients recovery from urine matrix

Urine treatment provides two main benefits. First, water recovered from urine can be immediately utilized for washing or flushing purposes. Second, nutrients recovered from urine can be used as fertiliser after effective treatment to make them safe. However, several difficulties accompany the use of urine as a liquid fertiliser. These include an imbalanced nutrient profile, an unpleasant odour, high pH in addition to the potential presence of disease-inducing organisms, hormones and pharmaceutical agents. Thus, several novel methods have been trialled and the following section

presents existing urine treatment technologies for the nutrients and water recovery.

2.3.1 Thermal driven processes

There have been numerous studies which evaluate the use of thermal methods, e.g. membrane distillation (MD) or distillation, for the extraction of water from human urine.

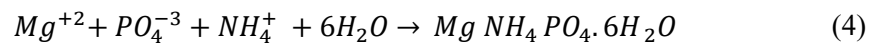
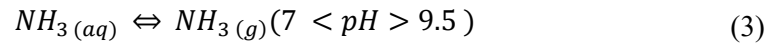
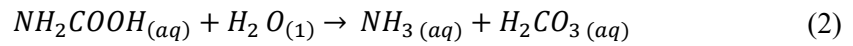
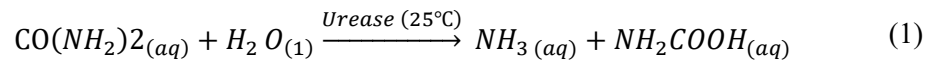
As long as there is suitable pre-treatment of the urine, these methods can generate distilled water of a high quality; which is particularly useful for space applications; and elevated factors of urine concentration (Maurer et al., 2006). Nevertheless, a disadvantage of urine evaporation is production of high titres of gaseous ammonia, as well as requiring significant thermal or electric energy. A vapour compression distillation plant with 85% energy recovery requires as much as 400 MJ.m⁻³ (Wood, 1982). Acidification or nitrification pre-treatment of urine can mitigate the loss of N (Fumasoli et al., 2016; Hellström et al., 1999). A marked decline in N attrition in the course of distillation and MD was noted when volatile NH₃ (g) underwent conversion to NH₄⁺ (l) or NO₃⁻ (l) (Tun et al., 2016). A small-scale pilot nitrification-distillation reactor was employed by Fumasoli et al. (2016) which generated 20-fold nitrified urine solution concentrate with negligible loss of N.

Further studies have assessed hybrid thermal-membrane techniques of MD trying to decrease energy consumption required by distillation. MD facilitates the passage of water vapour across a porous hydrophobic membrane whilst avoiding transfer of non-gaseous substances (Naidu et al., 2017). Since MD can function between 50-70 °C, sufficient heat can be provided from a waste heat or solar source.

2.3.2 Struvite precipitation

Currently, struvite precipitation is the most straightforward technique for recovering a portion of nitrogen and phosphorus from urine (Etter et al., 2011; Ronteltap et al., 2007). Eq. 1 and Eq. 2 outline the reactions for urea hydrolysis, catalysed by the urease enzyme, during which pH rises

over time correlated to temperature (Cook et al., 2007). The urine provides a source of phosphate; struvite precipitation is facilitated and the reaction leads to production of ammonium (Eq. 3) (Udert et al., 2003a; Udert et al., 2003b). When a source of Mg is added (Eq. 4), white crystalline phosphate struvite is formed (Zhang et al., 2009). Struvite precipitation occurs completely in a stirred or baffled reactor (Figure 2-1). After the urine is added, the Mg source is added to the stirred reactor. After the struvite crystals have formed, the solution is transferred to the filtration system, where the struvite crystals are separated from the effluent. The last stage of the process involves drying and collection of the struvite crystals (Rose et al., 2015). Two types of struvite are produced, i.e. magnesium potassium phosphate (MKP) and magnesium ammonium phosphate (MAP) (Stefov et al., 2005). Thus, urea hydrolysis can be a foundation for reclaiming ammonium, P and K, (although the recovery of N from NH_4 is less than 10% via struvite).



Furthermore, struvite is notably less favourable for macronutrients, which reduces its suitability as a fertiliser. Struvite precipitation's main value is for reclaiming phosphate. In order to achieve nearer to 100% P recovery, an extrinsic source e.g. Mg, has to be used to promote struvite precipitation (Wilsenach et al., 2007) thus increasing treatment costs. Use of Mg from different sources was assessed, e.g. Mg oxide (MgO), sulphate (MgSO_4) and chloride (MgCl_2) salts. Overall, the first source was the most cost-effective, however, in comparison to MgSO_4 or MgCl_2 , MgO took much longer to form a solution in urine (Sakthivel et al., 2012). It has been suggested

the greatest recovery of P struvite (90-97%) should occur when Mg, N and P are present in equimolar amounts (Lefebvre et al., 2016). For P recovery over 90%, pH 9–10 was needed. The ability of struvite to dissolve was mostly unaffected by additional organic complexing moieties or inorganic substances. The effect of other adsorbents, in combination with MgO ,to promote N, P and K recovery was assessed by Lind et al. (2000). They established that, for either fresh or stored urine, the use of zeolite in combination with MgO made N recovery more complicated, achieving about 80% recovery.

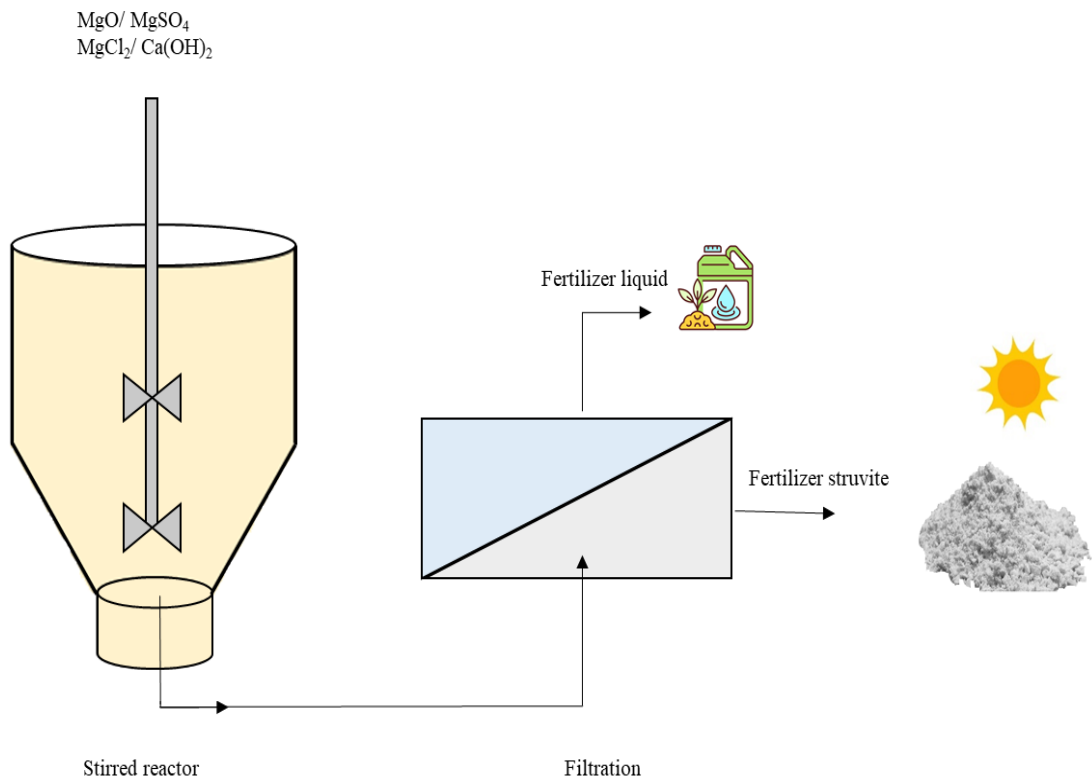


Figure 2-1 Illustration of the diagram struvite precipitation process to produce a fertiliser from urine (Patel et al., 2020).

2.3.3 Combined forward osmosis/ reverse osmosis

Combined use of both forward and reverse osmosis (FO-RO) as a hybrid method to enhance the recovery of water has been investigated. It was tested as a substitute for multi-bed filtration. In the hybrid FO-RO system, water is pulled across a selective FO membrane from a dilute solution

of wastewater to the more concentrated draw solution (DS). The surplus water is then reclaimed from the DS using RO, as shown in Figure 2-2. The two-fold treatment of the FO-RO system results in notable rejection of organic compounds, nutrients, and contaminants. The logic in selecting pre-treatment by FO included the potential to reduce susceptibility to contamination, lower energy requirements, and the fact that it is straightforward and dependable (Cath et al., 2005). Nevertheless, low rates of rejection of diminutive and charge neutral substances, e.g. urea, and volatile organic substances, was found when traditional hydrophilic polymeric FO and RO membranes were used.

In summary, the nutrients recovery from urine for use as agricultural fertiliser is a positive proposition, as urine can hold significant percentages of N, P and K. Recovery of nutrients direct from the urine stream should be more beneficial than their removal or production from other natural sources by conventional methods (Maurer et al., 2003). However, although the methods described have the potential for success, there is still concern that pharmaceuticals may also be recovered together with the nutrients, which prevents direct use as safe fertiliser. This literature review therefore also briefly considers existing knowledge of various micropollutants, their impact on humans and the environment, and current solutions for their removal.

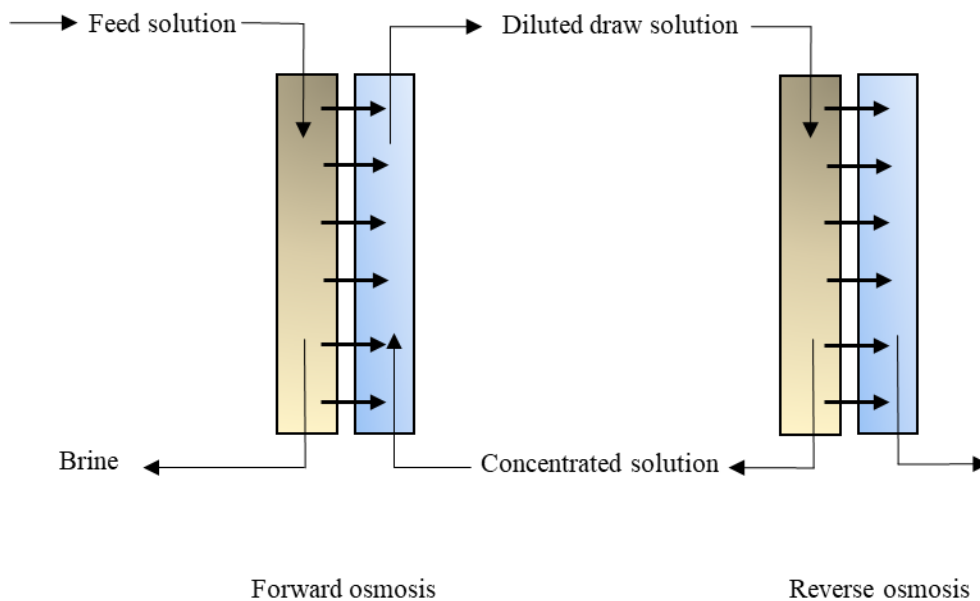


Figure 2-2 Illustration of the diagram hybrid forward osmosis – reverse osmosis (Shaffer et al., 2012).

2.4 Types of micropollutants and their influence on the human and aquatic environment

Micropollutants exist in different forms depending on the substance in which they occur. They are found in various chemicals, e.g., personal product care, pharmaceuticals, pesticides, and other industrial chemicals. The presence of pharmaceuticals in the water supply and WWTP effluents has been increasingly assessed over the past decade and detected at concentrations (ng/L -mg/L) as shown in Table 2-2. For instance, Kolpin et al. (2002) examined 139 streams of wastewater in US and identified more than 80 compounds with concentrations ranging about 0.01-10 µg/L. In the field of public health, the utilisation of antibiotics and pharmaceuticals has greatly enhanced the quality of people’s lives (Imwene et al., 2022). It is also significant to note that pharmaceuticals have different physicochemical characteristics such as lower cholesterol, managing symptoms of epilepsy, analgesics, and others. Thus, when micropollutants from these pharmaceuticals accumulate, they will also more likely bring about changes to the biological composition of plants and animals, and the entire ecosystem (Halling-Sørensen et al., 1998).

Pharmaceuticals are reported in the aquatic environment, and thus, it can have detrimental impacts on aquatic types, due to the potential toxicity caused by synergistic impacts of parent compounds or their metabolites (Quinn et al., 2009). Fish are affected by ibuprofen, which leads to the thinning of blood, alterations in the biological make-up, and genotoxicity (Brown et al., 2007; Virkutyte et al., 2010). In another study, the cause of death of white-backed vultures in India and Pakistan from 2000 to 2003 was studied. Results found that the vultures died from renal failure caused by accumulation of diclofenac. The research concluded that this accumulation was due to micropollutants in the environment (Oaks et al., 2004; Swan et al., 2006). The presence of these pharmaceuticals in the environment may cause unusual biological functions and fertility difficulties, increased cancer occurrences, the formation of antibiotic-resistant bacteria, and the likelihood of enhanced toxicity of chemical combinations. In many situations, the impacts of these pharmaceuticals on humans and aquatic environments are not well-defined (Kolpin et al., 2002). This presents challenges for WWTPs. Source separation urine systems aid separation of micropollutants from wastewater but require complementary processes to ensure that all toxic and hazardous substances are removed from wastewater, making it safe for healthy consumption or reuse in other industries.

Table 2-2 Occurrence of pharmaceuticals detected in surface water, wastewater, and urine.

Pharmaceutical Compounds	Concentration in aqueous solution		
	Surface (ng/L) ^a	water (ng/L) ^a	wastewater (ng/L)
Diclofenac	1.1-6.8	400	3200–72,000
Sulfamethoxazole	1.9-1900	1,000	7,740,000
Ibuprofen	5.5-2700	1000-3020	990,000
Naproxen	11	8,000	<10,000
Carbamazepine	4-5-1075	2,000	40,000

Trimethoprim	0.9-710	600	12,800,000
--------------	---------	-----	------------

^a (Alturki, 2013)

2.5 Pharmaceutical concentrations in source-separated urine

Urine can contain a variety of pharmaceutically active compounds, including prescription and non-prescription medications, personal hygiene products, cosmetic products, and preservatives used in food for human consumption. The base secretion pathway for most consumed pharmaceuticals is via urine. Table 2-3 shows the concentrations of common pharmaceuticals and antibiotics found in real human urine, as only a few studies have sought to identify these concentrations in source-separated urine, as shown in Table 2-3. Some pharmaceutical residue concentrations are found to be significantly (7,000 times) higher in urine than they are in groundwater and wastewater, as shown in Table 2-2. For example, the antibiotic sulfamethoxazole, is used to treat bacterial infections (e.g., urinary tract infections and prostatitis). A recent study by Ngumba et al. (2020) reported a sulfamethoxazole concentration value of 7.74 mg/L in source-separated urine, while Ternes et al. (2002) and Snyder et al. (2007) reported sulfamethoxazole concentrations in groundwater and wastewater of 410 and 1000 ng/L, correspondingly.

Table 2-3 Concentrations of pharmaceuticals and antibiotics found in human urine

Pharmaceutical Compounds	Measured concentrations in urine in eThekweni, South Africa ^a (µg/L)	Measured concentrations in fresh urine in a storage tank in the GIZ main building ^b (µg/L)	Mean values of pharmaceuticals in urine from a public urinal in Hamburg & Berlin ^c (µg/L)	Measured concentrations at UTS Waterless Urinals ^d in Australia (µg/L)	Measured concentrations in urine in Chunga area of Lusaka, Zambia ^e (µg/L)
Diclofenac	3.2–72	6	9-45	<10	NA
Sulfamethoxazole	<2–6,800	NA	NA	NA	7,740
N4 Acetyl-SMX	<1–3,500	NA	NA	NA	NA
Trimethoprim	<2–1,300	NA	NA	NA	12,800
Hydrochlorothiazide	<3–134	NA	NA	NA	NA
Atenolol acid	<4–1,100	NA	NA	NA	NA
Ritonavir	<1–4.6	NA	NA	NA	NA
Atenolol	<1–300	NA	NA	NA	NA
Emtricitabine	<6–920	NA	NA	NA	NA
Clarithromycin	<1	NA	NA	NA	NA
Ibuprofen	NA	990	398-794	497 ± 41	NA

Pharmaceutical Compounds	Measured concentrations in urine in eThekweni, South Africa ^a (µg/L)	Measured concentrations in fresh urine in a storage tank in the GIZ main building ^b (µg/L)	Mean values of pharmaceuticals in urine from a public urinal in Hamburg & Berlin ^c (µg/L)	Measured concentrations at UTS Waterless Urinals ^d in Australia (µg/L)	Measured concentrations in urine in Chunga area of Lusaka, Zambia ^e (µg/L)
Bisoprolol	NA	246	NA	NA	NA
Tramadol	NA	9	NA	NA	NA
β-Sitosterol	NA	NA	18-52	NA	NA
Carbamazepine	NA	NA	4-29	37 ± 3	NA
Pentoxifylline	NA	NA	3-9	NA	NA
Bezafibrate	NA	NA	192-846	NA	NA
Phenacetin	NA	NA	1-23	NA	NA
Triclosan	NA	NA	NA	48 ± 9	NA
Acetaminophen	NA	NA	NA	477 ± 278	NA
Fluoxetine	NA	NA	NA	12 ± 2	NA
Estriol	NA	NA	NA	6 ± 4	NA
Estrone	NA	NA	NA	<10	NA

Pharmaceutical Compounds	Measured concentrations in urine in eThekweni, South Africa ^a (µg/L)	Measured concentrations in fresh urine in a storage tank in the GIZ main building ^b (µg/L)	Mean values of pharmaceuticals in urine from a public urinal in Hamburg & Berlin ^c (µg/L)	Measured concentrations at UTS Waterless Urinals ^d in Australia (µg/L)	Measured concentrations in urine in Chunga area of Lusaka, Zambia ^e (µg/L)
Naproxen	NA	NA	NA	<10	NA
Norfloxacin	NA	NA	NA	NA	5.3
Tetracycline	NA	NA	NA	NA	2.8
Ciprofloxacin	NA	NA	NA	NA	660
Doxycycline	NA	NA	NA	NA	2–20
Amoxicillin	NA	NA	NA	NA	310
Nevirapine	NA	NA	NA	NA	5
lamivudine	NA	NA	NA	NA	1.9–10, 010

^a (Bischel et al., 2015)

^b (Schürmann et al., 2012)

^c (Hammer et al., 2005)

^d (Volpin et al., 2020a)

^e (Ngumba et al., 2020)

2.6 Granular activated carbon adsorption process

Activated carbon comes in various forms, including powder and granulated states. Granular Activated Carbon (GAC) is commonly used in fixed-bed columns due to its effectiveness, making it particularly suitable for scaling up from laboratory to industrial applications. It can handle substantial solution volumes and achieve high rates of micropollutant removal (de Franco et al., 2017). Research on GAC bed column adsorption is significant because it provides valuable data, such as breakthrough curves and treatment performance data, which are crucial for designing fixed-bed columns for practical applications. These data directly impact the technical and economic viability of the adsorption process. The breakthrough curve's shape offers insights into the dynamic behavior of the process, including aspects like in- and out-phase mass transfer and propagation, which influence the adsorption resistance. The Hydraulic Retention Time (HRT), often referred to as the Empty Bed Contact Time (EBCT) in GAC columns, provides a measure of the contact time, assuming GAC is completely porous. The performance of activated carbon is substantially influenced by a number of different variables in addition to the qualities of the solute to be adsorbed, such as charge, shape, size, hydrophobicity, concentration level, organic content, and contact time. These factors also include oxygen content, pore size distribution, surface area, and surface charge. All these factors play a crucial role in determining the rate and efficiency of adsorption. It's essential to consider these variables collectively to ensure the effective removal of micropollutants.

2.6.1 Application of granular activated carbon adsorption process

Activated carbon is commonly used to removing micropollutants, can be applied in both batch applications or fixed-bed columns, as shown in Figure 2-3 and 2-4, respectively. Several studies have confirmed the efficiency of GAC in removing micropollutants, making it a valuable asset in wastewater treatment (Snyder et al., 2007; Ternes et al., 2002). For example, in the study conducted by Kim et al. (2007), it was demonstrated that GAC could efficiently remove trace contaminants in drinking water treatment processes. This efficiency is primarily attributed to

GAC's porous nature and substantial surface area (Nguyen et al., 2013). Due to its commercial accessibility and porous nature, GAC is ideally suited for managing micropollutants with particular compositions. It also has stringent purity criteria. For instance, GAC has noteworthy effectiveness in the removal of micropollutants with certain physicochemical characteristics, such as those with prolonged perfluorocarbon chains. This effectiveness is attributed to the inclusion of functional perfluoroalkyl substances (PFAs) which actively participate in the adsorption and removal mechanisms (McCleaf et al., 2017). Numerous researchers have extensively discussed the occurrence of pharmaceuticals in wastewater treatment plant effluents (Lin et al., 2014).

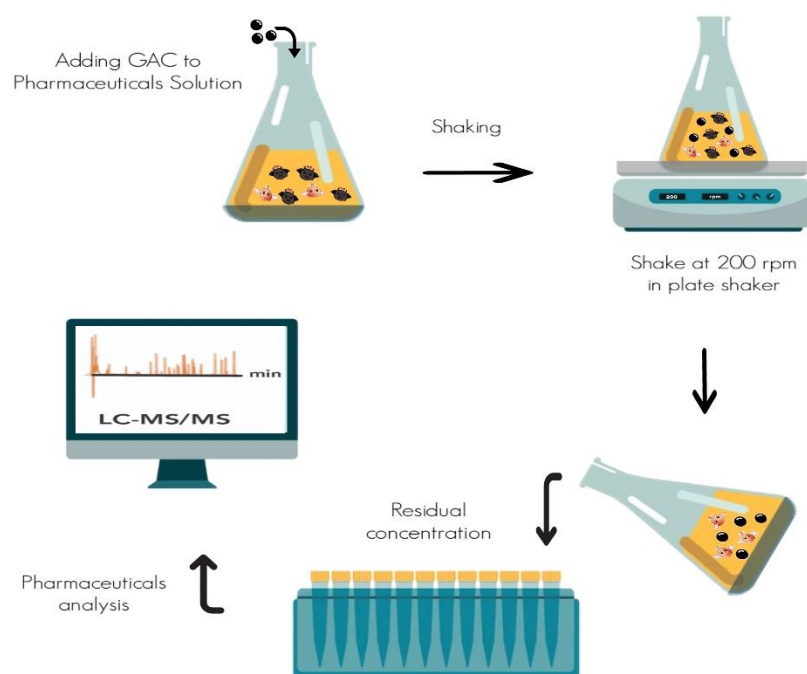


Figure 2-3 Schematic diagram of the batch test procedure

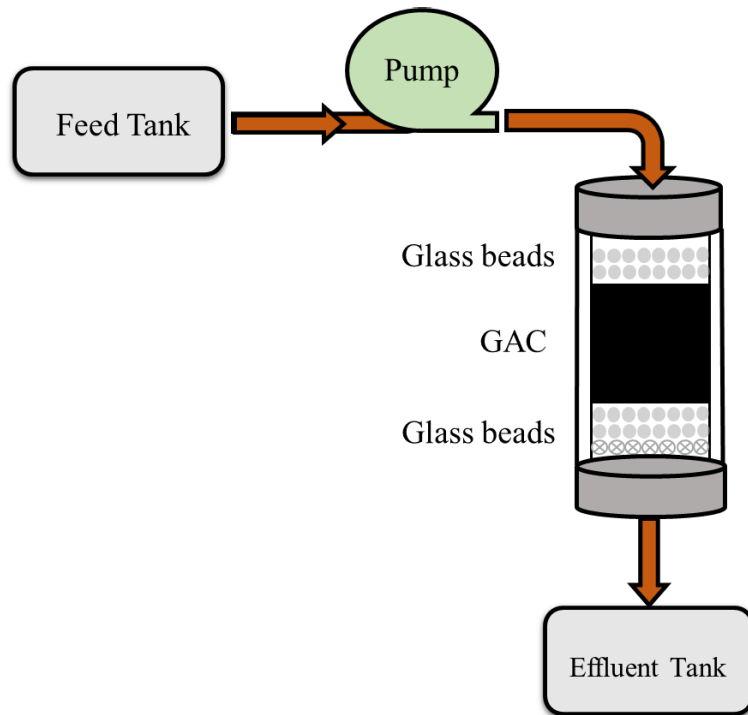


Figure 2-4 Schematic diagram of granular activated carbon column.

Conventional treatment methods have demonstrated their insufficiency in the successful elimination of these pharmaceuticals, as highlighted by Shanmuganathan et al. (2015); Westerhoff et al. (2005) conducted a study to evaluate the effectiveness of GAC in eliminating various pharmaceutical chemicals to solve this issue. According to their findings, a GAC dosage of 20 g/L resulted in clearance rates between 81% and 100%. A lower dosage of 5 g/L led to a 65% reduction in clearance rate. However, the efficiency of a five g/L GAC dosage varied depending on the substance.

Kim et al. (2007) evaluated the removal of 14 pharmaceuticals, 6 hormones, 2 antibiotics, 3 personal care items, and 1 flame retardant at full-scale and pilot-scale (inlet concentration at trace level, ng/L) during drinking water treatment methods. According to the findings, GAC was able to remove trace contaminants with high efficiency (99%) compared to conventional drinking water treatments. In order to evaluate the effectiveness of GAC in treating wastewater, Nguyen et al. (2012) focused primarily on eliminating trace organic pollutants, such as various hydrophilic substances including fenoprop, diclofenac, and carbamazepine. The findings of this investigation

demonstrated the effectiveness of GAC in the removal of these hydrophilic chemicals with a stunning 98% clearance rate. Similarly, Grover et al. (2011) carried out research on the effluent from a wastewater treatment facility and used pilot-scale granular activated carbon to assess the removal rates of pharmaceuticals and steroidal oestrogens. Their findings differed from those of the last study in terms of concentrations and removal rates, with high clearance levels of substances like mebeverine, indomethacin, and diclofenac being observed, ranging from 84% to 99%.

Deb et al. (2019) batch tested activated carbon for removal of three pharmaceuticals, at initial concentrations of 0.2 mM, in hydrolysed urine. The results showed that 2g/L of activated carbon removed 92.05% of ciprofloxacin, 89.70% of ibuprofen, and 82.60% of paracetamol during a 30-hour adsorption process. Application of the Langmuir model found ciprofloxacin to have highest adsorption (q_{\max}), followed by ibuprofen, and paracetamol (1310 $\mu\text{g/g}$, 860 $\mu\text{g/g}$, and 380 $\mu\text{g/g}$, respectively). Additionally, the artificial neural network (ANN) model of this work predicted 95% of the experimental removal values for the three pharmaceuticals.

A recent study by Köpping et al. (2020) assessed the rate of removal of 11 pharmaceuticals from nitrified urine using pilot-scale columns of coarse- and fine-grained activated carbon. They applied different empty bed contact times (25, 70, 92, and 115 minutes), which revealed that increased contact time is positively correlated to pharmaceutical removal. They showed that short bed contact times resulted in lower removal efficiency for all pharmaceutical compounds, particularly candesartan and clarithromycin. However, elevating the contact time from 25 to 70 minutes by increasing the bed height resulted higher removal rates for both candesartan (60%) and clarithromycin (90%). Köpping et al. (2020) employed fine GAC also in the same study. As for the coarse GAC column, the fine GAC column resulted in low breakthrough of pharmaceuticals in short contact times (in order: 25, 70, and 90 minutes) compared to coarse GAC column. Overall, the authors reported treatment time for pharmaceuticals was longer with fine GAC compared to coarse GAC for all empty bed contact times. This is due to the particle size

and surface area of GAC.

Duygan et al. (2021) combined aerobic biological treatment with post-treatment with powdered activated carbon (PAC) to test removal of 11 pharmaceuticals from urine. The results showed that levels of micropollutant removal corresponded to differences in their physical-chemical properties. Up to 90% of clarithromycin, ritonavir and atazanavir were removed in a 2-hour period, while atenolol, darunavir and trimethoprim degradation ranged from 30% to 70% during 12-hour aerobic biological treatment. On the other hand, sulfamethoxazole, hydrochlorothiazide, diclofenac and N4-acetyl sulfamethoxazole were only slightly degraded; by less than 20%; by aerobic biological treatment. The researchers applied additional treatment with PAC to attempt to remove all pharmaceutical compounds completely. Their study applied different PAC doses to test the impact on removal efficiency. With 25 mg/L of PAC adsorbent, approximately 70% of trimethoprim, ritonavir, and atazanavir were removed, while less than 20% of emtricitabine, N4-acetyl sulfamethoxazole, and sulfamethoxazole were removed. The five other pharmaceuticals were removed at rates from 20% to 70%. The study's results found that increasing PAC mass increases removal efficiency. At 100 mg/L of PAC, more than 50% of each pharmaceutical was removed, while 90% removal efficiency of all pharmaceuticals was achieved at 200 mg/L PAC.

Ternes et al. (2002) conducted research involving various drinking water treatment processes, including laboratory and pilot-scale experiments, as well as real water treatment facilities to remove selected pharmaceuticals (bezafibrate, clofibric acid, carbamazepine, diclofenac) with an initial concentration of target compounds below 2 µg/L. This investigation demonstrated that treatment with coal-based GAC was highly effective in eliminating the target pharmaceuticals, in addition to ozonation. Almost all of the pharmaceuticals were removed by GAC in pilot-scale experiments, with the exception of clofibric acid, which showed a removal rate of 57% in laboratory tests and 77% in water treatment facilities.

2.6.2 Granular activated carbon regeneration and reuse

Considering the application of GAC in micropollutant removal and modelling, regeneration and reuse of GAC are essential aspects to consider in the context of sustainable wastewater treatment. During the adsorption process, micropollutant compounds are adsorbed within the GAC pores and on its surface. Over time, the GAC gradually becomes saturated. When it reaches the saturation stage, or if GAC performance is inadequate before that point, the GAC process can no longer continue. Therefore, a regeneration operation is performed, which is a more cost-effective way to extend the life of the GAC instead of replacing or disposing of it. The presence of pharmaceuticals like metronidazole, which rapidly saturate the GAC, can lead to more frequent exhaustion of the adsorbent, requiring frequent regeneration (Almuntashiri et al., 2021; Nguyen et al., 2013).

Thermal regeneration is one of the most commonly used techniques for GAC regeneration. However, there are drawbacks to using this method, including the need to transport spent GAC to a specialized offsite facility for regeneration. Additionally, the repeated regeneration increases operational costs due to high GAC usage and reduced GAC service life. Typically, about 10% of GAC is lost during thermal regeneration due to excessive burn-off and attrition, requiring the replacement of lost GAC with virgin GAC. Because of these issues, various on-site regeneration studies have been conducted over the years as alternatives to thermal regeneration (Larasati et al., 2020; Marques et al., 2017).

One effective alternative for GAC regeneration is the chemical regeneration technique, which can be carried out on-site at a lower energy cost. This involves exposing the saturated GAC to chemical regenerants to desorb the micropollutants, resulting in minimal loss of GAC. It eliminates the need for specialized treatment, and the effectiveness of chemical regeneration depends on the interaction between GAC and micropollutants. Although there have been several investigations on chemical regeneration, the best regenerant solutions for desorbing a variety of aqueous pollutants have yet to be discovered. Finding the best regeneration solution, in particular,

is made more difficult by the presence of micropollutants that are weakly adsorbable. Additionally, the processes of these micropollutants adsorption and desorption on GAC have not been thoroughly studied. The desorption ratio attained during chemical regeneration was not included in several prior research that reported regeneration efficiency.

2.6.3 Artificial neural network modelling for pharmaceutical removal via adsorption

Building on our discussion of GAC's application in micropollutant removal and the need for advanced modelling techniques, we now turn our attention to the application of artificial neural network (ANN) modelling. It is expensive and time-consuming to run laboratory-scale column experiments and analyse samples for wastewater micropollutant removal assessment. On the other hand, using reliable modelling and simulation approaches to foretell micropollutant removal under various operational situations is a more beneficial and economical strategy for evaluating the probable performance of GAC column adsorption. Additionally, the use of numerical modelling can assist researchers in predesigning a process to make it more efficient and economical (Hosseinzadeh et al., 2020b; Hosseinzadeh et al., 2022). ANN can exhibit human-like behavior making it a powerful tool in this regard. Learning both non-linear and linear correlations between the dependent and independent parameters is one of ANN's primary capabilities. In ANN modelling, the network is trained using the actual findings from the experiment, and the trained model is subsequently verified and put to the test for prediction (Hosseinzadeh et al., 2020b). This adaptability, in contrast to other, more conventional models, is a result of ANN's ability to learn right away from empirical data without making assumptions about the physicochemical properties that can affect adsorption process.

ANN modelling has emerged as a powerful tool for modelling and optimizing wastewater treatment processes. It allows for the prediction of pharmaceutical removal efficiency and provides insights into the process's behavior (Pauletto et al., 2021; Vakili et al., 2019). More specifically, ANN has been used to create models for breakthrough curves (Moreno-Pérez et al., 2018), isotherms (Mendoza-Castillo et al., 2018; Pauletto et al., 2020b), kinetics (Gopinath et al.,

2020; Pauletto et al., 2020a), and process optimisation (Ghaedi et al., 2019). According to earlier research, ANN models are highly accurate in forecasting micropollutants adsorption. Almuntashiri et al. (2021) created ANN models, which had R^2 values of 0.984, 0.991, 0.99, and 0.992, respectively, predicted the elimination of ibuprofen, naproxen, metronidazole, acetaminophen, and carbamazepine. Additionally, several research in a variety of applications remarked on the excellent prediction and strength of ANN models.

In a research study conducted by Hosseinzadeh et al. (2020b), the ANN models exhibited high accuracy, with a score of 0.99, when predicting both actual and expected data regarding nutrient recovery from solid waste through vermicomposting. In comparison to response surface models, the findings of Hosseinzadeh et al. (2018) demonstrated the excellent accuracy of ANN models in forecasting the levels of benzene, toluene, xylene, and ethyl-xylene from contaminated airstreams in non-thermal plasma. An integrated sequencing batch reactor and powdered composite adsorbent were employed to optimize the removal of pharmaceutical products using the ANN modelling technique and RSM. Atenolol, ciprofloxacin, and diazepam are three pharmaceuticals that were specifically targeted and are found in synthetic wastewaters (Mojiri et al., 2020). Based on the modelling results, RSM determined the optimal concentration and removal efficiency as follows: Atenolol (90.2%), ciprofloxacin (94.0%), and diazepam (95.5%). In contrast, the ANN model demonstrated a high R^2 value exceeding 0.99 and a mean squared error below 1.0. As per the study by Mojiri et al. (2020), the R^2 value highlights the remarkable predictive accuracy of the ANN model. ANN models are expected to be used efficiently in forecasting pharmaceutical removal due to their high accuracy and prediction.

2.7 Alternatives treatment for pharmaceuticals removal

Pharmaceuticals are often present in wastewater, requiring effective removal methods. This section explores various treatment approaches, including Ultraviolet (UV) processes, ozonation, polymer resin adsorption, biochar application, membrane filtration, and membrane bioreactors.

These methods exhibit varying levels of efficacy depending on the specific pharmaceuticals and water treatment conditions.

2.7.1. Ultraviolet and Ultraviolet /peroxide processes

The ultraviolet (UV) processes efficacy in removing contaminants is contingent on the UV absorption of the contaminants (Kanakaraju et al., 2018). The significant parameters affecting direct UV photolysis degradation kinetics are; the ratio constants, k_{UV} , molar extinction coefficient (ϵ) and quantum yield. (Luo et al., 2018). A study by Zhang et al. (2016) provided insight into the degradation kinetics of antibiotics in stored urine using low-pressure (LP) -UV, UV/ PDS, and UV/H₂O₂. They found that antibiotics were degraded quicker by UV/PDS than by UV or UV/ H₂O₂. The highest degradation rates of eight sulfonamide antibiotics; sulfisoxazole, sulfathiazole, sulfamonomethoxine, sulfadimethoxypyrimidine, sulfamethazine, sulfamerazine, sulfamethoxypyridazine, and sulfadiazine; were 1.91×10^{-2} , 1.02×10^{-2} , 4.14×10^{-3} , 1.69×10^{-3} , 1.37×10^{-3} , 9.18×10^{-4} , 8.95×10^{-4} and 5.77×10^{-4} , respectively when exposed to UV/PDS. Furthermore, Zhang et al. (2015) also reported that three pharmaceuticals (sulfamethoxazole, trimethoprim and N4 -acetyl-sulfamethoxazole) in fresh and hydrolysed urine were degraded by LP-UV and UV integrated with PDS and H₂O₂. Under LP-UV, sulfamethoxazole was degraded more quickly than N4-acetyl-sulfamethoxazole or trimethoprim in both fresh and hydrolysed urine. The highest degradation rates were 1.22×10^{-2} , 2.0×10^{-3} and 1.5×10^{-5} for sulfamethoxazole, N4-acetyl-sulfamethoxazole and trimethoprim, respectively. When researchers applied UV in combination with H₂O₂ or PDS, no degradation of pharmaceuticals was noted in the first hour, but as the time passed (hours), degradation increased. The results showed that UV/PDS performed better than UV/ H₂O₂, the degradation rate of sulfamethoxazole was 3.1×10^{-3} and 5.35×10^{-3} for UV/PDS and UV/ H₂O₂, respectively. A study by Giannakis et al. (2017a) examined removal of venlafaxine from real human urine by UV and UV/ H₂O₂. The effectiveness of UV alone for degrading venlafaxine in hydrolysed urine was negligible, attributed to presence of light-absorbing compounds (e.g., phosphoro-, organic matter,

nitro-, and other groups). However, upon the addition of H₂O₂, venlafaxine degradation reached ~30%. By contrast, results of testing 10× diluted urine resulted in 80% of venlafaxine degradation and the addition of H₂O₂ further enhanced degradation, up to 100%. Subsequently Giannakis et al. (2017b) evaluated the influence of a UV/ H₂O₂/Fe combined process to remove iohexol from real hydrolysed urine. The combined process was found to remove more than 90% of the iohexol under laboratory conditions (100 ppm of Iohexol, 50 ppm H₂O₂, and 5 ppm Fe²⁺ dosage). Janssens et al. (2019) applied two ranges of wavelengths (UV-C and UV-A) to investigate the degradation of etoposide in urine at initial concentrations of 500 µg/L. The results showed rates of degradation improved proportionally with the catalyst titanium dioxide (TiO₂) at a concentration of 1500 mg/L. The etoposide degradation rate was 3.6 ×10⁻³ by UV, which increased to 35.9 ×10⁻³ and 37.3 ×10⁻³ for UV-C/TiO₂ and UV-A/TiO₂, respectively when the catalyst was added.

2.7.2. Ozonation process

Another promising method for removing micropollutants is the ozonation process, which can significantly reduce the micropollutant load in full-scale WWTPs (Hollender et al., 2009). In a study by Hernández-Leal et al. (2011), the effectiveness of ozonation in removing various micropollutants from biologically treated water was investigated. At an applied ozone concentration of 15 mg/L, all the chemicals were generally considerably eliminated (> 79%) from the biologically treated effluent. The majority of the targeted micropollutants were successfully removed at high ozone doses of 5 mg/L in a different research (Sui et al., 2010). More than 95% less of the drugs carbamazepine, diclofenac, indomethacin, sulpiride, and trimethoprim were present. Bezafibrate, on the other hand, was very resistant to ozonation and was only reduced by 14%. The use of O₃/H₂O₂ for the removal of a variety of micropollutants (pharmaceuticals and steroid hormones) during water reclamation was the topic of a research by Gerrity et al. (2011). For practically all of the target pollutants, the procedure demonstrated a high removal efficiency (> 90%), with the exception of TCEP (13%), TCP (26%), atrazine (69%), meprobamate (80%),

and ibuprofen (83%).

2.7.3. Polymer resin adsorption

Polymer resin adsorption is another approach for pharmaceutical removal. In a study conducted by Landry and Boyer (2013), the influence of different types of strong-base anion exchange resins on the removal of diclofenac from synthetic fresh and hydrolysed urine compositions was examined. Resin performance for removal of diclofenac from fresh urine was as follows: 78%, 60%, 44%, 9% for Dowex Marathon 11, Dowex 22, A520E, and IRA958 respectively, at an anion exchange resins dose of 1000 $\mu\text{l/L}$ and initial concentration of 200 μM . Diclofenac removal efficiency by the resin from hydrolysed urine was the same as for fresh urine; i.e. Dowex Marathon 11, Dowex 22, A520E, and IRA958, but at 5% lower rates. The researchers found that increased dosage of anion exchange resin from 2000 to 4000 $\mu\text{l/L}$ (except IRA958) increased removal efficiency rates, to about 20%, removal efficiency exceeded 95%. The authors suggested that the reason for this increase was the interaction between the deprotonated carboxylic acid of the adsorbate and the quaternary ammonium of the adsorbent material. They also suggested that anion exchange resins should be able to completely remove other pharmaceuticals similar to diclofenac e.g. ibuprofen and naproxen, due to the presence of the benzene rings and carboxyl group.

2.7.4. Biochar

Biochar is a carbonaceous residue of waste materials formed by pyrolysis (over 250°C) under low oxygen or sometimes oxygen-free conditions. The use of modified carbonaceous material is an established technique for removing inorganic and organic contaminants from wastewater streams (Imwene et al., 2022).

Solanki and Boyer (2017) examined the removal of seven pharmaceuticals (diclofenac, paracetamol, carbamazepine, citalopram, ibuprofen, acetylsalicylic acid and naproxen) at an

influent concentration of 200 μM . Four different types of biochar (bamboo, southern yellow pine, coconut shell and northern hardwood) applied at a dosage rate of 0.8 g/L removed 10% to 40% of pharmaceuticals. However, when the dose of biochar was increased to 40g/L, high removal efficiencies of more than 90% were achieved for all pharmaceuticals. Solanki and Boyer (2019) later used biochar to perform a pharmaceutical adsorption study (at initial concentrations of 0.2 mM) from synthetic fresh, synthetic hydrolysed, and real urine. The resulting removal rates of paracetamol and naproxen from synthetic hydrolysed urine were more than 95% and 50%, respectively, after 4 days of batch adsorption by 2 g/L of softwood biochar along with 8 ml/L of resin. From synthetic fresh urine, the removal rate decreased to 90% for paracetamol but increased to 70% for naproxen. The researchers observed no difference in the removal rate of paracetamol between real fresh or hydrolysed urine, achieving approximately 60% removal at the highest biochar dose (20 g/L).

Paredes-Laverde et al. (2018) researched use of coffee (*Coffea arabica*) husk and rice (*Oryza sativa*) husk wastes as adsorbents for norfloxacin removal from different water matrices including; distilled water, municipal wastewater and hydrolysed urine. The results found that approximately 30.60%, 81.45% and 96.95% of norfloxacin was removed within 60 minutes from urine, wastewater and distilled water, respectively when 3g/L of rice hulls were used as an adsorbent. Wastewater and urine compositions are characterized by high concentrations of inorganic. Thus, this interaction can be attributed to cations (e.g., Mg^{2+} , K, and Na) competing with pharmaceuticals for biochar surface sites, which reduce the adsorption rate of norfloxacin. The removal efficiency of norfloxacin was a somewhat higher in complex matrices using 3g/L of coffee husk as an adsorbent compared to rice husk. 83.54%, 95.63% and 99.66% of the norfloxacin was removed by coffee husk within 60 minutes of adsorption in urine, wastewater and distilled water, respectively. This might be because of the high surface area of coffee husk, along with the presence of deprotonated acidic groups, which contribute to improving the adsorption of norfloxacin. In general the results identified the use of coffee husk as an effective

alternate for pharmaceuticals removal (e.g. norfloxacin) in real applications.

Sun et al. (2018) tested batch treatment using combined biochar and hydrogen peroxide (H_2O_2) processes to remove five antibiotics (at an initial concentration of $10\ \mu M$) in hydrolysed urine. The results showed that sulfadimethoxine, sulfamethazine, sulfamethoxazole, N4-acetyl-sulfamethoxazole and sulfadiazine were removed at rates of 71%, 74%, 49%, 68% and 39%, respectively, at 1g/L after 5 days from the adsorption process. However, the authors indicated that after H_2O_2 (1 mM) was added to biochar (1g/L), sulfadimethoxine, sulfamethazine, sulfamethoxazole, and sulfadiazine were degraded by approximately 60% after 1 hour, but N4-acetyl-sulfamethoxazole did not degrade.

2.7.5. Membrane Filtration

Various membrane filtration technologies can be utilized to remove contaminants from wastewater. Nano-filtration (NF) and RO processes are driven by hydraulic pressure applied to the feed; the permeate crosses the membrane, and the concentrate is rejected as shown in Figure 2-5. Membrane filtration is a promising technique for removing contaminants from wastewater and has gained significant attention in recent decades. NF/RO and FO have the potential to remove micropollutants from wastewater (Al-Rifai et al., 2011; Alturki et al., 2010; Urtiaga et al., 2013), however they might not be suitable for treatment of urine because of their rejection for the nutrients and micropollutants together. Pronk et al. (2006) found that the PO_4-P and micropollutants were rejected by about 90% using the NF membrane in urine. It means additional treatment is needed to recover PO_4-P from micropollutants that exist in NF brine. Later Pronk et al. (2007) reported that prior treatment of the NF membrane by electro dialysis led to higher rates of micropollutant removal, although the technique is complicated.

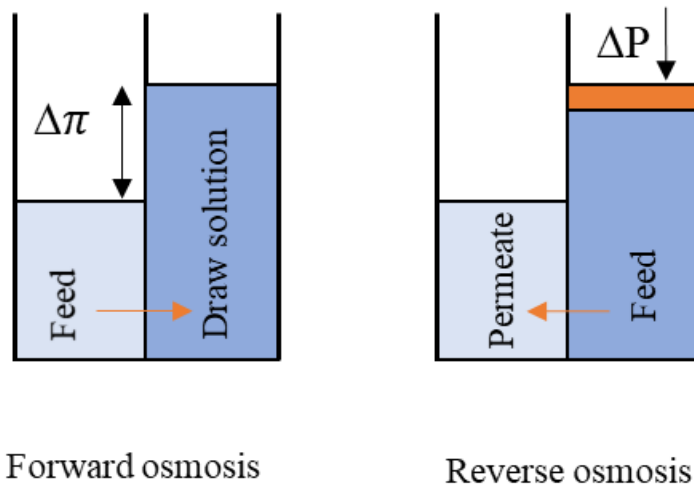


Figure 2-5 Principles of FO and RO (Cath et al., 2006).

2.7.6. Membrane bioreactor

One technology for removal of micropollutants in wastewater is the membrane bioreactor (MBR). This technology combines membrane separation with specific forms of biological treatment of targeted compounds. This is a promising alternative for removing micropollutants from wastewater (Caluwé et al., 2017). There are a number of parameters which affect MBR effectiveness; sludge age and concentration, overall composition of wastewater, pH levels of wastewater, wastewater conductivity, and operating temperature (Kovalova et al., 2012). These factors compromise the capacity of the membrane bioreactor to remove micropollutants from wastewater effectively. The MBR was able to remove pharmaceuticals with more than >95% removal rate for risperidone, enalapril, and atenolol. Despite the advantages of MBR, this technology does not yet fully remove contaminants from wastewater. Additional processes are required to remove remaining contaminants. Hai et al. (2011a); Tadkaew et al. (2011) reported that MBR rates of removal for metronidazole, acetaminophen, and naproxen were lower than 50%. In addition, hydrophilic substances e.g. sulfonamide antibiotics, cannot be easily removed, which results in low removal rates (Nghiem et al., 2009).

Overall, several techniques have been employed for pharmaceutical removal from wastewater, including UV process treatment, ozonation and membrane filtration. However, many of these

removal methods face challenges stemming from the generation of harmful byproducts and high operational costs. In contrast, polymer resin adsorption, biochar, and membrane bioreactors have displayed limitations in achieving complete pharmaceutical removal. An alternative with potential is GAC adsorption, thanks to its cost-effectiveness, flexibility, and reusability, as highlighted by (Jaria et al., 2019). Notably, there is a research gap in the utilisation of the GAC adsorption system for pharmaceutical removal from source-separated urine. Hence, this study aims to address this gap, offering reliable insights into the real-scale application of fixed-bed GAC column adsorption for the removal of pharmaceuticals from processed urine. Such an advancement has the potential to enhance the safety and value of urine-derived fertilisers.

2.8. Conclusion

This chapter presented some of the issues of pharmaceutical presence in urine and their adverse effect on public health and the environment if they are not removed from effluent. It also reviewed some currently available techniques for removing pharmaceutical compounds from wastewater. Based on the literature review, in theory, hydrolysed urine can be treated using a MBR that combines nitrification with a membrane filtration system. The two-step nitrification process converts ammonia to nitrite (NO_2^- -N) by *Nitrosomonas* bacteria, and the subsequent conversion of nitrite to nitrate by *Nitrobacter* bacteria. During this process more than 95% of dissolved organic carbon is removed. However, there are few studies on pharmaceuticals removal from urine using GAC adsorption. Therefore, there is a gap in current knowledge that needs to be investigated in more detail, i.e. the technical feasibility of GAC (batch study or fixed bed column) for the removal of pharmaceuticals from hydrolysed or nitrified urine. This hypothesis will be evaluated systematically in the proposed research and analysed through GAC breakthrough curves, kinetic studies, isotherm studies under different conditions by mathematical modelling.

CHAPTER 3 Pharmaceutical compounds removal from synthetic hydrolysed urine using GAC: Column study and predictive modelling

3.1 Abstract

Human urine contains high concentration of pharmaceuticals, a concern that must be addressed if used as a fertiliser. This chapter addresses the first objective of thesis by thoroughly assessing the removal of pharmaceuticals from hydrolysed urine before any treatment processes. This study systematically evaluated granular activated carbon (GAC) in removing pharmaceuticals five most found in the environment – naproxen (NAP), carbamazepine (CBZ), ibuprofen (IBP), acetaminophen (APAP) and metronidazole (MTZ) – from hydrolysed urine. Fixed-bed columns experiments were used to obtain breakthrough curve and assess GAC (1000 m²/g) performance in the adsorption of pharmaceuticals at different adsorbent mass (4–12 g/L), flow rate (1.15–4.32 L/d) and adsorption/contact time at ambient room temperature and pH 9. The highest adsorption capacity was observed at a lower adsorbent mass (4 g/L) and lower flow rate (1.15 L/d) for all micropollutants. The breakthrough curves showed the highest GAC adsorption capacity for CBZ (56.1 mg/g) while MTZ (32.2 mg/g) with the lowest adsorption will be the design limiting for column adsorption application. Thomas and Yoon-Nelson models fitted well for predicting empirical breakthrough curves for fixed-bed GAC column adsorption. The artificial neural network (ANN) modelling was able to predict the removal effectiveness of over 99% except for APAP at 84.5%. The overall results indicate that GAC is highly effective in removing targeted pharmaceuticals, supporting the thesis's overarching goal.

Keywords: ANN modelling; Breakthrough curves; GAC column adsorption; Hydrolysed urine; Pharmaceutical removal

3.2 Introduction

Over the past 50 years, studies have indicated that approximately 200,000 tons of pharmaceuticals are consumed worldwide annually (Lan et al., 2018). Based on the present consumption rate, global pharmaceutical use is expected to increase by approximately 15% by 2030 (Klein et al., 2018). Due to the frequent presence of pharmaceutical pollutants in the environment, there is growing concern about rise in the presence of antimicrobial-resistant bacteria. Furthermore, vast amounts of pharmaceutical pollutants have been reported in the groundwater, surface water and soil, so there are concerns about their harmful effects on humans and wildlife because of the potential toxicity caused by the synergistic effects of parent compounds and metabolites existing in the environment (Bradley et al., 2016; Madikizela et al., 2017). Most conventional wastewater treatment plants are not designed to remove organic contaminants such as pharmaceuticals and therefore cannot attain adequate removal of these organic compounds (Adams et al., 2002) which all finally lands up in the aquatic environment.

Nutrient recovery via urine collection, mainly from toilets, was first suggested in the 1990s because urine contains up to 88% of nitrogen, 67% of phosphorus, and 73% of potassium in the domestic wastewater (Almuntashiri et al., 2021; Badeti et al., 2021). Source separation of urine offers a unique opportunity for diversion of pharmaceuticals from the wastewater, because urine is the major source of pharmaceuticals that enters wastewater treatment plants although urine accounts less than 1% by volume of the total wastewater flow to the treatment plant (Lienert et al., 2007). However, only limited studies have been focussed so far on the pharmaceuticals removal from urine solutions.

Zhang et al. (2015) applied a combined UV and H₂O₂ processes while Dodd et al. (2008) investigated advanced oxidation process using ozone to remove micropollutants from hydrolysed urine. Both studies observed that micropollutants could be partially eliminated by oxidants formed from other compositions present in the urine. de Wilt et al. (2016) reported that

high levels of diclofenac, metoprolol and paracetamol (60%–100%) were removed, but trimethoprim and carbamazepine were only partially removed (30% and 60%, respectively) using biodegradation and photolysis. Sun et al. (2018) reported that a combination of biochar adsorption and H₂O₂ were able to remove 39%, 74%, 71% and 49% of sulfadiazine, sulfamethazine, sulfadimethoxine and sulfamethoxazole respectively, from urine at 1 gL⁻¹ biochar dosage. Pronk et al. (2006) observed that over 90% of micropollutants and nutrients present in the urine were removed via nanofiltration membrane process, so an additional step is necessary to separate the micropollutants from the nutrients. Using electro dialysis or microfiltration as pre-treatment step to nanofiltration, it resulted in higher micropollutant removal rates although the combined process is complicated and requires additional processes and longer operation times. Moreover, Zhang et al. (2020) observed that a fixed bed biochar column adsorption combined with peroxydisulfate removed 75% of N4-acetyl-sulfamethoxazole and 98% of sulfamethoxazole from the urine. Duygan et al. (2021) reported that over 90% of pharmaceuticals is removed from the nitrified using 200 mg/L of powdered activated carbon.

Granular activated carbon (GAC) is widely employed in the removal of natural or synthetic micropollutant compounds and hence can be utilized in fixed-bed columns and stirred-tank reactors. Most recent studies are related to GAC removal of pharmaceuticals from the surface water and wastewater (Del Vecchio et al., 2019; Grover et al., 2011; Hernández-Leal et al., 2011; Kim et al., 2010; Li et al., 2018; Nguyen et al., 2012) and only limited studies are dedicated to the removal of pharmaceuticals from the urine matrix (Almuntashiri et al., 2021; Duygan et al., 2021; Köpping et al., 2020). GAC column adsorption is one of the most common technologies for water and wastewater treatment because of its high treatment efficiency, ease of expansion into industrial applications and simple operations (Sotelo et al., 2014). GAC adsorption may result in high pharmaceutical removal nevertheless however with time, the GAC bed column will become saturated needing regeneration or replacement (Nguyen et al., 2013). Studies on bed column adsorption is important because it can provide valuable information such as breakthrough curves and acquire treatment performance data essential for system design for actual applications.

Following column saturation, GAC can be generally regenerated and reused making the process more sustainable and economical (Jaria et al., 2019).

Lab-scale column experiments and sample analysis of micropollutants to evaluate their removal performances from wastewater is both expensive and time-consuming. Predicting micropollutant removal through robust modelling and simulation under various operating conditions is a more useful and cost-effective approach to understanding the likely performances of the GAC column adsorption. In addition, the application of numerical modelling can help researchers with the process predesign making it more efficient and cost-effective (Hosseinzadeh et al., 2020b; Hosseinzadeh et al., 2022). As a machine, artificial neural network (ANN) is inspired by human brain, where this machine can demonstrate human-like behaviour. One of the key abilities of ANN is learning both non-linear and linear relationships between the dependent and independent factors. In ANN modelling, the actual results with the experimental condition feed the network to train it and the trained model is then validated and tested for prediction (Hosseinzadeh et al., 2020b). Therefore, the trained ANN models have been employed effectively to forecast micropollutants removal systems' efficiency during the wastewater treatment process (Pauletto et al., 2021; Vakili et al., 2019). More precisely, ANN has been used to develop models for kinetics (Gopinath et al., 2020; Pauletto et al., 2020a), isotherms (Mendoza-Castillo et al., 2018; Pauletto et al., 2020b), breakthrough curves (Moreno-Pérez et al., 2018), as well as process optimisation (Ghaedi et al., 2019). Unlike other, traditional models, this versatility is due to the fact that ANN learns immediately from empirical results without making suppositions about the nature of physicochemical which influence mechanism adsorption.

Although few studies have been published on the fixed-bed columns adsorption for pharmaceutical removal from a urine matrix (Duygan et al., 2021; Köpping et al., 2020; Zhang et al., 2020), to the best of our knowledge, an analysis of GAC's breakthrough curves and behaviour under various conditions using ANN predictive modelling of pharmaceuticals in hydrolysed urine has not yet been evaluated. Therefore, the objectives of the study include evaluating the

pharmaceutical removal from hydrolysed urine by fixed bed GAC column including understanding the impacts of major operating conditions, apply mathematical models to reproduce breakthrough curves for pharmaceutical adsorption and, acquire column adsorption parameters and apply it for ANN modelling to predict pharmaceutical removal from the hydrolysed urine.

3.3 Material and methods

3.3.1 Adsorbent and adsorbate

Five pharmaceutical compounds were selected for this study: CBZ, NAP, IBP, APAP and MTZ (Sigma Aldrich, Australia). Pharmaceutically active compounds were selected based on their frequent occurrence and in high percentage (up to 90%) in the urine matrix, molecular structure, and various physicochemical properties such as hydrophobicity and molecular size as shown in Table 3-1. Stock solutions of each micropollutant were prepared by dissolving them in 100% MeOH solution due to their low solubility in water. The concentrations of all five pharmaceutical in the hydrolysed urine were spiked to an initial concentration of 0.2 mM to work within a detectable limit. The coal-based GAC (MDW/4050CB) used in this study was supplied by James Cumming & Sons Pty Ltd., Australia. Before use, the GAC was washed with water to eliminate surface impurities, then drier at 100 °C for 24 h in an oven. The BET surface area of GAC was $S_{BET} = 1000 \text{ m}^2/\text{g}$ and GAC particle size ranging from 0.42 to 1.68 mm with majority within 0.42–0.60 mm range (Jamil et al., 2019). The synthetic hydrolysed urine composition used for all the tests in this work are shown in Table S3-1.

Table 3-1 The physicochemical pharmaceuticals properties.

Pharmaceutical Compounds	Compound Class	MW	Log K _{ow} ^a	pK _a	Excretion percentage ^c
CBZ	Antiepileptic	236.27	1.89 ± 0.59	13.94 -0.49 ^c	72%
NAP	Analgesics	230.26	2.88 ± 0.24	4.20 ^b	80 %
IBP	Analgesics	206.28	3.50 ± 0.23	4.90 ^b	60 %
APAP	Pain reliever	151.16	0.48 ± 0.21	1.72 9.86 ^b 14.44	(60%-90 %)
MTZ	Antibiotics	171.15	-0.14 ± 0.30	2.58 ^c	77 %

^a (Nguyen et al., 2012)

^b (Jamil et al., 2019)

^c (Almuntashiri et al., 2021)

3.3.2 Fixed-bed column experiments

The column adsorption experiments were performed using acrylic columns with 2 cm internal diameter and 30 cm length. A stainless steel mesh was placed at the bottom to prevent the GAC adsorbent from flowing out with the effluent. The fixed-bed column was filled with GAC and supported by glass beads at the top to improve influent flow distribution and ensure full wetting of the adsorbent, as shown in Figure S3-1. The influent was fed in down-flow mode at a controlled flow rate using peristaltic pump (Masterflex, Cole-Parmer, USA). The hydrolysed urine flow varied between 1.15 L/d and 4.32 L/d and all tests were performed at 25°C.

3.3.3 GAC column adsorption analysis

The micropollutant adsorption on the fixed-bed GAC column were assessed by plotting breakthrough curves C_t/C_0 (where C_0 is the initial concentration of micropollutants, and C_t represents the micropollutants concentration at the end of the fixed-bed at a time t) against operation time (days). The breakthrough point was determined using breakthrough curve experiments, which identify the time at which the concentration of the effluent reaches a relatively specified percentage of the influent concentration, and is usually 5% (de Franco et al., 2017). Saturation time was defined as when the effluent concentration of micropollutants reached the 95% of influent concentration. The breakthrough point, which allows the system to calculate treated effluent volume, is an important parameter. The region above the breakthrough curve, therefore, determines the highest capacity of adsorption, q_t (mg/g), and can be calculated as follows:

$$q_t = \frac{Q \cdot C_0}{m} \int_{t=0}^{t=total} \left(1 - \frac{C_t}{C_0}\right) dt \quad (1)$$

where m represents the adsorbent mass in the column (g) Q represents the flow rate (L/d); and t represents the total time (d) (de Franco et al., 2017).

The height of mass transfer zone (h_{MTZ}) is the adsorbent length in the fixed bed, which is unsaturated and thus contributes to mass transfer. The form of the h_{MTZ} is depended on the adsorption mechanism, the mass transfer conditions, operational conditions related to bed length and the flow rate (Sotelo et al., 2013). The h_{MTZ} calculation can be expressed as follows:

$$h_{MTZ} = \left(1 - \frac{q_b}{q_t}\right) h \quad (2)$$

where h represents the bed height (cm); q_b and q_t are the adsorption capacity (mg/g) at the

breakthrough point (effluent concentration reaches 5% of influent) and the highest adsorption capacity at saturation (effluent concentration reaches 95% of influent), respectively.

Additionally, the adsorbent usage rate (U_r), the fraction of bed utilisation (FBU) and empty bed contact time (EBCT) are helpful factors for the breakthrough curves analysis. FBU is linked to h_{MTZ} and EBCT or time of residence, which impacts the influent treatment volume and the breakthrough curve's nature, can be expressed as follows:

$$U_r = \left(\frac{m}{V_a} \right) \quad (3)$$

$$FBU = \left(\frac{q_b}{q_t} \right) \quad (4)$$

$$BECT = \left(\frac{V}{Q} \right) \quad (5)$$

Here, V represents the fixed-bed volume (L); V_a represents the volume that was treated at breakthrough (L) (Jaria et al., 2019).

3.3.4 Data collection and ANN modelling

To establish a sophisticated and accurate analysis of the process, the empirical results of a series of fixed-bed column adsorption were used to evolve computer models under various conditions involving contact time, adsorbent mass and flow rate. To decrease the complication of the computation and evade overtraining, the empirical data of the input and output were randomized and ranged from 0.1 to 0.9, as expressed in Eq. (6):

$$\text{Normalized value } (A_i) = \frac{A_i - A_{max}}{A_{max} - A_{min}} \times (0.9 - 0.1) + 0.1 \quad (6)$$

where A_{min} and A_{max} represent the values of minimum and maximum of the network's inputs or outputs, whereas A_i represents the value of any input or output (Hosseinzadeh et al., 2020a).

In this work, five feed-forward ANN models were developed using MATLAB R2018b to predict each pharmaceutical removal by fixed-bed GAC column adsorption. ANN modelling is carried out in three phases, for example, training, validation, and testing. In the training phase, the model is trained and developed, and then, the developed model is validated and tested in the validation and testing phases, respectively. Each developed ANN model has three layers: the input, hidden, and output layers. The numbers of the input and output variables show the numbers of the neurons in the input and output layers. The number of neurons in a hidden layer is determined through modelling process. The contact time, adsorbent mass and flow rates were used as input variables in all five models, whereas the percentages of NAP, CBZ, IBP, APAP and MTZ removal were considered the output variables for each of the developed models. To calculate the precision of the models in all three training, validation and testing phases, the determination coefficient (R^2) and the mean square error (MSE) were used as statistical indicators depending on which model was chosen as shown in Table 3-2. To model the processes, all the experimental data were randomly sectioned on two divisions of 80% and 20%. The first division was employed with fractions of 70%, 15% and 15% for training, validation and test, respectively, while the second division was employed for an additional test to check more the viability of the models.

Levenberg-Marquardt was used as a backpropagation training algorithm to develop the models. Furthermore, the output and hidden layers employed a function of linear transfer (purelin) and a function of a tangent sigmoid transfer (tansig), respectively. Various numbers of neurons ranging

from 1 to 20 were studied in the hidden layer of the neural networks to determine the most suitable number. Additionally, such modelling was repeated five times to develop a model with minimum errors ratio and maximum precision and output predictions.

Table 3-2 Error functions equations

Index	Equations
Determination coefficient	$R^2 = 1 - \frac{\sum_{i=1}^N (y_{prd,i} - y_{Act,i})}{\sum_{i=1}^N (y_{prd,i} - y_m)}$
Mean square error (MSE)	$MSE = \frac{1}{N} \sum_{i=1}^N (y_{prd,i} - y_{Act,i})^2$

where $y_{Act,i}$ represents actual empirical values;, $y_{prd,i}$ represents the predicted ANN model values;, N is the total number of data; and y_m is the mean of empirical values (Hosseinzadeh et al., 2020a).

3.3.5 Breakthrough curve modelling

The breakthrough occurrence time and the saturation curve shape are fundamental properties for process design and dynamic response, as they directly influence² the technical and economic feasibility of the adsorption process. To design a fixed-bed column to facilitate adsorption, accurate predictions for the effluent's breakthrough curve are needed. The shape of the curve provides insight into the dynamic behaviour of the process in which in- and out-phase mass transfer and propagation increase resistance to adsorption (Blagojev et al., 2019).

Many mathematical models can be employed to describe the fixed-bed column adsorption process. The model developed by Thomas is one of the most widely and commonly applied in fixed-bed column performances (de Franco et al., 2018). This model, supposes that the rate of adsorption can be described using the kinetics of Langmuir adsorption, disregarding intraparticle

mass transfer, external liquid film resistance and pivotal dispersion in the column (Jaria et al., 2019). It is expressed as follows:

$$\frac{C_0}{C_t} = \frac{1}{1 + \exp \frac{K_{th}}{Q} (q_0 m - C_0 Q t)} \quad (7)$$

where q_0 and k_{th} represent the theoretical adsorption capacity (mg/g) and the Thomas model rate constant (L/d/mg), respectively.

Regarding the Yoon-Nelson model, it was developed to reduce the error ratio related to the Thomas theory at periods of time. This model supposes that the rate of decrease in the micropollutant adsorption eventuality is proportionate to the eventuality of the micropollutant adsorption and the eventuality of micropollutant breakthrough on the adsorbent (Jaria et al., 2019). The model can be represented as follows:

$$\frac{C_0}{C_t} = \frac{\exp(K_{yn}t - t_{50\%}K_{yn})}{1 + \exp(K_{yn}t - t_{50\%}K_{yn})} \quad (8)$$

where k_{yn} and $t_{50\%}$ represent the rate constant of the Yoon-Nelson (d^{-1}) and the time required to reach 50% of micropollutant breakthrough (d), respectively.

3.3.6 Pharmaceutical compounds analysis

The pharmaceutical concentrations were analysed using liquid chromatography mass spectrometry (LCMS-8060), provided using a CORTECS C18+ Column, 2.7 μ m, with dimensions of 2.1 mm and 75 mm for inner diameter and length, respectively. The ESI negative mode was used for the analyses of IBP and NAP, whereas the ESI positive mode was employed for CBZ, APAP, and MTZ. All analytes were revealed simultaneously. Two mobile phases were applied for these analytes: A was 100% methanol, and B was Milli-Q water. The gradient

elution used for the flow rate was persistent at (0.6 mL/ min) as follows: mobile phase A remained at 50% (0.01–0.10 min), increased to 95% (0.10–1.50 min) and remained at 95% (1.50–3.50 min) and declined to 50% after that (3.51–5.50 min). The multiple reaction modes chosen for the analytes were as follows: APAP (152 > 110, ES+), MTZ (172 > 128, ES+), CBZ (237 > 194, ES+), IBP (205 > 161, ES-) and NAP (229 > 185, ES-). Calibration curves were also created for all micropollutants at various concentrations of (2–5000 nM), and also the determination coefficient (R^2) was more than 0.99.

3.4 Results and discussion

3.4.1 Influence of operational conditions on pharmaceuticals removal

3.4.1.1 Influence of flow rate

The empirical breakthrough curves for the pharmaceutical adsorption in urine by GAC column are shown in Figure 3-1. The breakthrough curves exemplify the rate of final concentration (C_t) at different times and the initial concentration (C_0) against time. The breakthrough curves exemplify the rate of final concentration (C_t) at different times and the initial concentration (C_0) against time. The plot shows how the column adsorption of micropollutants onto GAC is influenced by the flow rates. Moreover, the breakthrough curve is significantly affected by the adsorption ratio or the mass moving from solution to adsorption active sites inside the GAC particles. The plots were nearest to an S-shaped breakthrough curve, especially at lower flow rates, which indicated a higher adsorption rate and slower process. On the other hand, the breakthrough point time or $t_{5\%}$ and saturation time decreased as the flow rate increased from 1.15 L/d to 4.32 L/d for all micropollutants, as shown in Table 3-3. This is expected because of the increased mass loading of micropollutants into the column at higher flow rates thereby saturating faster. The trend in the values of breakthrough point ($t_{5\%}$), volume treated at breakthrough (V_a) and highest adsorption capacity at saturation (q_t) were CBZ > NAP > AAP > IBP > MTZ indicating that GAC adsorption is most favourable for CBZ while the MTZ being least favourable will be the limiting design of GAC column adsorption

amongst the five studied micropollutants.

The maximum adsorption capacities calculated were 56.1, 53.4, 36.3, 34.9 and 32.2 mg/g at a flow rate of 1.15 L/d, which decreases to 46.9, 40.1, 26.2, 21.7 and 12.1 mg/g at the highest flow rate of 4.32 L/d for CBZ, NAP, IBP, APAP and MTZ, respectively. Although the micropollutant loading rate increases at higher flow rates however, the decrease in the adsorption capacity at higher flow rates could be attributed to insufficient residence time for micropollutants to adsorb in the column and also potential hydraulic short circuiting. Similar findings were reported for the adsorption of flumequine on activated carbon (Sotelo et al., 2013), and were explicated by the lower residence time in the column at higher flow rate.

Competence and mass transfer parameters obtained from empirical breakthrough curves on the column experiment of micropollutants from the urine matrix are displayed in Table 3-3. These parameters indicate that a low flow rate may produce a longer operating time to $t_{5\%}$, along with a larger of V_a . FBU, which represents the ratio of the micropollutants adsorbed at breakthrough point (q_b) to total adsorbed at saturation (q_t) varied 0.32 – 0.12 at flow rate of 1.15 L/d but decreased to 0.22 – 0.01 at 4.32 L/d. These FBU values are within the range reported in the literature. The decrease in the FBU values at higher flow rates can be due to the inadequate contact time between the GAC and micropollutants as reported in other studies (Deokar & Mandavgane, 2015; Jaria et al., 2019; Tor et al., 2009). The U_r value increases at higher flow rate, which is a significant increase from 1.15 to 4.32 L/d. This is expected because the high flow rates reduce the liquid film thickness surrounding the GAC particles, which results in a lower resistance of mass transfer and a higher mass transfer rate, the explanation being that the value of U_r increases as the flow rate increases.

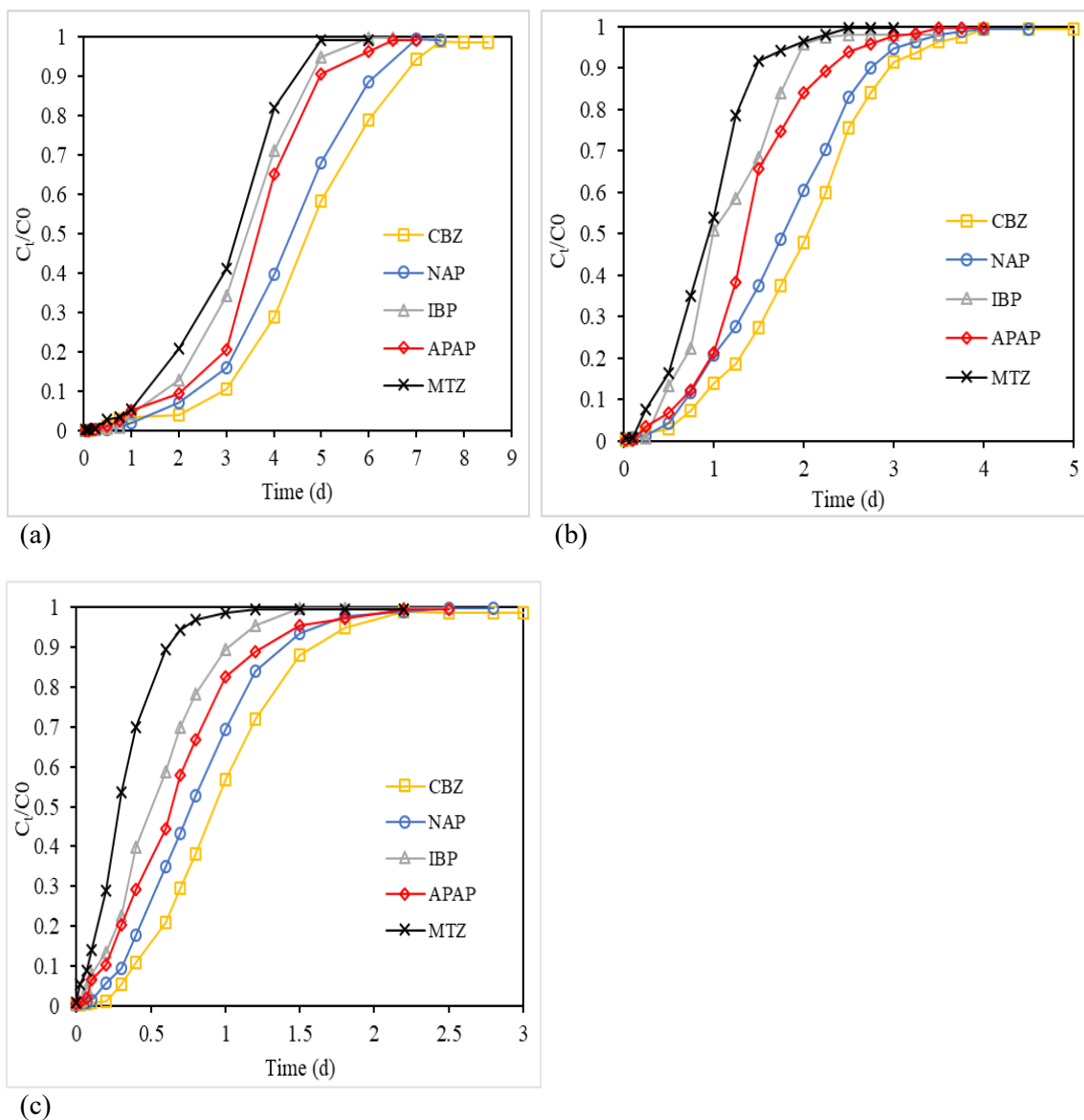


Figure 3-1 Breakthrough curves of pharmaceuticals adsorption onto GAC at various flow rates of (a) 1.15 L/d; (b) 2.59 L/d and (c) 4.32 L/d; $m = 4$ g and $C_0 = 0.2$ mM.

Table 3-3 Parameters of competence and mass transfer obtained from empirical breakthrough curves for pharmaceuticals adsorption by GAC on fixed-bed column. $t_{5\%}$ (time and breakthrough), V_a (volume treated at breakthrough), q_b (adsorption capacity at the breakthrough point), q_t (highest adsorption capacity at saturation), EBCT (empty bed contact time), h_{TMZ} (height of mass transfer zone) and U_r (usage rate), $t_{exp.50\%}$ (the experimental time required to reach 50% of micropollutant breakthrough).

Pharmaceuticals	Experiments condition		$t_{5\%}$ (d)	V_a (L)	q_b (mg/g)	q_t (mg/g)	EBCT (d)	FBU	h_{TMZ} (cm)	U_r (g/L)	$t_{exp.50\%}$ (d)
	Flow rate (L/d)	adsorbent mass (g)									
CBZ			1.8	2.07	18.05	56.07		0.32	2.32	1.93	4.83
NAP			1.4	1.61	16.13	53.35		0.30	2.39	2.48	4.4
IBP	1.15	4	0.8	0.92	7.94	36.25	0.0095	0.18	2.67	4.34	3.5
APAP			1	1.15	7.71	34.85		0.22	2.67	3.47	3.6
MTZ			0.5	0.575	3.957	32.22		0.12	3.00	6.95	3.13
CBZ			0.7	1.813	14.89	50.96		0.29	2.43	2.20	2.15
NAP			0.5	1.295	11.93	48.77		0.24	2.59	3.08	1.9
IBP	2.59	4	0.25	0.6475	4.54	26.93	0.0042	0.16	2.85	6.17	1.1
APAP			0.3	0.777	3.83	25.58		0.14	2.92	5.14	1.4
MTZ			0.2	0.518	2.18	18.27		0.11	3.02	7.72	0.97

Pharmaceuticals	Experiments condition		$t_{5\%}$ (d)	V_a (L)	q_b (mg/g)	q_t (mg/g)	EBCT (d)	FBU	h_{MTZ} (cm)	U_r (g/L)	$t_{exp.50\%}$ (d)
	Flow rate (L/d)	adsorbent mass (g)									
CBZ			0.23	0.9936	10.43	46.68		0.22	2.66	4.02	0.93
NAP			0.18	0.7776	7.61	40.1		0.19	2.78	5.14	0.8
IBP	4.32	4	0.075	0.324	2.59	26.19	0.0025	0.1	2.96	12.34	0.52
APAP			0.09	0.3888	1.90	21.68		0.08	3.03	10.28	0.64
MTZ			0.01	0.0432	0.22	12.11		0.01	2.99	26.45	0.3
CBZ			3.1	3.56	23.8	49.37		0.48	2.69	1.68	6
NAP			2.6	2.99	22.52	46.84		0.48	2.70	2.01	5.8
IBP	1.15	6	1.5	1.72	9.43	32.03	0.014	0.29	3.67	3.48	4.6
APAP			1.8	2.07	8.87	27.6		0.31	3.53	2.89	5.3
MTZ			1.2	1.38	5.21	23.46		0.22	4.05	4.34	4
CBZ			6.4	7.36	25.68	43.2		0.6	4.22	1.63	11
NAP			6	6.9	25.2	41.04	0.028	0.61	4.01	1.73	10.7
IBP	1.15	12	3.3	3.8	11.78	27.21		0.43	5.90	3.15	9.2
APAP			4	4.6	10.92	24.77		0.44	5.82	2.60	9.5

Pharmaceuticals	Experiments condition		$t_{5\%}$	V_a	q_b	q_t	EBCT	FBU	h_{MTZ}	U_r	$t_{exp.50\%}$
	Flow rate (L/d)	adsorbent	(d)	(L)	(mg/g)	(mg/g)	(d)		(cm)	(g/L)	(d)
		mass (g)									
MTZ			2.5	2.875	7.85	21.80		0.36	6.22	4.17	8

3.4.1.2 Influence of adsorbent mass

Fixed-bed experiments were conducted at different mass of adsorbent denoted by adsorbent column height of 4.0 g (3.50 cm), 6.0 g cm (5.2 cm) and 12.0 g (10.4 cm) to study the influence of adsorbent mass on the breakthrough curve and adsorption performance, as presented in Figure 3-2. As expected, smaller height bed height resulted in a quicker breakthrough compared to higher bed height leading to the faster saturation and exhaustion of the adsorbent. A higher bed height can result in longer breakthrough time and obviously higher volume of urine treatment. Besides providing increased adsorption surface area, the use of more GAC mass increases the column length and hence the travel length and contact time of the micropollutants with the adsorbent resulting in a much higher adsorption at breakthrough (Salman et al., 2011; Zhang et al., 2019). Table 3-3 shows the symmetrical and calculated lengths of the mass transfer. The trend in the values of $t_{5\%}$, V_a and q_t were $CBZ > NAP > AAP > IBP > MTZ$ similar to the one observed earlier at different flow rates. The mass adsorption capacity q_b increased when a higher adsorbent height is used while the q_t decreased. A possible explanation for the reduced adsorption capacity could be the π -bond intervention of the extra GAC with each other, which prevents the fashioning of π -bonds between the pharmaceuticals and GAC in the column (Tian et al., 2013). Although this resulted in gradual increase in the FBU which is good, but this also contributed to increased h_{MTZ} especially at the highest column height of 10.4 cm indicating the increase in the nonideality of the adsorption process at larger adsorbent height. This is further supported by the decrease in the U_r at higher adsorbent height. A smaller h_{MTZ} is preferable as this brings the adsorption process closer to ideal resulting in higher utilisation rates and less adsorbent wastage. However, for practical applications, the adsorbent height cannot be too short as this could significantly increase the column area/diameter resulting in increased footprint, which is less desirable. The FBU values increased when larger mass of adsorbent was used. Besides providing increased adsorption surface area, the use of more GAC mass increases the column length and hence the travel length and contact time of the micropollutants with the adsorbent resulting in a much higher adsorption at breakthrough resulting in improved FBU (Sotelo et al., 2013).

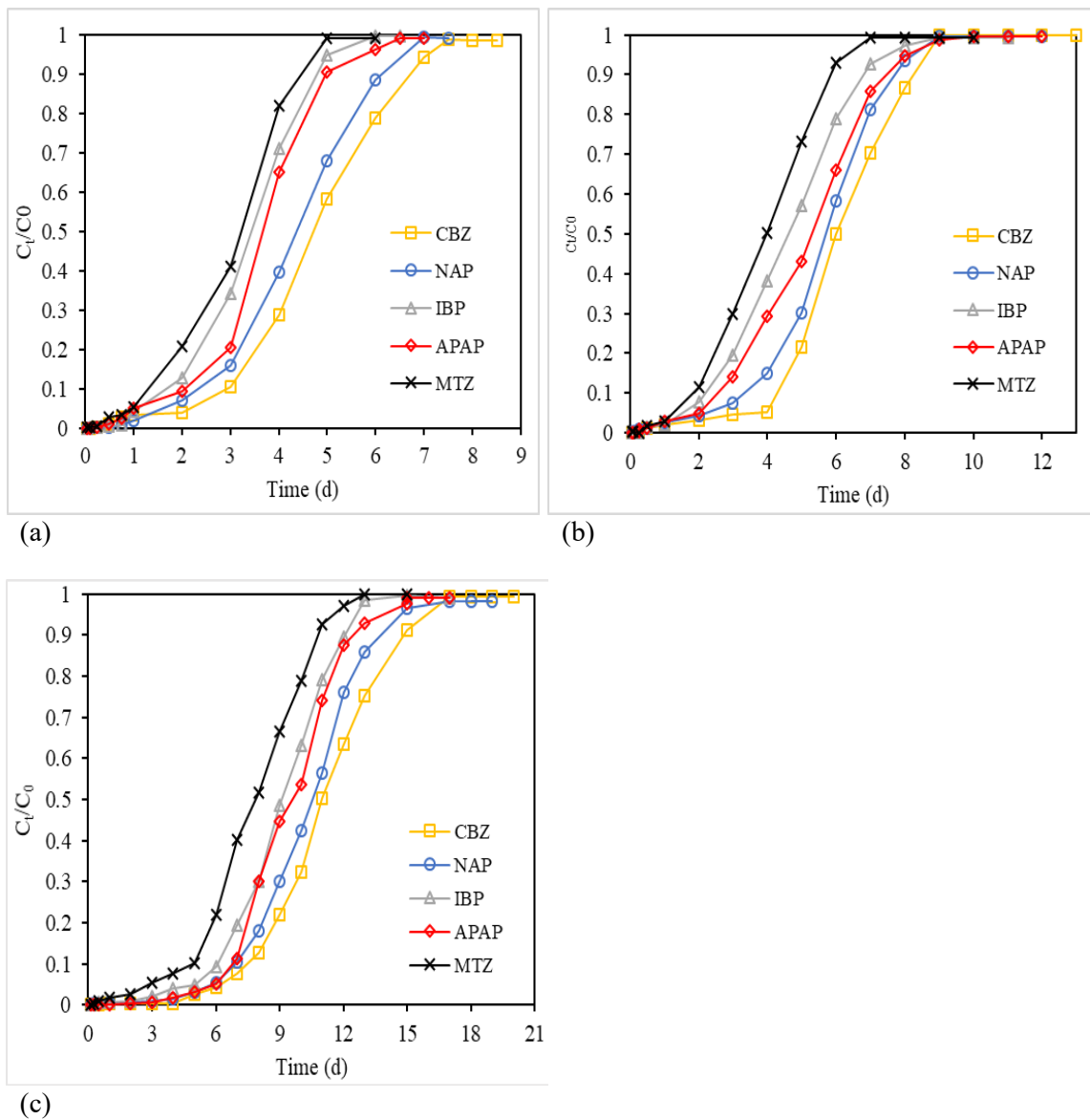


Figure 3-2 Breakthrough curves of pharmaceuticals adsorption onto GAC at various mass of adsorbent of adsorbent column heights of (a) 4.0 g; (b) 6.0 g and (c) 12.0 g; $Q = 1.15$ L/d and $C_0 = 0.2$ mM.

3.4.2 Breakthrough curves modelling

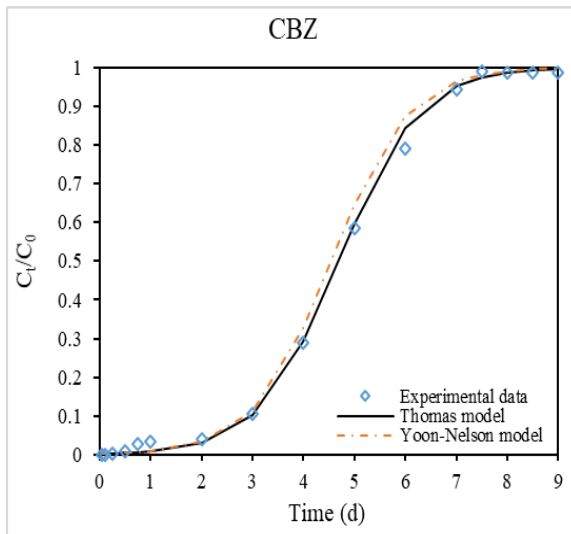
The performance of GAC column adsorption can be predicted via an analytical modelling approach of the breakthrough curves. The analytical models of Thomas and Yoon-Nelson were used to describe the empirical data of the breakthrough curves as shown in Figure. 3-3.

Mathematical parameters and coefficients of determination of modelling under various operating conditions of the empirical design are presented in the Table 4.

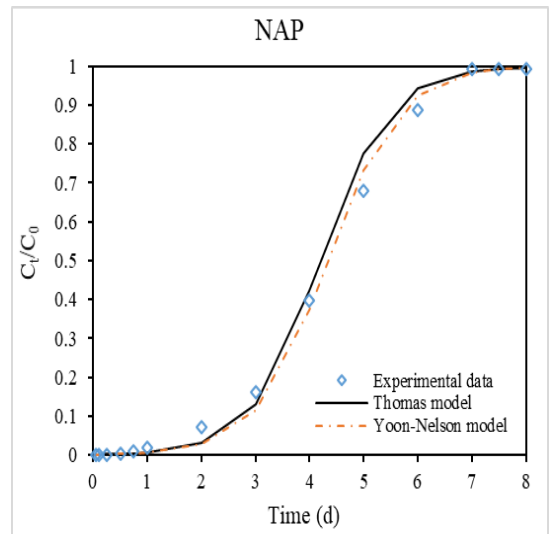
The Thomas equation is a two-parameter neutralisation that has a kinetic constant (k_{th}). From Table 3-4, it can be seen that the k_{th} value increased at higher flow rates but decreased at higher adsorbent mass or bed height, indicating that the mass transfer resistance reduces and, proportionally, the pivotal dispersion and fluid-film thickness on the surface of particle also decrease (Jaria et al., 2019). Similar observations were found by de Franco et al. (2018) that reported higher k_{th} values at lower adsorbent for the adsorption of the diclofenac onto the GAC. Sotelo et al. (2013) also found lower k_{th} values at lower flow rates for a fixed-bed column of flumequine by activated carbon. Thus, it could be supposed that the high flow rates increased the driving strength of the mass transfer in the liquid film. In addition, the maximum adsorption capacity for the micropollutants has been calculated using Thomas model (q_0) the predicted values were somewhat similar to experimentally calculated values in Table 3. Results showed that the maximum capacity (q_0) of micropollutants decreased in the following order: CBZ > NAP > IBP \approx APAP > MTZ similar to the trend reported earlier in 3.1.1 Influence of flow rate, 3.1.2 Influence of adsorbent mass. However, the value of q_0 decreased when a larger adsorption bed height was used. The regression coefficient R^2 values of the Thomas kinetic model are 0.95, 0.96, 0.95, 0.92, and 0.96 for CBZ, NAP, IBP, APAP, and MTZ, respectively, in Figure 3-3, indicating good agreement with the empirical results.

Regarding the Yoon-Nelson model, it assumes the predicted time required to reach 50% of micropollutant breakthrough ($t_{pred.50\%}$). As can be seen in Table 3-4, the value of the model parameter of $t_{pred.50\%}$ increased at a higher adsorbent mass but decreased at a higher flow rate. With an increase in the flow rate from 1.15 to 4.32 L/d, the estimated $t_{pred.50\%}$ values decreased from 4.59-2.90 to 1.20-0.375 (day), respectively, close to the experimental calculated values in Table 3-3. The value of rate constant K_{yn} , however, increased at a higher flow rate but decreased at a higher adsorbent mass as shown in Table 4. Figure 3-3 shows the breakthrough curve of the Yoon-

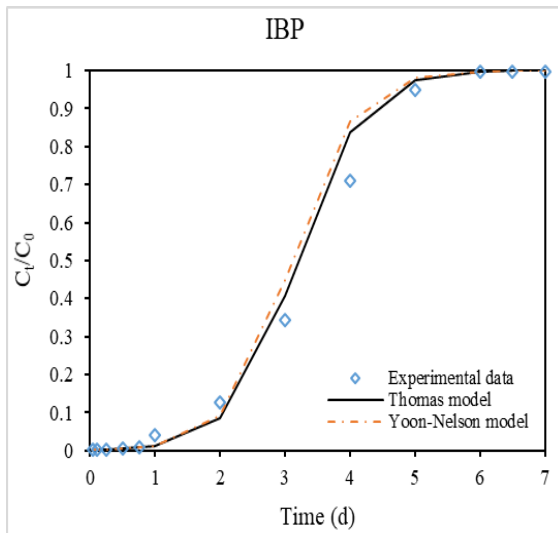
Nelson model fitting with the experimental data, as well as high Yoon-Nelson regression coefficients R^2 values, which are 0.95, 0.96, 0.95, 0.92, and 0.96 for CBZ, NAP, IBP, APAP, and MTZ, respectively. Therefore, the outcomes presented in Table 3-4 indicate that the Thomas and Yoon-Nelson models are suitable for predicting the breakthrough curves for pharmaceutical adsorption onto GAC in the fixed-bed column.



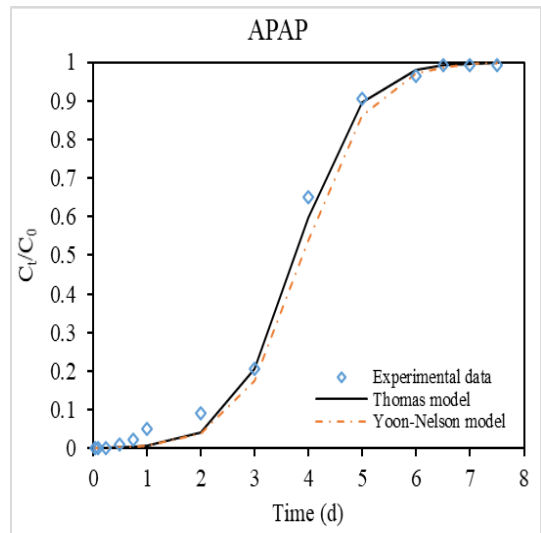
(a)



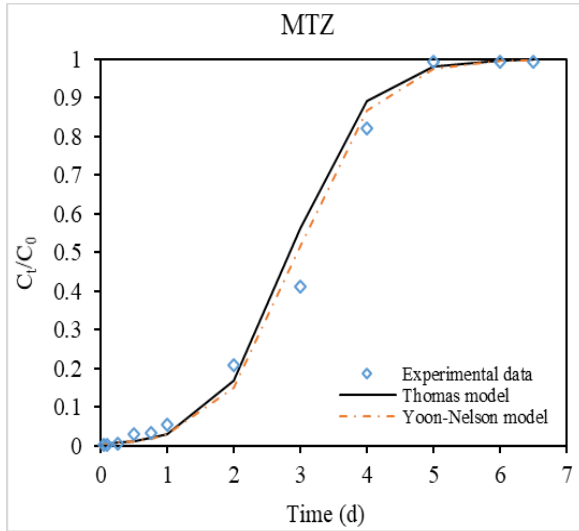
(b)



(c)



(d)



(e)

Figure 3-3 Modelling breakthrough curve for fixed- bed adsorption of pharmaceuticals onto GAC

($Q = 1.15$ L/d; $C_0 = 0.2$ mM and $m = 4.0$ g).

Table 3-4 Thomas and Yoon-Nelson models parameters for pharmaceuticals adsorption by GAC on fixed-bed column.

k_{yn} (Yoon-Nelson rate constant), $t_{pred.50\%}$ (the predicted time required to reach 50% of micropollutant breakthrough), q_0 and (theoretical adsorption capacity) and k_{th} (Thomas model rate constant).

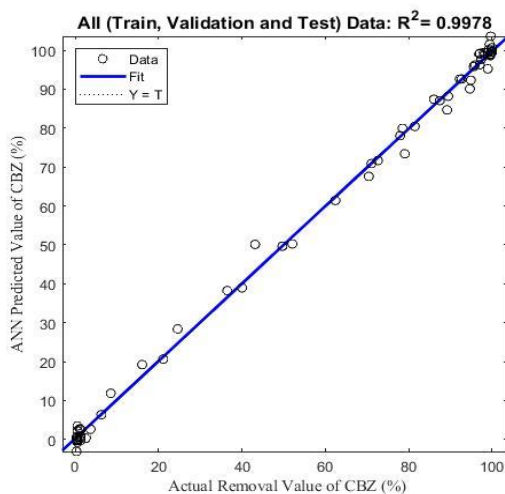
Pharmaceuticals	Experimental conditions		Thomas model			Yoon-Nelson model		
	Flow rate (L/d)	Mass (g)	q_0 (mg/g)	K_{th} (L/d/mg)	R^2	$t_{pred.50\%}$ (d)	K_{yn} (d ⁻¹)	R^2
CBZ			69.22	0.025	0.95	4.59	1.35	0.95
NAP			59.01	0.029	0.97	4.13	1.50	0.97
IBP	1.15	4	39.59	0.045	0.95	3.23	1.93	0.95
APAP			37.74	0.046	0.92	3.81	1.63	0.92
MTZ			31.08	0.050	0.96	2.98	1.86	0.96
CBZ			61.31	0.051	0.98	2.07	2.35	0.98
NAP			52.07	0.049	0.94	2	1.96	0.94
IBP	2.59	4	29.23	0.095	0.90	1.3	2.4	0.90

Pharmaceuticals	Experimental conditions		Thomas model			Yoon-Nelson model		
	Flow rate	Mass	q_0	K_{th}	R^2	$t_{pred.50\%}$	K_{yn}	R^2
	(L/d)	(g)	(mg/g)	(L/d/mg)		(d)	(d ⁻¹)	
APAP			32.95	0.094	0.92	1.6	2.68	0.92
MTZ			22.13	0.10	0.94	1.08	2.88	0.94
CBZ			53.03	0.10	0.94	1.1	4.03	0.94
NAP			47.52	0.1	0.95	0.94	4.58	0.95
IBP	4.32	4	28.58	0.13	0.93	0.64	5.71	0.93
APAP			27.41	0.14	0.91	0.83	4.53	0.91
MTZ			14.08	0.23	0.93	0.37	8.08	0.95
CBZ			54.16	0.018	0.92	6.07	1	0.92
NAP			45.04	0.020	0.96	5.50	0.89	0.96
IBP	1.15	6	36.93	0.024	0.95	4.85	1.07	0.95

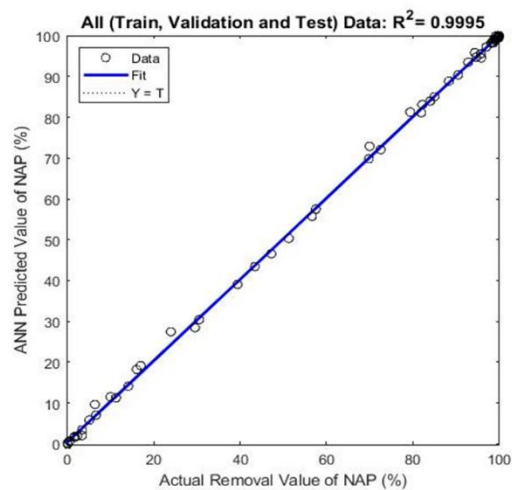
Pharmaceuticals	Experimental conditions		Thomas model			Yoon-Nelson model		
	Flow rate	Mass	q_0	K_{th}	R^2	$t_{pred.50\%}$	K_{yn}	R^2
	(L/d)	(g)	(mg/g)	(L/d/mg)		(d)	(d ⁻¹)	
APAP			33.41	0.036	0.97	5.25	0.8	0.97
MTZ			27.95	0.34	0.94	4.1	1.1	0.94
CBZ			48.67	0.013	0.98	11.1	0.64	0.98
NAP			42.06	0.014	0.97	10.3	0.62	0.97
IBP	1.15	12	32.74	0.017	0.96	8.9	0.68	0.96
APAP			26.94	0.024	0.95	9.8	0.82	0.95
MTZ			22.65	0.023	0.90	7.8	0.78	0.90

3.4.3 Modelling of Pharmaceuticals removal using ANN

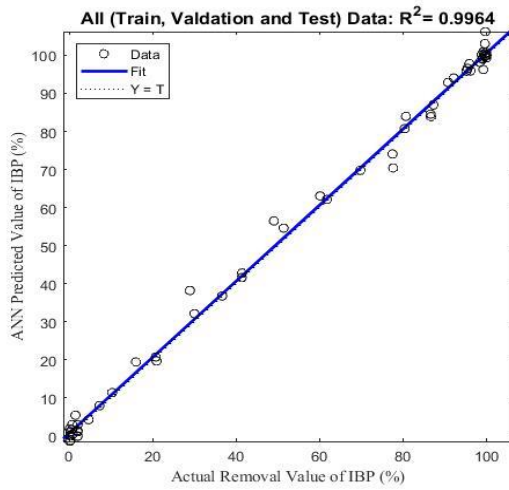
The results point out that the topologies of 3-12-1, 3-16-1, 3-16-1, 3-5-1, and 3-12-1 pointing out 12, 16, 16, 5, and 12 neurons in hidden layers were the best fit for CBZ, NAP, IBP, APAP and MTZ models, respectively. The determination coefficients for all (training, validation, and testing) provided good performance for the models in the forecast of the outputs (Figure S3-2-S3-6). Figure 3-4 shows the values of R^2 for all data of the evolved models, which were 0.997, 0.999, 0.996, 0.844 and 0.995 for CBZ, NAP, IBP, APAP and MTZ, respectively. Furthermore, Figure 3-5 shows residual errors from the established models. As noted the MSE of the models were respectively, 3.92, 0.913, 6.54, 276.158 and 7.95 for CBZ, NAP, IBP, APAP and MTZ that are negligible. The evolved models, therefore, can foresee the effectiveness of the removal of the CBZ, NAP, IBP, APAP and MTZ from urine solutions with 99.7%, 99.9%, 99.6%, 84.5% and 99.5% respectively.



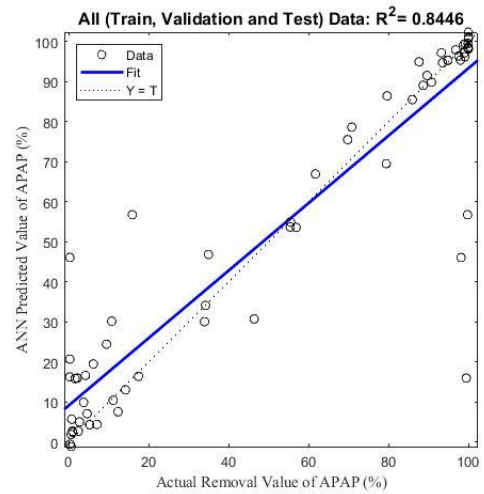
(a)



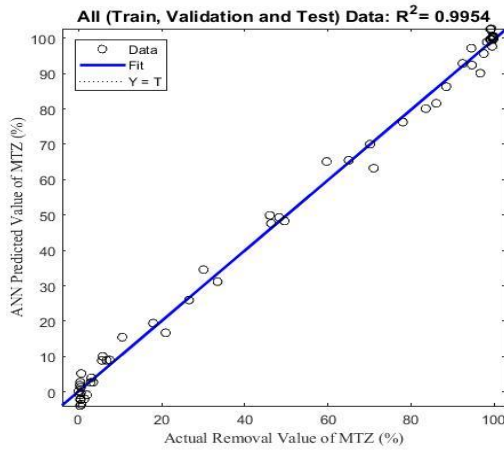
(b)



(c)



(d)



(e)

Figure 3-4 Elucidation the experimental and ANN predicted data for all three phases of (a) CBZ, (b) NAP, (c) IBP, (d) APAP and (e) MTZ removal models.

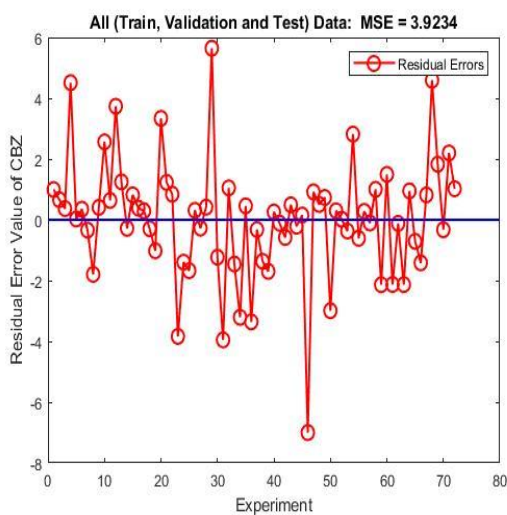
Equation (9) shows the prediction for the removal of all micropollutants using the ANN models.

The values of the weights and biases for five micropollutants are displayed in Tables (S3-2-S3-6):

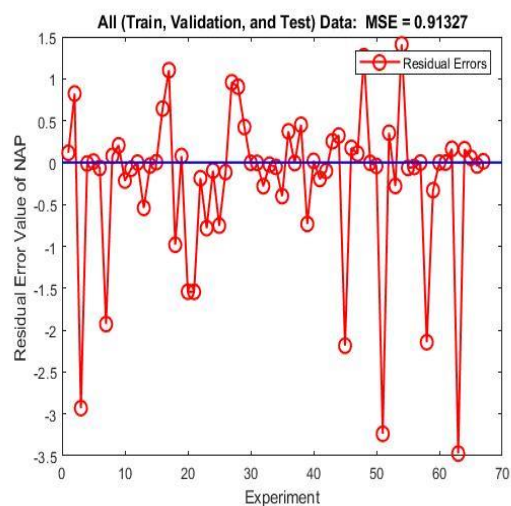
$$ANN \text{ equation} = \text{Purelin}(LW \times \text{tansing}(IW \times [\text{contact time}; \text{adsorbent mass}; \text{flow rate}]b1) + b2)$$

As shown in Figure 3-5, the residual error distribution was very low in the prediction of CBZ, NAP, IBP and MTZ, whereas the residual errors of APAP model in which five experimental results

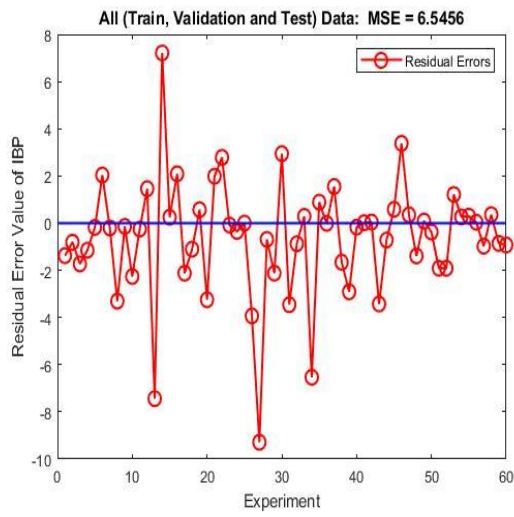
could not fit very well with the developed model. As mentioned in other studies, the results of these modelling procedures can be different in various applications and the nature of the data are very important in this regard; therefore, it can be attributed to the mentioned reasons (Hosseinzadeh et al., 2020a; Hosseinzadeh et al., 2020c). Nevertheless, all of the other 78 data sets from 83 ones could mimic very well with the model and demonstrated very low errors (Figure 3-5). In a way that the additional test for APAP removal model indicted better performance in Figure 3-6 with $R^2 = 0.934$ and MSE 73.36, it means that the mentioned five actual data, which increase the residual errors of the model and decline the R^2 of the model, could not generally decrease the performance of the developed model. Furthermore, as APAP, the additional tests were accomplished for other four compounds' models with 20% of the experimental data as well. As observed in Figure 3-6, the R^2 and MSE of the additional tests for the CBZ, NAP, IBP and MTZ models are (0.986, 0.914, 0.995 and 0.958) and (3.427, 1.746, 3.27 and 6.41) correspondingly.



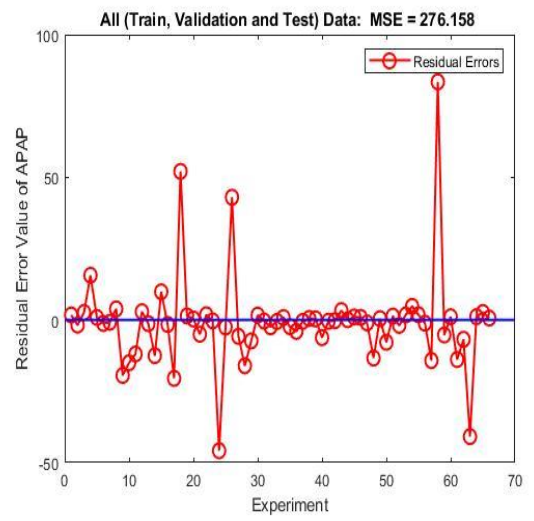
(a)



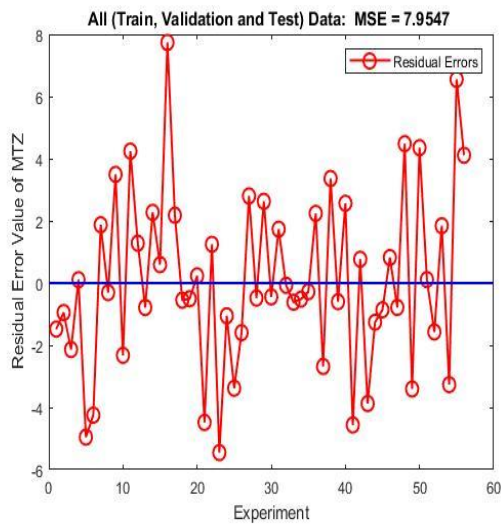
(b)



(c)

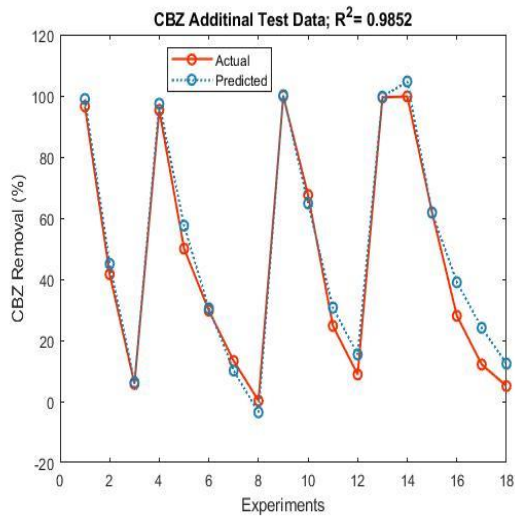


(d)

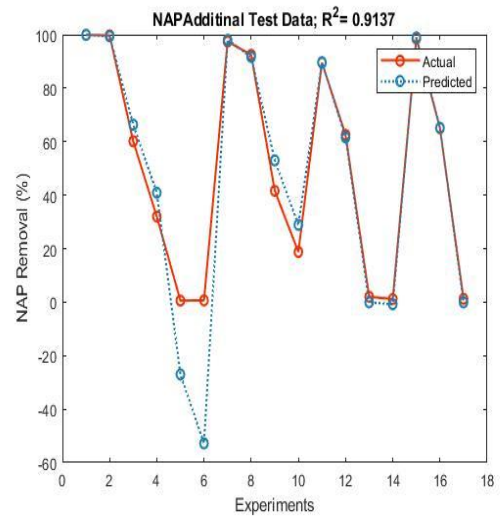


(e)

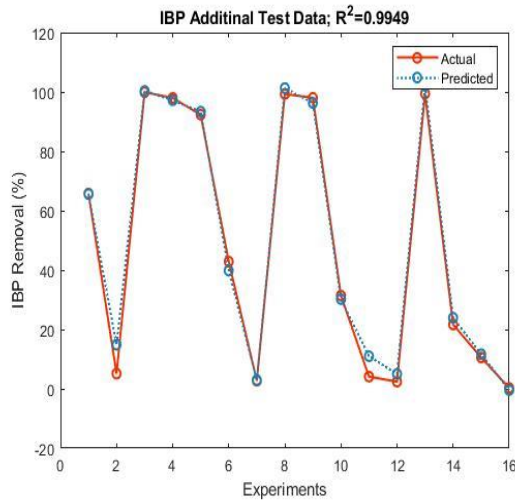
Figure 3-5 Illustration the residual errors of the evolved ANN models for (a) CBZ, (b) NAP, (c) IBP, (d) APAP and (e) MTZ.



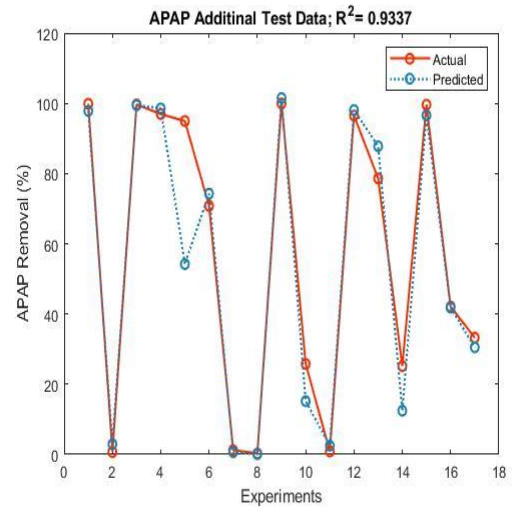
(a)



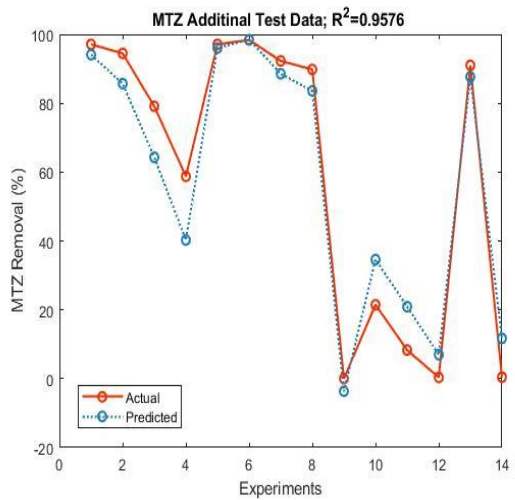
(b)



(c)



(d)



(e)

Figure 3-6 Elucidation the experimental and ANN predicted data for additional tests of (a) CBZ, (b) NAP, (c) IBP, (d) APAP and (e) MTZ removal models.

Previous studies reported that ANN models can predict pharmaceutical adsorption with high accuracy. Almuntashiri et al. (2021) predicted the removal of ibuprofen, naproxen, metronidazole, acetaminophen, and carbamazepine via the developed ANN models, which feature R^2 values of 0.984, 0.991, 0.991, 0.99, and 0.992, respectively. In addition, the high prediction and strength of ANN models were reported in other studies in various applications. Hosseinzadeh et al. (2020b) found that the ANN models were able to foresee experimental and predicted values of nutrient recovery from solid waste by vermicomposting with high accuracy of 0.99. The results of Hosseinzadeh et al. (2018) indicated the high accuracy of ANN models in predicting levels of benzene, toluene, xylene and ethyl-xylene from polluted airstreams in non-thermal plasma, as compared to response surface models. Due to the high accuracy and prediction of ANN models, such models are projected to be employed effectively in predicting pharmaceuticals removal.

3.4.4 Adsorption of pharmaceuticals onto GAC

GAC characteristics are very important in determining the adsorption capacity of different micropollutants (e.g., surface area, specific surface area, porosity and pore size distribution, etc.). Most of the adsorption process occurs when the macro-pores act as paths for the adsorbate to reach micro-pores. On the other hand, the acidity constant (pK_a) and octanol-water partition coefficient (K_{ow}) of these micropollutants could have a fundamental effect on the ratio and level of adsorbent adsorption (Sotelo et al., 2014); consequently, all properties have been documented in earlier literature reviews.

Based on the literature, hydrophobicity is a valuable factor in evaluating the sorption capacity of pharmaceuticals, which affects the sorption capacity of pharmaceuticals on the adsorbent, as expressed by $\log K_{ow}$. The $\log K_{ow}$ values of the five compounds ranked in decreasing order are IBP, NAP, CBZ, APAP and MTZ. NAP, however, displayed relatively less adsorption affinity

compared to CBZ, results similar to those observed by Yu et al. (2008) and Westerhoff et al. (2005), who applied various dosages of activated carbon in pure water spiked with micropollutants. This is due to the dissociation of the acid at values of pH (6.4–8.2), which was noted in these studies.

The pK_a of pharmaceuticals varies according to their molecular structure. Ionisable compounds might manifest either as anions or cations based on their pH in the aqueous solution. Additionally, the surface charge of GAC has an important role in the removal process. Zeta potential, that measures the charge of external surface for the GAC enhances the understanding of how the adsorption process occurs (Sotelo et al., 2013). The surface charge of the GAC, therefore, possesses an oscillating character that could have either a negative or positive charge depending on pH values, thereby resulting directly in an effect regarding electrostatic interactions (Almuntashiri et al., 2021; Calisto et al., 2015). Consequently, when the value of pH is lower than the point of a zero-charge pH_{PZC} value, the surface of the GAC is positively charged and hence favours absorbing the anionic compounds, and vice versa. The value of the pH_{PZC} of the GAC was determined to be pH 4.8 in our previous study (Almuntashiri et al., 2021). This shows that the surface of the GAC possessed a negative charge during the adsorption mechanism because the pH_{PZC} value was less than the pH of the hydrolysed urine.

In our study, the five active pharmaceutical compounds have been divided into two groups based on their pK_a values compared to the pH of the aqueous solution (pH ~ 9) as shown in the Table 3-1. NAP and IBP possessed negative charges, while CBZ, APAP and MTZ possessed neutral charges. Although both NAP and IBP being negatively charged in the urine matrix are expected to experience electrostatic repulsion with the negatively charged GAC surface however, their high removal rates indicates the less role of the electrostatic interactions. Their interaction with the GAC surface might be because of other interactive forces such as π - π bonding, H-bonding, van der Waals forces, etc. that might have contributed to their removal (Jamil et al., 2019) which needs further studies to understand its actual removal mechanism.

On the other hand, CBZ, APAP and MTZ are neutral in the urine matrix, and are therefore expected to exhibit more electrostatic interactions with a negative charge on the GAC surface compared to NAP and IBP. The results showed that MTZ was the least adsorbed in the fixed-bed column compared to other micropollutants. From this, it can be deduced that MTZ adsorption onto GAC is probably fundamentally physio sorption with a pH range of 4–11 (Rivera-Utrilla et al., 2009; Sotelo et al., 2014). In contrast, CBZ exhibited the highest sorption affinity to the GAC surface due to the fact that physicochemical properties such as the pKa described above and high molecular weight play an important role in the adsorption processes (Ahmed, 2017; Sotelo et al., 2014).

Human urine can contain hundreds or even thousands of different types of pharmaceuticals and at wide ranging concentrations and this column adsorption study has shown that depending on their properties such as physio-chemical properties, molecular weight, surface charges, pKa values, etc. their removal mechanism, breakthrough curve and their maximum removal rates (Jamil et al., 2019) by GAC adsorption can also vary significantly. The breakthrough curve results of the five studied pharmaceuticals indicates that the GAC column can be saturated much earlier for certain pharmaceutical (e.g. MTZ) than the other pharmaceuticals that can have a significant impact on the process design and the capital costs. These results also show that the designer must consider options such as multiple column (different adsorbent in each column) adsorption or multi-adsorbent column (different adsorbent mixed as multi-sorption media) in order to optimise both the removal effectiveness and their costs. While the former option can be simulated, using the empirical breakthrough models (Thomas model and Yoon Nelson model) applied in this study however, the second option will need further studies using different adsorbent media targeting those micropollutants that are less adsorbed and removed by GAC.

3.5 Conclusion

A fixed-bed GAC column adsorption was studied for the removal of five selected pharmaceuticals from hydrolysed urine (synthetic). The GAC column study revealed that adsorbent mass and flow rate influenced both breakthrough point and saturation time. A higher flow rates led to a quicker breakthrough resulting in the faster saturation and exhaustion of the adsorbent. A smaller bed height resulted in faster breakthrough time and lower volume for urine treatment. The adsorption affinity of the micropollutants were as follows $CBZ > NAP > AAP > IBP > MTZ$ indicating for GAC column adsorption application, MTZ would be the limiting micropollutants in the adsorption column design amongst the five studied micropollutants. This study showed that the GAC adsorption of pharmaceuticals depends on their physicochemical properties, $\log K_{ow}$ and molecular weight. The Thomas model fitted well in describing the empirical breakthrough curves by GAC column adsorption while the Yoon Nelson model described well for 50% of the column saturation time under the operation conditions tested in this study. The ANN models employed were capable to estimate the empirical and predicted values of pharmaceuticals removal from hydrolysed urine very effectively. This study has shown that GAC column adsorption can be highly effective in the removal of micropollutant from the hydrolysed urine. However, it must be acknowledged that this study was not extensive in the range of performance parameters tested such as GAC properties, types of pharmaceuticals and concentration range, GAC regeneration capacity, etc., which must be considered for future studies including the impact of competing organics such as creatinine and the regeneration capacity of the GAC adsorbent.

Acknowledgements

This study was supported by the Bhutan trust Fund for Environmental Conservation (Project Grant No No. MB0167Y16, UTS Cross - faculty collaboration scheme (PRO21-12519) and the Saudi Arabian Cultural Mission in Australia (SACM) for PhD scholarship of Abdulaziz Almontashiri.

CHAPTER 4 Removal of pharmaceuticals from nitrified urine

4.1 Abstract

Building on the previous chapter's findings, this chapter addresses the second objective of this thesis, which involves pharmaceutical compound removal from synthetic nitrified urine. This represents a more advanced stage, where urine has undergone a biological nitrification process. In this study, granular activated carbon (GAC) was examined for the removal of five of the most detected pharmaceuticals (naproxen, carbamazepine, acetaminophen, ibuprofen and metronidazole) from a nitrified urine to make the urine-derived fertiliser nutrient safe for food crops. Batch experiments were conducted to investigate the adsorption kinetics that described the removal of micropollutants (equal concentrations of 0.2 mM) from the synthetic nitrified urine at different GAC dosages (10 – 3,000 mg/L). Artificial neural network modelling was also used to predict and simulate the removal of pharmaceuticals from nitrified urine. Langmuir and Freundlich isotherm models described the equilibrium data, with the Langmuir model providing slightly higher correlations. At the highest dose of 3,000 mg/L GAC, all the pharmaceuticals showed a removal rate of over 90% after 1 hour of adsorption time and 99% removal rates after 6 hours of adsorption time. This study concludes that GAC is able to remove the targeted xenobiotics without affecting the concentration of N and P in the urine, suggesting that nitrified urine could be safely used as a nutrient product in future, supporting with the overarching thesis objective of sustainable nutrient recovery.

Keywords: Micropollutants; Granular activated carbon; Nitrified urine; Adsorption; Modelling

4.2 Introduction

Approximately \$325.8 billion were spent in the USA on pharmaceutical products in 2012 alone (Zhang et al., 2015). Most pharmaceuticals are processed through the human body and excreted as metabolites in the faeces or urine, meaning they end up in the sewage system and finally at the sewage treatment plant. Estimations made by Lienert et al. (2007) suggest that around 64% of active ingredients in the pharmaceuticals are excreted together with the urine and the rest with the faecal matter. The biggest problem with this is that most existing wastewater treatment plants (WWTPs) are unable to remove all the micropollutants from the wastewater (Zhang et al., 2015). This means that vast quantities of micropollutants are released into the environment, which can significantly impact on the quality of land and soil fertility, as well as aquatic life and marine ecosystems.

Source-separation of urine is a novel approach that is attracting more and more attention in an effort to recover and recycle nutrient to enhance the circular economy of nutrients. Diverting urine from the wastewater is considered a promising alternative to decrease the overall loading of pharmaceuticals and nutrients in the WWTPs. Since urine contributes more than 80% of the total nitrogen and 50% of phosphorus present in wastewater (Badeti et al., 2021; Volpin et al., 2018), diverting urine not only reduces the nutrient load to the WWTPs but can also help recover and reuse as a valuable source of fertiliser to grow food again (Volpin et al., 2020b). Thus, the recovery of nutrients from the urine stream directly could be more economical and sustainable than the fresh fertiliser produced using natural resources most of which are depleting (Maurer et al., 2003). Several studies on the biological and physio-chemical techniques have been reported for the nutrient recovery from source separated urine such as combined forward osmosis-membrane distillation systems, nitrification-denitrification, ammonia stripping, etc. (Etter et al., 2014; Volpin et al., 2019). Even though these technologies are able to recover nutrients from the urine however, there is still concern about the existence of pharmaceuticals in the recovered nutrients from the urine.

Many researchers have tested methods of removing pharmaceuticals from urine. Sun et al. (2018) investigated the adsorption of four parent sulfonamide antibiotics on biochar/ H₂O₂ combination. It was found that the removal of sulfadimethoxine, sulfamethazine, Sulfamethoxazole, and sulfadiazine present in hydrolysed urine were 71%, 74%, 49%, and 39% respectively using 1 g/L dosage of the adsorbent. Dodd et al. (2008) tested an advanced oxidation process using ozone, and Zhang et al. (2015) used UV and H₂O₂ combinations. Both the studies found that pharmaceuticals could only be partially removed because the oxidants reacted with other compounds present within the urine. de Wilt et al. (2016) tested the elimination of micropollutants through biodegradation and photolysis with algae growth and recovered nutrients from the biomass. They found that they were able to remove high levels of metoprolol, paracetamol, and diclofenac (60-100%), and to partially remove trimethoprim and carbamazepine (30 and 60% respectively). Other studies investigated the removal of pharmaceuticals using membranes. For example, Pronk et al. (2006) discovered that more than 90% of pharmaceuticals and PO₄-P in fresh urine were rejected by Nano-filtration (NF) membranes. This means that a further process was required to separate micropollutants from the PO₄-P as both are present as NF brine. The use of microfiltration or electrodialysis as a pre-treatment step to the nanofiltration process resulted in a high level of pharmaceutical removal although the process is complex (Pronk et al., 2007). Moreover Landry and Boyer (2013) explored the impacts that pharmaceutical adsorption had on the resins of anion exchange polymers and observed that there were undesirable side-effects including the concomitant desorption of chloride.

Granular activated carbon (GAC) is widely used to eliminate natural or synthetic organic micropollutants from water (Delgado et al., 2012). There are many advantages of using adsorption processes for micropollutant removal. Firstly, adsorption process has much lower energy consumption compared to other processes such as oxidation methods, membrane processes, etc. Secondly, the adsorption process can be used either as a batch process or as a continuous process and are relatively inexpensive and can be regenerated for reuse by thermal methods (Mohanty et

al., 2006). Furthermore, there are various reactor configurations that can be used for adsorption, such as mixed slurry or fixed bed configurations, and it is possible to apply GAC in convenient filter beds to facilitate potential reactivation and reuse (Crittenden et al., 1999). Experimental analysis of all the different micropollutants for their removal from the municipal wastewater is both time consuming and highly expensive. But modelling and simulating the impacts of specific operating conditions on micropollutants removal is one approach of cost-effectively predicting removals thereby significantly helping reduce operation times and analytical costs (Hosseinzadeh et al., 2020b). Furthermore, a review of research indicates that there are limited modelling studies about pharmaceuticals removal process from source separate urine stream.

Therefore, the main objective of this study is to evaluate the removal of pharmaceutical compounds from the nitrified urine by GAC adsorption including understanding their adsorption kinetic and apply predictive modelling using artificial neural network (ANN). ANN modelling can learn the linear and nonlinear relationships between dependent and independent variables in a set of examples using strong algorithms. In other words, ANN can model and simulate various types of processes without fully understanding their complex nature, background, and mechanisms. Many studies have shown the ANN procedure is highly efficient in modelling and hence ANN modelling has been applied in this study (Hosseinzadeh et al., 2020c). Our hypothesis is that, removing micropollutants from the nitrified urine by GAC adsorption is much easier than their removal from the fresh urine or hydrolysed urine. The urea in the urine is hydrolysed due to the urease enzyme converting into ammonia/ammonium and bicarbonate which increases the pH of the urine. This hydrolysed urine is treated by a membrane bioreactor (MBR) at pH 6.2 via a combination of a biological nitrification and an ultrafiltration (UF) membrane. Nitrification is a process of biological oxidation by which $\text{NH}_4^+\text{-N}$ is converted into $\text{NO}_2^-\text{-N}$ by ammonia oxidizing bacteria (AOB). The $\text{NO}_2^-\text{-N}$ is further oxidized to $\text{NO}_3^-\text{-N}$ by nitrite oxidizing bacteria (NOB), and during this biological nitrification process, about 95% of dissolved organic carbon (DOC) in the urine is removed (Figuerola & Erijman, 2010; Volpin et al., 2020b). The urine MBR effluent is therefore termed as nitrified urine, which is a much more stable form of N in urine and

contains very low dissolved organic matter. This technique has been recently suggested as an innovative means to remove the pharmaceuticals from industrial and wastewater (Caluwé et al., 2017). The results obtained by the MBR system were appropriate for removing pharmaceuticals (e.g., >95% removal rate for atenolol, enalapril, and risperidone). However, further treatment is essential for the maximum removal of all sorts of micropollutants present in urine because MBR is not effective in removing some of the pharmaceuticals. For example, removal rates for metronidazole, naproxen, and acetaminophen are lower than 50% (Hai et al., 2011b; Tadkaew et al., 2011), as shown in Table 4-1. Synthetic nitrified urine has been therefore used in this study that simulates the MBR effluent from a nitrified urine. Although GAC has been used for the removal of micropollutants from the nitrified urine in one study so far (Köpping et al., 2020), however, to the best of our knowledge, GAC adsorption kinetics and ANN predictive modelling of micropollutants in the nitrified urine has not yet been reported.

Table 4-1 Removal of micropollutants by biological treatment

Chemical compounds	Removal by MBR %	References
Acetaminophen	40 – 50	(Hai et al., 2011b)
Carbamazepine	9-35	(Hai et al., 2011a; Tadkaew et al., 2010)
Ibuprofen	75	(Tadkaew et al., 2010)
Metronidazole	<40	(Hai et al., 2011b)
Naproxen	<50	(Tadkaew et al., 2010)

4.3 Materials and methods

4.3.1 Pharmaceuticals and adsorbent

Carbamazepine, naproxen, acetaminophen, ibuprofen and metronidazole were purchased from Sigma Aldrich, Australia. A set of five pharmaceutically active compounds are selected according to their molecular structure, widespread occurrence in urine and diverse physicochemical

properties (e.g. molecular size and hydrophobicity) as well as high percent of their excretion from human urine ranging (60-90%) as shown in Table S4-1 (supporting information). The stock solutions for each pharmaceutical were prepared by dissolving in 100% methanol solution since these pharmaceuticals have low solubility in water. Each of the micropollutant was spiked into the synthetic nitrified urine at initial concentration of 0.2mM for more accurate analysis of pharmaceuticals in the urine samples. The adsorbent used was a commercial GAC, supplied by James Cumming & Sons Pty Ltd., Australia. The adsorbent was dried at 90 °C for 24 hr in thermostatic oven before adsorption. The physical properties of GAC are shown in Table S2. The composition of the synthetic nitrified urine along with the pharmaceuticals used for all the experiments in this study are listed in Table 4-2 (Etter et al., 2014).

Table 4-2 Compositions of synthetic nitrified urine.

Compositions	Quantity
NH ₄ NO ₃	19.2 g
NaH ₂ PO ₄	2.7 g
KCl	3.4 g
KHCO ₃	1.1 g
Na ₂ SO ₄	2.3 g
NaCl	3.6 g
HCl 32%	0.4ml

4.3.2 Batch adsorption experiments

Batch experiments were conducted to investigate the removal of pharmaceuticals and nutrients by GAC adsorption. For the kinetic study, a set of five pharmaceuticals with various GAC doses (10, 25 80, 800, 1500 and 3000 mg/L) were added to 125 mL of synthetic nitrified urine in conical flasks. For isotherm study, one more GAC dose, 160 mg/ L, was added to provide more reliable adsorption data. All the conical flasks were placed on a mechanical shaker table at 200 rpm for 4

days to provide enough contact time to reach equilibrium. Moreover, the flasks were wrapped with aluminium foil to avoid photolysis. All samples were then directly filtered using 0.45 μm cellulose esters filters and stored in glass bottles at 4 $^{\circ}\text{C}$ prior to their analysis. Both Langmuir and Freundlich linear models were employed in the present study to explain the pharmaceuticals' adsorption equilibrium. The adsorption isotherm equations discussed in supplementary materials and also summarised in Table S3. The amount of micropollutants adsorbed by the GAC at any time (t) was determined as follows:

$$q_e = \frac{V(C_0 - C(t))}{m} \quad (1)$$

here, q_e is the instantaneous mass of adsorbed pollutants ($\mu\text{mol/g}$) over a unit mass of adsorbent, V stands for the volume of the solution (L), C_0 and $C(t)$ are the initial and instantaneous concentrations ($\mu\text{mol/L}$) of the micropollutants, and m is the mass of the GAC dosed into the solution.

4.3.3 ANN Modelling

A feed-forward ANN model was employed using MATLAB R2018b to simulate the pharmaceuticals removal from the nitrified urine by GAC adsorption process. When designing the model and its structure, the number of neurons that would be included in the input and output layers was determined based on how many input and output variables were involved. The GAC dose and contact time were considered as the input variables for the models, whereas the percentage removal of the micropollutants was taken as the output variable. Using (Eq. 2), all of the input and output data were normalized between 0.1-0.9 for the stable convergence of the weight and bias of the network (Hosseinzadeh et al., 2018):

$$\text{Normalized value } (X_i) = \frac{X_i - X_{\text{max}}}{X_{\text{max}} - X_{\text{min}}} \times (0.9 - 0.1) + 0.1 \quad (2)$$

where X_{min} and X_{max} are the minimum and maximum values of the input or output of the network, whereas X_i is any input or output value of the range.

Multiple neural networks were created by varying the number of neurons from one to twenty in the hidden layers to ensure the minimum error in the simulation. To analyse the accuracy of the models during the training, validation and test stages, the determination coefficient (R^2) (Eq. 3) and mean square error (MSE) (Eq. 4) were calculated and subsequently used as statistical indices to decide which model was the best (Hosseinzadeh et al., 2020b).

$$R^2 = 1 - \frac{\sum_{i=1}^N (y_{prd,i} - y_{Act,i})}{\sum_{i=1}^N (y_{pr,i} - y_m)} \quad (3)$$

$$MSE = \frac{1}{N} \sum_{i=1}^N (y_{pr,i} - y_{Act,i})^2 \quad (4)$$

where $I_{Act,i}$ is values of actual experimental. $y_{prd,i}$ represent the values of predicted ANN model. N represents the total number of data; and y_m represents the mean of experimental value.

During the modelling process, 60 datasets for each micropollutant (300 datasets for all five micropollutants) was divided into two groups, the first of which consists of 80% data. In this group, 70%, 15% and 15% data were employed, for training, validation and test, respectively. The remaining 20% was used to carry out an additional test.

Levenberg-Marquardt algorithm was used to train the network until it approximates a model associating the input and output of the process. According to this algorithm, the weights and biases of the network are iteratively updated to minimize the error which is given by,

$$X_{k+1} = X_k - [J^T J + \mu I]^{-1} J^T e \quad (5)$$

where, X_k is the current weight and bias of the network, whereas X_{k+1} are the updated values of the parameters. Besides, e is the network error, J represents the jacobian matrix of the errors, μ is a scaler whose value is reduced by the steps of the iteration, J^T represents the transpose of the error

matrix, and I is the identity matrix.

Moreover, in the output layer, a linear transfer function was employed and a tangent sigmoid transfer function was used in the hidden layers. The tangent sigmoid transfer function constrains the output within a range of -1 to +1 employing the following model in (Eq. 6):

$$a = \frac{2}{(1 + e^{-2n})} - 1 \quad (6)$$

where a and n are the input and output of neurons of the hidden layer.

Finally, the MSE values were worked out through the MSE equation (2-4) (Hosseinzadeh et al., 2020c). Neurons with diverse numbers between 1 and 20 in the hidden layer were investigated to determine the most effective number of neurons to apply. Besides, five replications were carried out during all three stages of the process (training, validation and testing) to ensure that there were no errors and to enhance the accuracy of estimations of the network weights and output predictions.

4.3.4 Micropollutant compounds and nutrients analysis

The micropollutants were concentrated by solid-phase extraction (SPE) using Oasis MCX 3 cc Vac Cartridge (60 mg Sorbent per Cartridge, 30 μ m). The analysis involved liquid chromatography with mass spectrometry (LCMS-8060 Shimadzu), supplied with a CORTECS C18+ Column, 2.7 μ m, 2.1 mm X 75 mm (Waters). The ionisation worked on ESI mode. The ESI positive mode was applied for the analysis of carbamazepine, acetaminophen, and metronidazole, while the ESI negative mode was applied for ibuprofen and naproxen. All the analytes were detected simultaneously. Mobile phase A was Milli-Q water and mobile phase B was 100% methanol. The gradient elution was conducted at a persistent flow rate (0.6 mL/min) as follows: the mobile phase B was kept at 50% (0.01-0.10 min), augmented to 95% (0.10–1.50 min) and kept at 95% (1.50-3.50 min), and then reduced to 50% (3.51–5.50 min). The multiple reaction modes (MRMs) selected for the analytes were: acetaminophen (152 > 110, ES+), metronidazole (172 > 128, ES+), carbamazepine (237 > 194, ES+), ibuprofen (205 > 161, ES-), naproxen (229

> 185, ES-). Individual calibration curves were made for each micropollutants at different concentrations of 1, 5, 10, 50, 100, 1000, and 5,000 nM the coefficient of determinations (R^2) were more than 0.999. To evaluate the loss of micropollutants during the extraction processes, the recovery ratio, which is the ratio of the peak areas before and following the extraction, was used. The final concentration was then calculated by multiplying the measured concentrations with the obtained recovery ratio. TN and PO₄-P concentrations were measured by colorimetric analysis (Merck 214 KGaA, Darmstadt, Germany) using a spectrophotometer (Spectroquant NOVA 60).

4.3.5 Analyzing the zeta potential for GAC

Zeta potential is the electric potential nearby particles' surfaces where ions or ionic compounds from samples are absorbed and are then correlated to charge the surface. Samples of 800 mg/L GAC in deionised water were prepared at different pH (2 – 12), which were adjusted by 0.1 M HNO₃ or 0.1 M NaOH solutions. The samples were placed in a mechanical shaker table for 24 h at 200 rpm, followed by measuring the final pH. Zeta potential was analysed using the Zetasizer nano device (3600, Malvern, UK).

4.4 Results and discussions

4.4.1 Micropollutant removal by GAC adsorption

The GAC dose and contact time play a significant role in the micropollutant removal from any aqueous phase and their adsorption kinetics. Figure 4-1 shows the variations of the micropollutant normalised effluent concentrations (naproxen, carbamazepine, acetaminophen, ibuprofen and metronidazole) in the nitrified urine effluent with adsorption time at different GAC doses.

Figure 4-1 (a-b) shows the decrease in the normalised effluent concentrations (C_i/C_0 : ratio of effluent concentration to the initial concentration) curve with the adsorption time finally flattening after about 60 min of adsorption time. As the micropollutants are adsorbed in the GAC, their effluent concentrations continue to decrease reaching a saturation beyond which no significant decrease in the effluent concentrations were observed after about 1hr adsorption time, while

Figure 4-1© shows sharp higher adsorption of micropollutants, therefore, occurred within the first 2 hrs at a 3000 mg/L GAC dose.

At 10 mg/L GAC dose, the highest C_i/C_0 was observed for metronidazole (0.9) followed by ibuprofen (0.83), acetaminophen (0.81), naproxen (0.79) and carbamazepine (0.75) corresponding to their removal rates of 13%, 17%, 19%, 21% and 23%, respectively at 60 min adsorption time. This low removal is expected because of the very low adsorption surface available at a very low dose of just 10 mg/L GAC and also the competition between urine compositions and micropollutants that might be adsorbed onto GAC. However, at higher GAC doses, the removal rates of the micropollutants were increased because of the larger adsorption surface available for the micropollutants. For example, at the GAC doses of 80 mg/L, the highest removal (at 60 min adsorption time) was observed for carbamazepine (52%) followed by naproxen (50%), acetaminophen (43%), ibuprofen (39%) and metronidazole (35%) as presented in Fig 1(b). At even higher GAC dose of 3,000 mg/L, the removal rates were carbamazepine (97%), naproxen (95%), acetaminophen (93%), ibuprofen (91%) and metronidazole (89%). These results indicated that carbamazepine and naproxen consistently showed the best removal efficiencies while metronidazole was the lowest although even metronidazole was removed 99% from the nitrified urine at 360 min of adsorption time. The variations of normalised effluent concentrations (C_i/C_0) with adsorption time for different GAC concentrations are all presented in Figure S1 of the supporting information. These micropollutant removal rates are comparable to previous works by Solanki and Boyer (2017) where the removals of naproxen, ibuprofen, and carbamazepine by activated carbon at dose 0.8 g/L were reported to be more than 90%.

Figure 4-1(d) shows the mass of the micropollutants adsorbed per unit mass of GAC adsorbent for 800 mg/L GAC dose. At around 6 hr of adsorption, the mass of micropollutant adsorbed reaches maximum beyond which no more adsorption is observed. The highest GAC adsorption affinity was shown for carbamazepine (54.64 mg/g) followed by naproxen (53.94 mg/g), ibuprofen (44.6 mg/g), acetaminophen (34.81 mg/g) and lowest with metronidazole (33.2 mg/g).

Regarding the adsorption of micropollutants to GAC, the time needed to reach the adsorption equilibrium might differ from less than half an hour (Calisto et al., 2015) to many days (Solanki & Boyer, 2019) due to the different characteristics of both the adsorbate and adsorbent. In our study, about 6 hours of contact time was adequate to reach adsorption equilibrium whereas there was little or no significant change in the effluent concentration of all micropollutants from 2 hours to 6 hours. Overall, this could be mostly attributed to the fact that increasing the amount of the adsorbent contribute to rise the surface area and the number of active (Sun et al., 2018).

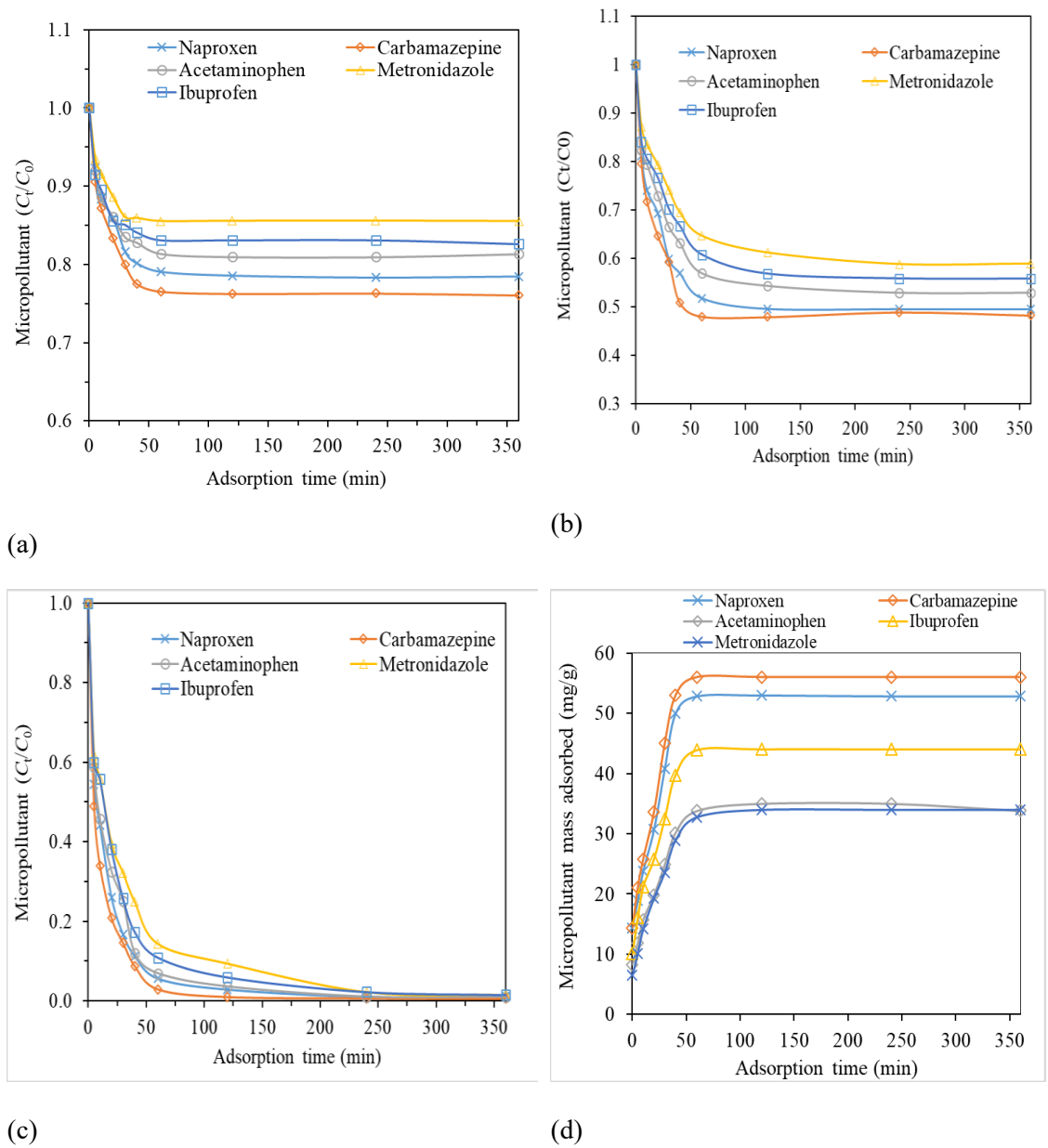
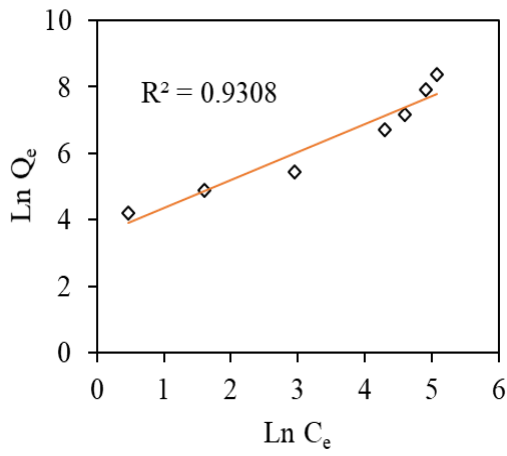


Figure 4-1 Variations in the normalised effluent concentrations C_t/C_0 with adsorption time for

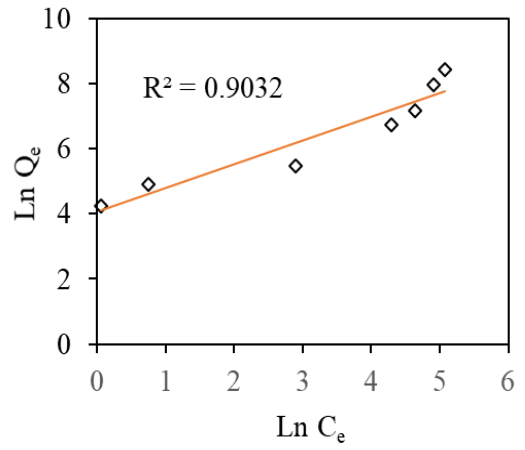
different GAC doses of (a) 10 mg/L, (b) 80 mg/L and (c) 3,000 mg/L, and (d) mass of micropollutant adsorbed per unit GAC mass for 800 mg/L GAC dose.

4.4.2 Adsorption isotherms

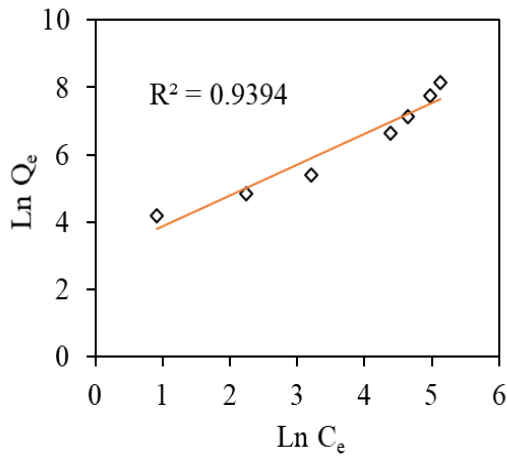
An isothermal adsorption study reveals the characteristics of the adsorption layers. In this paper, both Freundlich and Langmuir isotherms were used to illustrate the micropollutants adsorption equilibrium with the GAC. The Freundlich isotherm refers to heterogeneous surfaces, and isotherm parameters provided essential details about the interactions that take place between adsorbent and adsorbate. Figure 4-2 shows that the experimental data was well described by the Freundlich model. After linearly plotting the experimental data for $\ln(q_e)$ and $\ln(C_e)$, the intercept and slope were used for calculating the values of k_f and $1/n$. Therefore, the Freundlich regression coefficients were 0.94, 0.96, 0.90, 0.92, and 0.93 for naproxen, carbamazepine, acetaminophen, ibuprofen, and metronidazole respectively. In general, the K_f and $1/n$ values calculated for synthetic urine and summarized in Table S4-4 indicates that urine compositions did favourably adsorb onto GAC. According to this model, the maximum and minimum Freundlich constants were shown by carbamazepine and metronidazole, respectively. Since carbamazepine is more hydrophobic than the other organic compounds, it showed the maximum adsorption capacity while metronidazole is hydrophilic and so showed the least adsorption capacity on the GAC surface which is hydrophobic. It can be also elucidated via (e.g. high molecular weight, polarizability, octanol-water partition coefficient) which are the major physicochemical properties that play an essential role in mechanisms of adsorption (Ahmed, 2017). More detailed explanation is discussed in section 3.4. Although the regression coefficients in Fig 2 were above 0.9, it is also evident that the plot is non-linear for all micropollutants at higher $\ln(C_e)$ values which also explains one of the limitations of Freundlich isotherm in general (Singh, 2015). This indicates that at higher micropollutant concentrations, amount of micropollutant adsorbed also increases rapidly because of the heterogenous surfaces of GAC with exponential distribution of active sites and their energies (Ayawei et al., 2015).



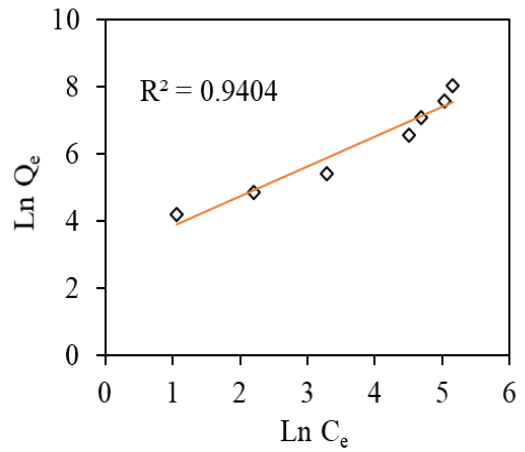
(a)



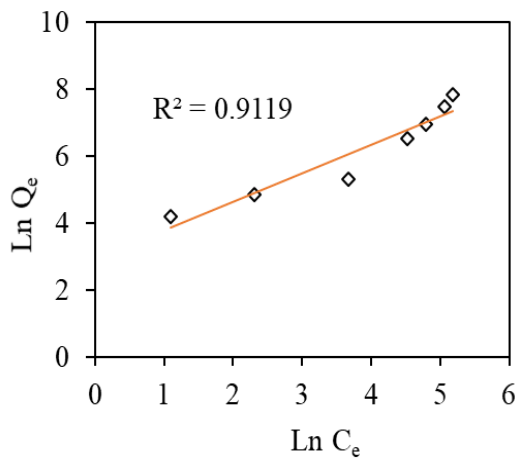
(b)



(c)



(d)



(e)

Figure 4-2 Experimental data (dots) and linear Freundlich isotherm (line) for adsorption of

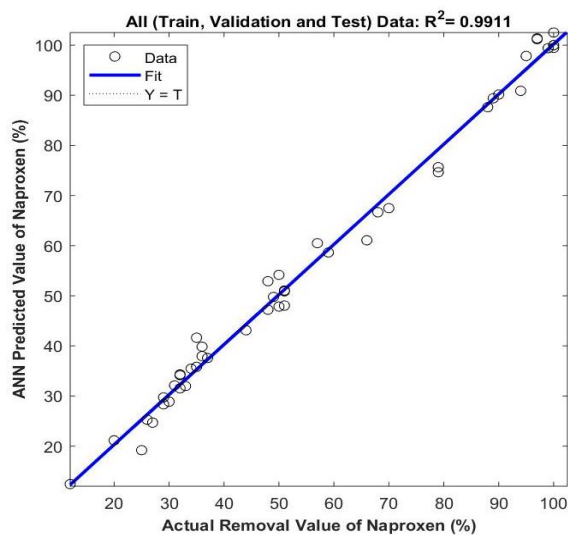
naproxen (a), carbamazepine (b), acetaminophen (c) ibuprofen, (d) and metronidazole (e).

The Langmuir model assumes monolayer adsorption (when the layer of adsorbed is one molecule thick) that only takes place at specific localized identical sites and the lateral interactions or steric hindrances are unable to take place among the adsorbed molecules, even on sites that are next to each other. Figure S2 shows the experimental data that well described by the Langmuir model. After linearly plotting the experimental data for $1/q_e$ and $\ln(1/C_e)$, the intercept and slope was used to calculate the values of q_{max} and K_L for each micropollutants. As shown in Table S4, Langmuir adsorption capacity values of acetaminophen and ibuprofen are slightly similar, indicating sorption sites for them were probably similar. The q_{max} value of acetaminophen and carbamazepine were similar to that reported in previous literature for the activated carbon under comparable conditions (Cabrita et al., 2010; Nguyen et al., 2013).

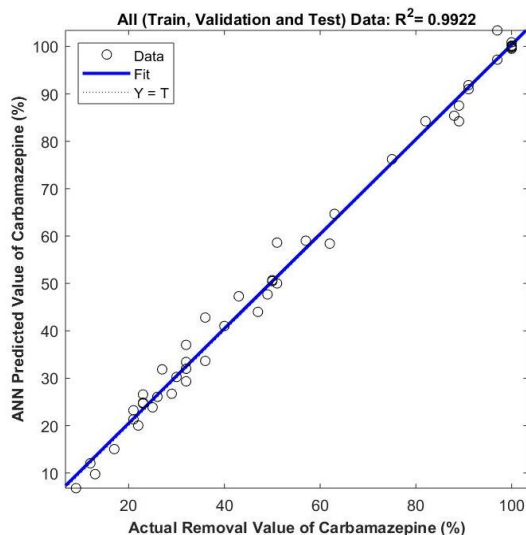
4.4.3 Micropollutants removal modelling by ANN

Several topologies with 1 to 20 neurons in the hidden layer were constructed to model the GAC efficiency in removal of the naproxen, carbamazepine, acetaminophen, ibuprofen, and metronidazole from nitrified urine solutions using ANN. In these models contact time and different doses were used as inputs of the developed ANN models. The results indicate that the topologies of 2-12-1, 2-14-1, 2-14-1, 2-7-1, and 2-17-1 indicating 12, 14, 14, 7, and 17 neurons in hidden layers were the best ones for naproxen, carbamazepine, acetaminophen, ibuprofen, and metronidazole models consecutively. It is worth highlighting that the first and third numbers in these topologies were the number of inputs and outputs. The correlation coefficients for training, validation, and testing datasets in all three models demonstrated great performances of the developed models in the prediction of the outputs (Figures S3-S7). As can be seen in Figure 4-3, the R^2 values for all data of the developed models were 0.9911, 0.9922, 0.9895, 0.9842, and 0.9808 for naproxen, carbamazepine, acetaminophen ibuprofen, and metronidazole respectively. Moreover, the residual errors of the constructed models are presented in Figure 4-5. As observed, the MSE of the models were 0.0005, 0.0005, 0.0007, 0.0006, and 0.0005 for naproxen,

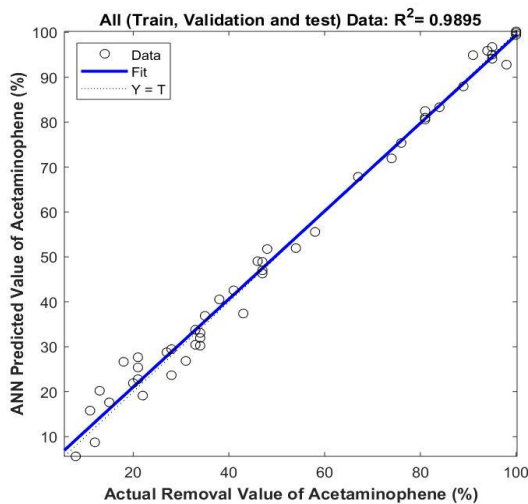
carbamazepine, acetaminophen, ibuprofen, and metronidazole, respectively which are all negligible. Therefore, the developed models can predict the removal efficiencies of the naproxen, carbamazepine, acetaminophen, ibuprofen, and metronidazole from aqueous solutions with 99.1%, 99.2% , 98.9% 98.4% and 98.1% respectively.



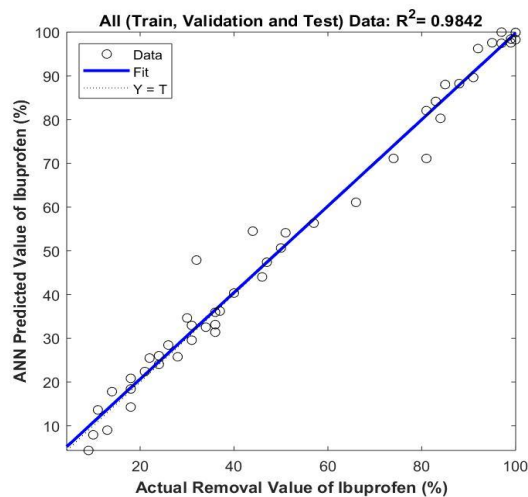
(a)



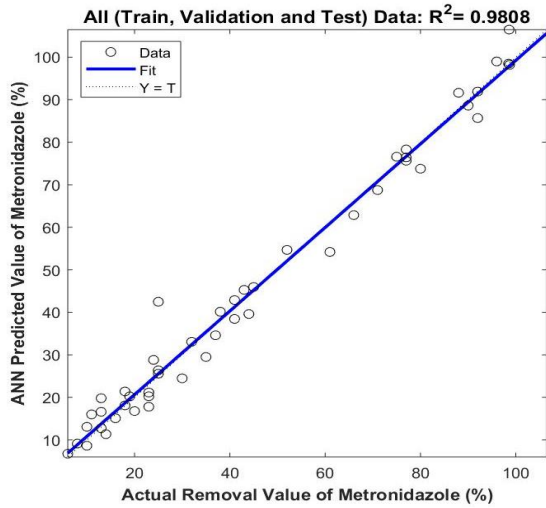
(b)



(c)



(d)



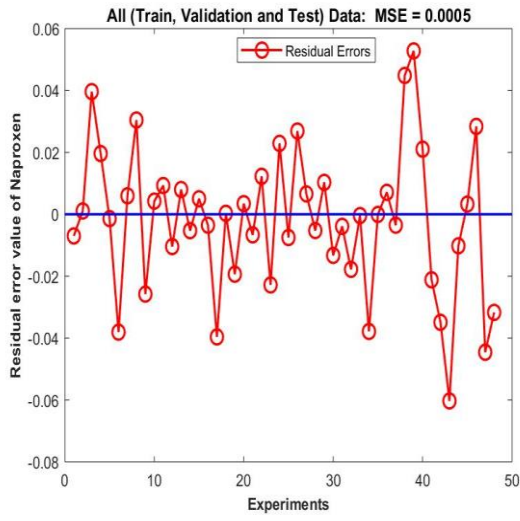
(e)

Figure 4-3 Scatter plots of the predicted and actual values of the (a) naproxen, (b) carbamazepine, (c) acetaminophen, (d) ibuprofen, and (e) metronidazole.

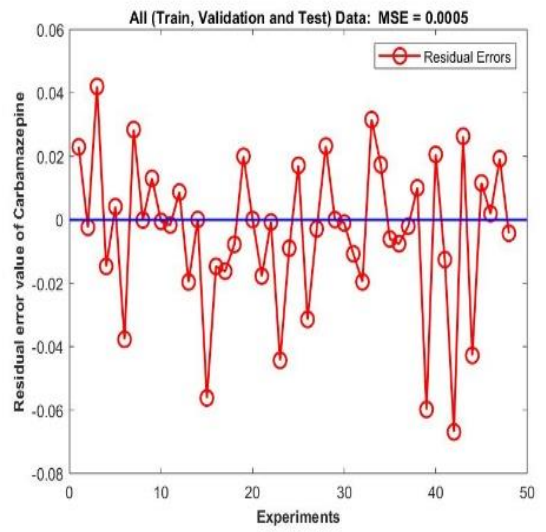
The ANN model for five micropollutants removal prediction is shown in equation (7) weights and biases values for all micropollutants are shown Table (S5-S9):

$$\begin{aligned}
 \text{ANN equation} = & \text{Purelin} (LW \times \text{tansig} (IW \times [\text{contact time}; \text{adsorbent dosage}] b1) \\
 & + b2)
 \end{aligned}
 \tag{7}$$

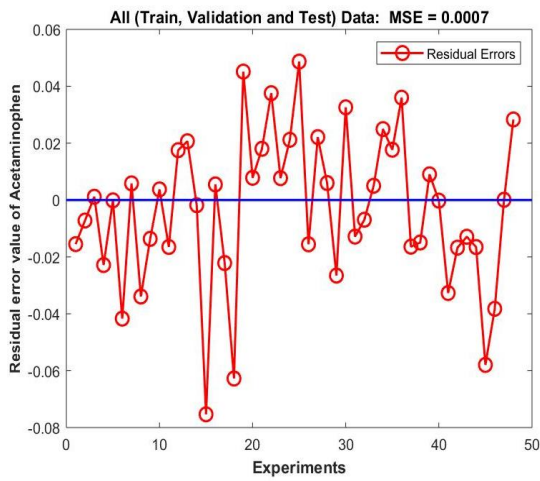
Figure 4-4 illustrates the residual error distribution in naproxen, carbamazepine, acetaminophen, ibuprofen, and metronidazole prediction, which is close to zero. Hence, in the GAC system, it is reasonable to conclude that the developed ANN model can imitate the behaviour of all five micropollutants. Figure 4-5 shows that the twelve additional experiments undertaken matched well with the prediction for the removal efficiency of naproxen, carbamazepine, acetaminophen, ibuprofen, and metronidazole with ANN models showing R^2 values of 0.9852, 0.9729, 0.9133, 0.9762, and 0.9764, respectively. Therefore, the developed models could predict the removal efficiency with strengths of 98.52%, 97.29%, 91.33%, 97.62% and 97.64% for naproxen, carbamazepine, acetaminophen, ibuprofen, and metronidazole corespondingly.



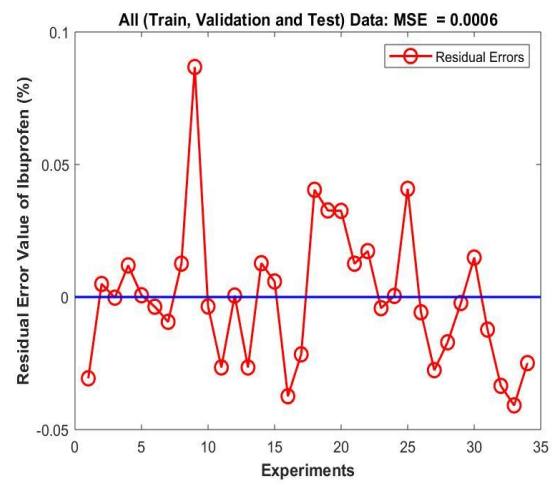
(a)



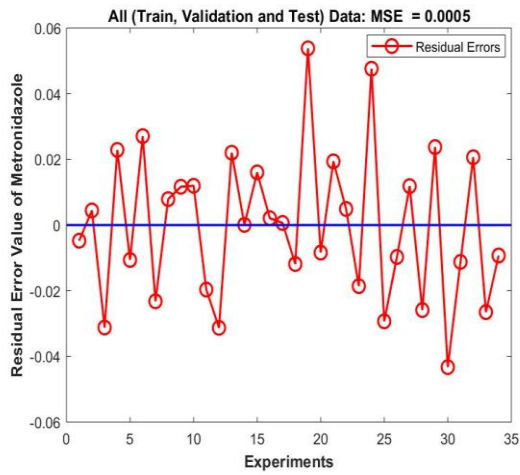
(b)



(c)

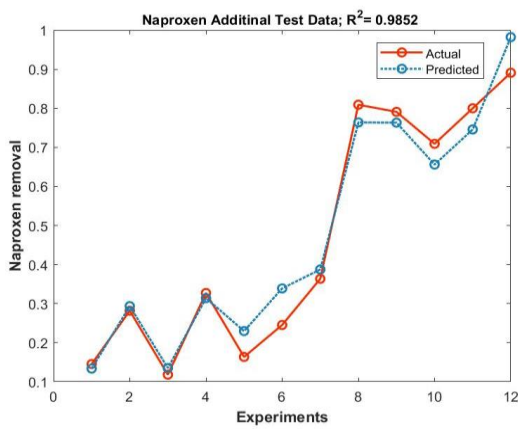


(d)

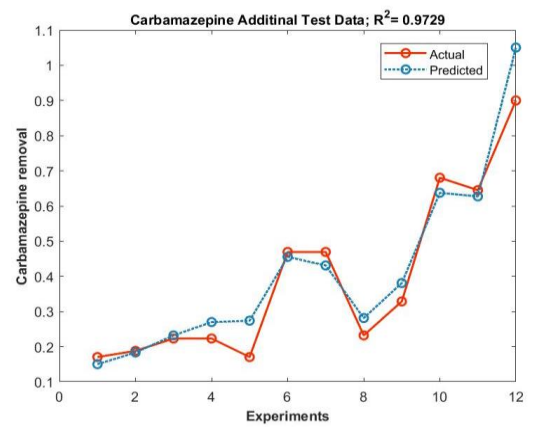


(e)

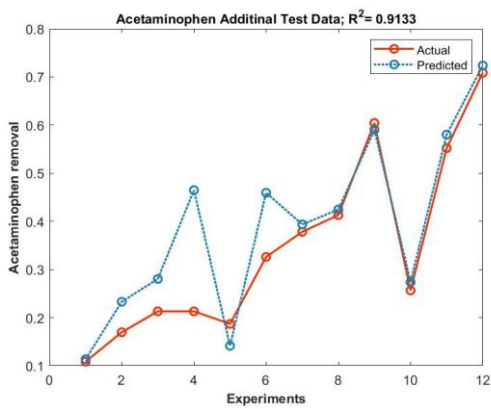
Figure 4-4 The residual errors of the developed ANN models for (a) naproxen, (b) carbamazepine, (c) acetaminophen, (d) ibuprofen, and (e) metronidazole.



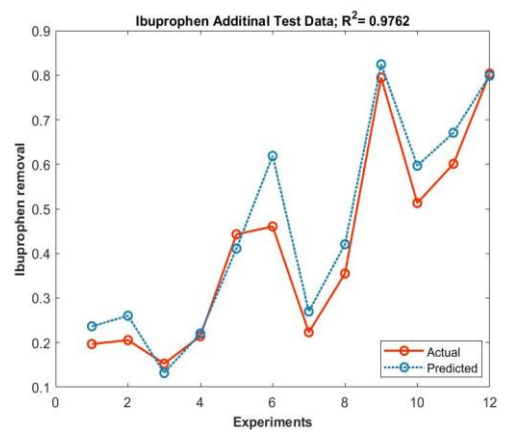
(a)



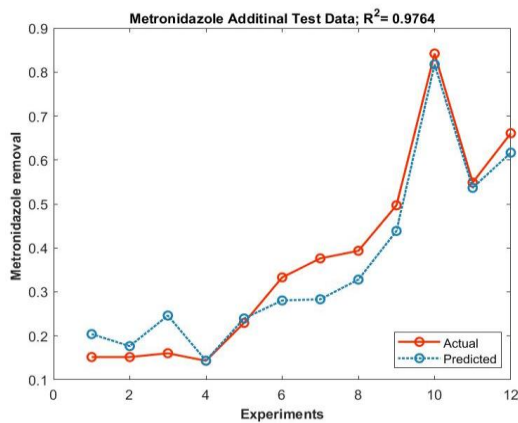
(b)



(c)



(d)



(e)

Figure 4-5 Illustration the predicted data versus the experimental data of normalized removal from ANN for (a) naproxen, (b) carbamazepine, (c) acetaminophen, (d) ibuprofen, and (e) metronidazole.

A high accuracy prediction for micropollutant adsorption were also reported earlier using ANN models. Mojiri et al. (2019) predicted naproxen, ibuprofen, and diclofenac removal, by ANN models with R^2 value of 0.990, 0.998, and 0.998, respectively. Other similar studies also predicted ANN model accuracy, though the experimental set-up and materials varied from ours. Hosseinzadeh et al. (2020a) reported ANN models' high ability to predict nutrient recovery from solid wastewater with R^2 value of 0.99. In another study, Hosseinzadeh et al. (2018) compared the strengths of ANN and response surface methodology (RSM) models in elimination of volatile organic carbons from air stream by non-thermal plasma and demonstrated the great capability of ANN model than the RSM one. Due to the high prediction strengths of these models, it is expected that these models can be applied to estimate the micropollutants removal from nitrified urine very effectively.

4.4.4 Effect the GAC onto pharmaceuticals

The properties of GAC and in particular the specific surface area is therefore expected to significantly affect the adsorption of pharmaceuticals. GAC comes in a range of specific surface area and GAC with larger specific surface area is expected to have much higher removal efficiencies. For example, powdered activated carbon (PAC) with higher specific surface area

(800 – 1500 m²/g) compared to GAC can achieve better pharmaceutical removal efficiencies (Kim et al., 2010; Mailler et al., 2015), however, GAC is much easier to handle unlike PAC where additional process is required to prevent washout and hence GAC was used for the adsorption of pharmaceuticals in this study. Most sorption occurs when macropores act as passages for the sorbate to reach in micropores. Thus, the GAC surface charge plays a significant role in the adsorption of pharmaceuticals. Zeta potential measures the external charge of the GAC surface; therefore, enhancing the understanding of the ways in which the adsorption mechanism occurs is necessary (Sotelo et al., 2013). When the pH value is greater than the value of the point of a zero charge pH_{PZC}, meaning the GAC surface possesses a negative charge and hence favors absorbing the cationic species, and vice versa. In our study, the pH_{PZC} value of the GAC was observed to be at pH 4.8 as shown in Figure S8 which indicates that the GAC was negatively charged during the adsorption process since the pH of the nitrified urine was higher than the pH_{PZC} of GAC. In addition, the octanol-water partition coefficient (K_{ow}) and acidity constant (pK_a) of these pharmaceutical compounds might have an important influence on the rate and level of GAC adsorption; thus, all characteristics have been documented from previous literature reviews, as shown in Table S1.

According to the literature hydrophobicity is an important element in assessing the adsorption capacity of micro pollutants, which influences the adsorption capacity of micropollutants onto GAC, as represented by log K_{ow} (Choi et al., 2005; Jamil et al., 2019; Yu et al., 2008). The log K_{ow} values of the five compounds ranked in decreasing order are ibuprofen, naproxen, carbamazepine, acetaminophen, and metronidazole. However in this study, naproxen and ibuprofen showed a relatively less sorption affinity compared to carbamazepine, results similar to those reported by Yu et al. (2008), using different doses of GAC in an ultra-pure water matrix spiked with pharmaceuticals. This outcome could be due to the acidic dissociation at pH values that observed in these earlier works. Yu et al. (2008) suggested utilizing the modified value of log K_{ow} to understand the sorption affinity of an acidic or basic pesticides. Using Eq. 8 (Yu et al., 2008), the modified log K_{ow} values of naproxen and ibuprofen are calculated to be 1.42 and 1.63,

respectively, at pH 6.2 (nitrified urine), which is lower than the value for carbamazepine, thereby supporting the above-mentioned differences in the adsorption affinity.

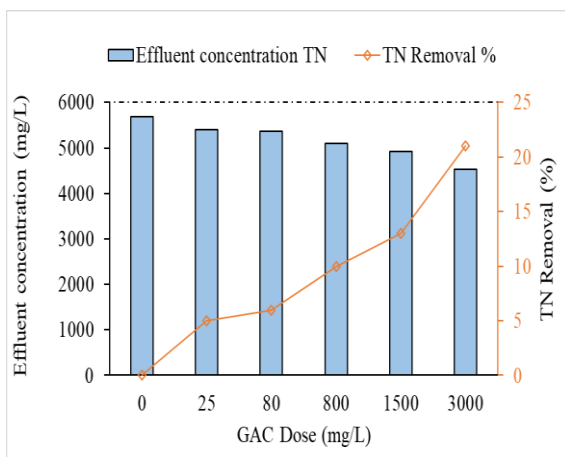
$$\text{Log } K_{ow} = \frac{K_{ow}}{(1 + 10^{(pK_a - pH)})} \quad (8)$$

The acid dissociation constants (pK_a) of micropollutants differed based on their molecular structure. Ionizable compounds could exist either as cations or anions according to their pH in the aqueous phase. On the other hand, the GAC surface charge has an oscillating character, whereby its surface could be negatively or positively charged based on the pH values, which has a direct effect on electrostatic interactions (Calisto et al., 2015; Jamil et al., 2019), as described above. The Pk_a values of naproxen and ibuprofen are lower than the pH of the solution (pH 6.2), which means they were negatively charged in the nitrified urine, thus indicating a lower tendency to react or electrosorb with the negatively charged GAC surface. Therefore, the interaction of these compounds with GAC surface could be due to other interacting forces such as van der Waals forces, π - π bonding or H-bonding (Jamil et al., 2019). Carbamazepine, metronidazole and acetaminophen, however, are neutrally charged in nitrified urine, thereby allowing to show electrostatic interactions (Solanki & Boyer, 2017). The metronidazole was the least absorbed on GAC compared to the acetaminophen. From this, it can be concluded that the adsorption of metronidazole on GAC is likely to be mainly physisorption and very weakened with the pH range. Another study showed that the pH range of solution does not have any considerable effect on the removal of metronidazole (Rivera-Utrilla et al., 2009). However, the pH value in the aqueous phase may play an important role to maximize the removal of micropollutants (e.g. acetaminophen to 2 -7) by GAC adsorption. Al-Khateeb et al. (2014) found that the removal of acetaminophen using graphene nanoplatelets was not a function of pH at a range of 2 -7, but the removal efficiency dropped from 88.7% to 73.8% when the pH value was increased from 7 to 11. Precisely, a study was conducted on removal of acetaminophen from three wastewater sources, namely fresh urine, hydrolysed urine, and effluent wastewater. The outcomes showed

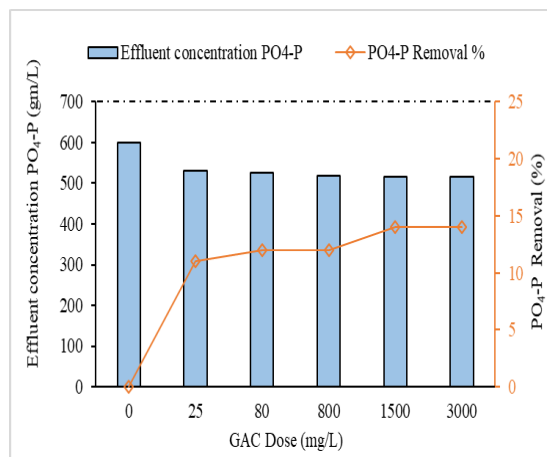
that the highest removal efficiency was obtained from fresh urine followed by wastewater and then hydrolysed urine due to different pH values (Solanki & Boyer, 2017). This agrees with our hypothesis that removing hydrophilic compounds such as acetaminophen from nitrified urine is better than removing them from hydrolysed urine.

4.4.5 Effect the GAC onto TN & PO₄-P

The positively charged NH₄⁺-N ion and negatively charged NO₃⁻-N ions are the two major forms of total nitrogen (TN) constituents in nitrified urine and are therefore expected to interact with the GAC surface. TN is the major nutrient in the nitrified urine containing about 6,000 ± 520 mg/L of N as in this study. Figure 4-6a illustrates the percentage of TN removal at various GAC dosages. At the highest GAC dose of 3000 mg/L, only about 21% of the TN was removed from the nitrified urine via GAC adsorption, which might be because of the negatively charged GAC surface that enable electrosorption of the positively charged NH₄⁺ ions. These outcomes shows that GAC lacks adsorption capacity for TN because it typically has a nonpolar surface because of manufacturing conditions at high temperatures, which is a drawback for some applications due to poor interaction with some polar adsorbates. Moreover, the surface of activated carbon is hydrophobic and does not have more sorption affinity toward TN in aqueous solution (Halim et al., 2010). According to previous studies, the GAC displays negligible ammonium-ions removal via physical adsorption, which could be attributed to the ions' solubility and polarity in the aqueous solution (Nguyen et al., 2013). Figure 4-6b shows the percentage removal of phosphorus (PO₄-P) during GAC adsorption at different dosages. The results show that only about 14% of the PO₄-P is removed by the GAC adsorption from the nitrified urine irrespective of the GAC dosages used. This low adsorption affinity of the PO₄-P can be attributed to the electrostatic repulsion of the negatively charged PO₄³⁻ ions by the negatively charged GAC surface. Although these results indicate that GAC can simultaneously adsorb both the nutrients (N and P) from the nitrified urine, however, it is significant that GAC is more effective in removing the micropollutant without significantly adsorbing the nutrient present in the nitrified urine. The lower nutrient adsorption by GAC is essential so that micropollutants do not have to compete with the nutrients for adsorption.



(a)



(b)

Figure 4-6 Total nitrogen concentrations upon completion of batch tests at 25-3000 mg /L doses in a nitrified urine.

4.5 Conclusion

Batch experiments were conducted to evaluate the adsorption kinetics that described the removal of micropollutants from nitrified urine. The following conclusions are drawn from this adsorption study:

- (1) Higher GAC dose and contact time resulted in enhanced removal of pharmaceutical contaminants in nitrified urine. Removal of pharmaceuticals can therefore be maximised by adjusting the adsorbent dose and contact time.
- (2) The ANN models used in this study were able to predict quite accurately matching 99.1%, 99.2% , 99.0% 98.4% and 99.1% with the experimental values and predicted values of naproxen, carbamazepine, acetaminophen, ibuprofen, and metronidazole removal, respectively.
- (3) The linear Freundlich and Langmuir isotherms fitted well for the GAC adsorption of the five pharmaceuticals.

(4) The removal of carbamazepine, acetaminophen and metronidazole was observed to be mainly due to electrostatic interactions between the negatively charged GAC surface and the ionic pollutants.

(5) Although not desirable, GAC adsorption also removed little nutrients (21% TN and 14% PO₄-P) along with micropollutants and although this is not very significant, however, it can reduce the micropollutant adsorption capacity of the GAC due to competitive adsorption.

This study on the GAC adsorption of pharmaceuticals was however limited to synthetic nitrified urine only. Hence, the future studies must assess the removal of pharmaceutically active compounds from the real nitrified human urine, which can contain various organic species that can compete with the micropollutants for GAC adsorption.

Acknowledgements

This study was supported by the Bhutan trust Fund for Environmental Conservation [Project Grant No. MB0167Y16] and the Saudi Arabian Cultural Mission in Australia (SACM) for providing a PhD scholarship to Abdulaziz Almontashiri.

CHAPTER 5 Removal of antibiotics from a biologically nitrified real human urine using granular activated carbon adsorption

5.1 Abstract

In this chapter, it focuses the third objective of the thesis, which is the removal of sulfonamide antibiotics from nitrified urine. This represents urine that has undergone biological nitrification in a membrane bioreactor. The presence of antibiotics in urine poses challenges for its safe use as a fertiliser. The present study studied the efficacy of using granular activated carbon (GAC) adsorption to remove three of the most common antibiotics detected (sulfamethoxazole or SMX, sulfadiazine or SDZ and sulfamethazine or SMZ) in the real nitrified human urine obtained from a pilot-scale urine membrane bioreactor subjected to biological nitrification. In addition, the artificial intelligence network procedure with Levenberge-marquate training algorithm was used to model the removal of antibiotic compounds. Fixed-bed column tests were performed to obtain breakthrough curves and evaluate the performance of GAC in the antibiotics adsorption under various operating parameters, such as particle sizes (425–1000 μm), adsorbent mass (0.5–1.5 g/L), flow rates (0.06–1.8 L/hr) and adsorption/contact time at pH 6.2. For all the antibiotics, the maximum antibiotics adsorption capacity was found with lower particle sizes of adsorbents, at lower flow rate or higher hydraulic retention time and higher mass of adsorbent. According to the breakthrough curves, SMZ revealed the greatest adsorption capacity (4.33 mg/g) onto GAC and the lowest adsorption capacity for SDZ (4.01 mg/g). Meanwhile, various adsorption models have been employed to evaluate the breakthrough curves of the antibiotics (Thomas, Yoon–Nelson, and Yan models). This study also revealed that artificial neural network can effectively predict (over 99%) antibiotic removal from a real nitrified urine.

Keywords: Antibiotics, Artificial neural network modelling, Column adsorption, Nitrified urine, Granular activate carbon

5.2 Introduction

In the past fifty years, researchers have reported that over two hundred thousand tons of drugs are used annually worldwide to treat human illnesses, including steroid hormones, anti-inflammatory drugs, and antibiotics (Lan et al., 2018). Previous studies have shown that 30%-90% of drugs (either active metabolites or parent compounds) are secreted with faeces and urine (Lienert et al., 2007). Many studies have indicated the presence of pharmaceutical pollutants in the soil and groundwater (Madikizela et al., 2017; Nguyen et al., 2012). Therefore, pharmaceutical contaminants are of growing concern due to their toxicity and their harmful impacts on the aquatic environment, humans, and other wildlife (Adams et al., 2002; Bradley et al., 2016; Madikizela et al., 2017). Many conventional wastewater treatment plants are not specialized to eliminate pharmaceuticals and thus, cannot achieve sufficient removal of these micropollutants, which all end up in the environment (Adams et al., 2002; Feizi et al., 2021). The micropollutant removal from a wastewater treatment plant is not easy because of the sheer volume of the wastewater that needs to be subjected to treatment.

Source separation of urine from a wastewater stream and treatment is seen as a unique opportunity and an effective method of recovering nutrients and reusing as liquid fertiliser for food crops to support agricultural production. Nevertheless, due to the presence of pharmaceuticals in the urine, the direct application of urine derived fertiliser requires additional treatment to remove pharmaceuticals. Various techniques have been employed to remove pharmaceutical from the urine matrix, including advanced oxidation processes such as ozonation or oxidation (Dodd et al., 2008; Sun et al., 2018) and membrane separation (Pronk et al., 2006) and these technologies are limited by high capital and maintenance costs. One of the alternatives is a granular activated carbon (GAC) adsorption processes which is seen as a relatively simple and yet effective approach for removing pharmaceuticals compared to other energy intensive processes such as membrane processes, oxidation methods, etc. (Sotelo et al., 2014). GAC can be employed either as a stirred-tank reactor or fixed-bed column, but GAC columns are considered the most popular due to their

simplicity for industrial applications, high removal efficiency and simple operation. Many studies have shown that GAC removes pharmaceuticals effectively from water resources (Del Vecchio et al., 2019; Grover et al., 2011; Hernández-Leal et al., 2011; Li et al., 2018; Nguyen et al., 2012; Sotelo et al., 2014), but a limited number of studies have focused on pharmaceutical removal from a real nitrified human urine (Almuntashiri et al., 2021; Duygan et al., 2021; Köpping et al., 2020). Fixed-bed column adsorption studies are essential since they can provide valuable information (e.g., processing performance data essential for practical system design and breakthrough curves) (Feizi et al., 2021; Reynel-Avila et al., 2015).

Laboratory-column tests and study for removal efficiencies involving hundreds of samples is time-consuming and expensive. Under various operating conditions, robust modelling and simulation to predict the removal of pharmaceuticals is the most beneficial and cost-effective way to understand the possible performance of the fixed bed column adsorption. Moreover, numerical modelling applications could be investigated easily in the predesign process, making it more cost-effective and efficient (Hosseinzadeh et al., 2020b; Hosseinzadeh et al., 2022). Micropollutant adsorption modelling is challenging because operating conditions also affect the adsorption mechanism along with the interactions among the micropollutants and adsorbent material. An artificial neural network (ANN) can demonstrate human-like behaviour inspired by the human brain. ANN modelling has been used successfully to forecast removal of pharmaceuticals during the adsorption process for wastewater treatment (Pauletto et al., 2021; Vakili et al., 2019). In particular, ANN models have been developed for accurate prediction of breakthrough curves (Almuntashiri et al., 2022; Moreno-Pérez et al., 2018), isotherms (Mendoza-Castillo et al., 2018; Pauletto et al., 2020b), kinetics modelling (Gopinath et al., 2020; Pauletto et al., 2020a) and process improvement (Ghaedi et al., 2019). ANN models, unlike other traditional models, learn immediately from experiential outcomes without imposing assumptions about the physicochemical nature which impacts the adsorption mechanism.

GAC adsorption can be employed in any form of urine (fresh urine, hydrolysed urine, nitrified urine and concentrated nitrified urine) for pharmaceutical removal however GAC being excellent adsorbent to most components in the urine and hence treatment must be targeted so that GAC adsorption is effective for removing pharmaceuticals only. If GAC adsorption is used with fresh urine or hydrolysed urine, adsorption of pharmaceuticals will have to compete with the other organics present in the urine for adsorption and hence GAC adsorption capacity may be significantly affected. In a biologically nitrified urine using MBR, most of the suspected solids and organics (over 95%) are all removed during biological decomposition and hence GAC active surfaces is now mostly available for the adsorption of the remaining pharmaceuticals thereby increasing its adsorption capacity and the replenishment costs. In this study, GAC fixed bed column adsorption has been studied to investigate the removal of three commonly found antibiotics from a real nitrified urine obtained from a pilot urine membrane bioreactor (MBR). This is an extended study of one of our earlier studies using GAC adsorption for pharmaceutical removal using a synthetic nitrified urine. Nitrification is a biological oxidation process in which the ammonia/ammonium present in the hydrolysed urine is converted into nitrite via ammonia-oxidizing bacteria. The nitrite is then further converted into nitrate via nitrite-oxidizing bacteria. The urine processed through a biological nitrification in a MBR is termed as nitrified urine. The nitrification process has been recommended recently as a promising approach to remove drug contaminants from contaminated water (Caluwé et al., 2017). The nitrification process was found to be suitable for removing drugs such as risperidone, enalapril, and atenolol over a 95% removal rate. Nevertheless, other treatment processes are vital for effective removal of drugs from urine since nitrification cannot remove all the drugs. For instance, sulfadiazine (SDZ), sulfamethoxazole (SMX), and sulfamethazine (SMZ) removal rate were lesser than 50% (Lastre-Acosta et al., 2020). The characteristics of actual nitrified urine could differ substantially from synthetic urine, particularly in terms of its complex chemical composition, encompassing biological, organic constituents and other chemistry. This variation can notably influence the efficacy of pharmaceutical removal by GAC adsorption. Besides, in a real nitrified urine, the concentration of pharmaceuticals is relatively lower than that of other organic and inorganic

components, potentially altering the referencing of adsorption sites during GAC adsorption processes. Furthermore, limited research exists on the application of Artificial Neural Network (ANN) modelling specifically for predicting pharmaceutical removal from biologically nitrified urine. This underlines the necessity for an enhanced understanding of the unique attributes of real nitrified urine to optimize the performance and predictive modelling accuracy of GAC adsorption in pharmaceutical removal processes. A review of existing literature demonstrates that there is limited research about a continuous fixed-bed column for drugs (antibiotics) removal from real nitrified urine, (Almuntashiri et al., 2022; Duygan et al., 2021; Köpping et al., 2020; Solanki & Boyer, 2019; Zhang et al., 2020), and the findings from this work is intended to fill this gap, to help understand how key operational conditions can affect antibiotic adsorption. Using mathematical models, breakthrough curves of antibiotic adsorption can be designed and obtained and the parameters of column adsorption can be used in ANN modelling to predict how antibiotics will be removed from nitrified urine.

5.3 Materials and methods

5.3.1 Antibiotics and the reagents

Three antibiotics SDZ, SMX, and SMZ (Sigma Aldrich, Australia) were chosen for this work based on their frequent presence in the urine or wastewater. The physicochemical antibiotic characteristics are presented in Table S5-1 of the Supplementary Materials. The stock solution was prepared by dissolving each antibiotic in MeOH solvent because of their water solubility, and they were diluted until the concentration of each antibiotics compound was 10 μM . The GAC (James Cumming & Sons Pty Ltd., Australia) used as adsorbent was sieved to 425, 600 and 1000 μm particle sizes and then washed in water before use to remove surface scums and dried at 90°C for 1 day. The GAC's point of zero charge was 4.8 (Almuntashiri et al., 2021). Quantachrome instrument (Autosorb iQ2) was used to measure Brunauer-Emmett-Teller (BET) specific surface area and pore volume of GAC. The other properties of GAC are presented in Table 5-1.

Table 5-1 The GAC characteristics in various particle sizes.

Particles size (μm)	pore size (nm)	BET Surface area (m^2/g)	Pore volume (cm^3/g)
425	7.374	988.751	0.576
600	7.374	921.034	0.535
1000	7.374	878.311	0.498

5.3.2 Source separated nitrified urine

A biologically nitrified urine used in the GAC column adsorption experiments was obtained from a pilot-scale MBR (100 L/day capacity) used for the treatment of hydrolysed (or stored urine) at the University of Technology Sydney, Australia. A source-separated urine is collected from the waterless male urinals of the Faculty of Engineering and Information Technology building (building 11) at UTS using dedicated urinal pipes and stored in the 5,000 litres tank at the basement. The hydrolysed urine from the tank is then subjected to biological nitrification using a pilot-scale MBR using ultrafiltration as a membrane (Ren et al., 2021) and this MBR effluent was used as a nitrified urine for all the fixed-bed column adsorption experiments. The nitrified urine was measured for dissolved organic carbon (DOC), cations (Na^+ , K^+ , Mg^{2+} , Ca^{2+}), anions (SO_4^{2-} , Cl^- , PO_4^{3-} -P, NO_3^- -N), pH, NH_4^+ -N and NO_2^- -N as well as the target pharmaceuticals compounds in the column adsorption experiment. Table 5-2 shows the nitrified urine composition utilized for all the experiments.

Table 5-2 Properties and ionic composition of the nitrified urine before and after GAC

	Nitrified urine (MBR permeate)	After GAC column (Adsorption permeate)
pH	6.2	6.2
DOC (mg/L)	63.9	58
NH ₄ ⁺ -N (mg/L)	1750	1620
NO ₃ ⁻ -N (mg/L)	1507.47	1376.87
NO ₂ ⁻ -N (mg/L)	<1	<1
Na ⁺ (mg/L)	749.50	665
K ⁺ (mg /L)	1286	1240
Mg ²⁺ (mg/L)	5.6	3.8
Ca ²⁺ (mg/L)	31.6	21
Cl ⁻ (mg/L)	1246.40	1215.82
PO ₄ ³⁻ -P (mg/L)	191.45	140.27
SO ₄ ²⁻ (mg/L)	253.90	251.24

5.3.3 Fixed-bed GAC adsorption column and analysis

Acrylic columns were used for the experiments, and cotton based was inserted at the end of the column to avoid the GAC from flowing out with the liquid. The column adsorption experiments were performed using acrylic columns. A stainless steel mesh was placed at the bottom to prevent the GAC adsorbent from flowing out with the effluent, as shown in Figure S5-1 of supporting materials. The GAC (James Cumming & Sons Pty Ltd., Australia) used as adsorbent was sieved to 425, 600 and 1000 µm particle sizes and then washed in water before use to remove surface scums and dried at 90°C for 1 day. The down-flow mode was applied to ensure a continuous flow at a constant flow rate utilizing a peristaltic pump (Masterflex, Cole-Parmer). The nitrified urine flow varied between 0.06 L/hr, 0.12 L/hr and 0.18 L/hr and all tests were performed at 25 °C. The

experimental columns were set at different heights, reflected by the GAC mass of 0.5 g (0.45 cm), 0.8 g (0.7 cm) and 1.5 g (1.3 cm), to assess the effect of column height on adsorption performance and the breakthrough curve. The antibiotic removal using GAC column was investigated via plotting breakthrough curves (C_t/C_0), where C_0 and C_t are the influent and effluent concentrations of antibiotic at a time t , respectively, versus operating time (hr). Both the time of breakthrough point and saturation were identified by a breakthrough curve, when the concentration of effluent arrived at (5% and 95%) of the concentration of influent, respectively (Almuntashiri et al., 2022). The breakthrough point is an essential factor that helps the system compute the treated effluent volume. Therefore, to identify the highest adsorption capacity q_t (mg/g) of the antibiotics, the area above the breakthrough curve was calculated by the equation:

$$q_t = \frac{Q \cdot C_0}{m} \int_{t=0}^{t=total} \left(1 - \frac{C_t}{C_0}\right) dt \quad (1)$$

Where Q , t and m represent the flow rate (L/hr), the time (hr) and the GAC mass in the column (g), respectively (Almuntashiri et al., 2022).

The height of the mass transfer zone (h_{MTZ}) refers to the length of the unsaturated GAC in the fixed bed column which contributes to mass transfer. The critical parameters determining the shape of the h_{MTZ} , including the mass transfer conditions, adsorption mechanism, and operating conditions associated with flow rate, length of bed and type of mass adsorbent. (Sotelo et al., 2013). The h_{MTZ} is calculated can follows:

$$h_{MTZ} = \left(1 - \frac{q_b}{q_t}\right) h \quad (2)$$

Where h represents the bed length (cm); q_t is the maximum adsorption capacity (mg/g) at saturation; q_b represents the adsorption capacity (mg/g) at the breakthrough point.

The empty bed contact time (*EBCT*), fraction bed utilisation (*FBU*), and the GAC usage rate (*U_r*) are useful parameters to analyse the breakthrough curve. *FBU* is associated with *EBCT*/residence time, and *h_{MTZ}*, which influences the breakthrough curve's nature and the influent treatment volume, can be calculated by equations:

$$EBCT = \left(\frac{V}{Q} \right) \quad (3)$$

$$FBU = \left(\frac{q_b}{q_t} \right) \quad (4)$$

$$U_r = \left(\frac{m}{V_a} \right) \quad (5)$$

where, *V* represents column volume (L); *V_a* represents the treated effluent volume at breakthrough (L) (Almuntashiri et al., 2022).

5.3.4 Mathematical breakthrough modelling

Both the breakthrough time and saturation curve are major characteristics for dynamic response and process design, as they immediately affect strongly affect the practicality of the process in terms of technical and economic aspects. Accurate forecasts for the breakthrough curve is necessary to create a column experiments and simplify the micropollutant adsorption process.

Numerous mathematical models to describe adsorption kinetics can be utilized to illustrate column adsorption experiments. Among the most common models developed and employed in column performances is the Thomas model. This model shows that the adsorption ratio process can be illustrated by Langmuir kinetics and ignoring intraparticle mass transfer, resistance of

external fluid film and pivotal dispersal in the columns adsorption, and it is represented as follows (Almuntashiri et al., 2022):

$$\frac{C_0}{C_t} = \frac{1}{1 + \exp \frac{K_{th}}{Q} (q_0 m - C_t Q t)} \quad (7)$$

where k_{th} and q_0 represent the rate constant of Thomas model (L/hr/mg) and the adsorption capacity (mg/g), respectively.

Yan et al. (2001) put forward the Yan Model (sometimes referred to as the Modified Dose-Response Model) to reduce the difference between the predicted breakthrough curve and the empirical data derived using the Thomas model, particularly when operating times are extremely short or extremely long. The expression below can be used to describe the model:

$$\frac{C_0}{C_t} = 1 - \frac{1}{1 + \left(\frac{C_t Q t}{q_Y m} \right)^\alpha} \quad (8)$$

where α and represents a model parameter and q_Y represents the adsorption capacity (mg/g).

In contrast, the key purpose of the Yoon-Nelson Model is to minimise breakthrough-curve errors associated with the Thomas model during shorter or longer timeframes (Jaria et al., 2019). The expression below can be used to describe the model.

$$\frac{C_0}{C_t} = \frac{\exp(K_{yn} t - t_{50\%} K_{yn})}{1 + \exp(K_{yn} t - t_{50\%} K_{yn})} \quad (9)$$

where $t_{50\%}$ and k_{yn} represent the time required to reach 50% of antibiotics breakthrough (hr) and the constant rate of Yoon-Nelson (hr^{-1}), respectively.

5.3.5 Data collection and ANN modelling

The findings of continuous column tests were used to develop computer models involving several different parameters, including adsorbent mass, particle size, contact time and flow rate. The key objective of this was to perform a complex and accurate process analysis. The empirical values of input and output are normalized and ranged between 0.1 - 0.9. This reduced the complexity of the calculations and avoided overtraining.

$$\text{Normalized value } (A_i) = \frac{A_i - A_{min}}{A_{max} - A_{min}} \times (0.9 - 0.1) + 0.1 \quad (10)$$

In this equation, A_{min} and A_{max} represent the network's minimum and maximum value, respectively, whilst A_i is any value (Hosseinzadeh et al., 2020a).

For this study, MATLAB R2018b was used to develop ANN models to predict the antibiotics removal using a GAC adsorption column. The three stages carried out in ANN modelling are train, validate, and test. Thus, the models are trained and evolved at the training stage, after which the developed models were validated and tested. The input, hidden, and output layers are present in every ANN model created. A model process is performed to identify the number of neurons in the hidden layer. The percentage removals of SMX, SMZ and SDZ were employed as output variables for the generated models, whereas particle sizes, contact duration, flow rates, and adsorbent mass were utilized as input variables. This was applied to all three models. The mean absolute error (*MAE*) and the coefficient of determination (R^2) were applied as statistical markers to calculate the accuracy of the models in all the train, validate, and test stages, as displayed Table 5-3. The empirical results were separated randomly into two sections of 80% and 20% to model the processes. For the first section, the following percentages were employed for the train, validate and test stages: 70%, 15% and 15% respectively. The second section was used as an extra test to confirm the model's viability.

Table 5-3 Error functions equations

Index	Equations
Mean absolute error	$MAE = \frac{1}{N} \sum_{i=1}^N y_{prd,i} - y_{Act,i} $
Determination coefficient	$R^2 = 1 - \frac{\sum_{i=1}^N (y_{prd,i} - y_{Act,i})}{\sum_{i=1}^N (y_{prd,i} - y_m)}$

where $y_{prd,i}$ and $y_{Act,i}$ represent predicted ANN model values and actual empirical values, respectively, y_m is the mean of experiential data; and N is the total number of data (Chen et al., 2022; Hosseinzadeh et al., 2020a).

The models were developed using the Levenberg-Marquardt backpropagation training technique. In addition, hidden layers used the tangent sigmoid transfer function (tansig), while the output used a linear transfer function (purelin). Several different neurons in the hidden layer of neural networks (ranging from 1 - 20) were evaluated to determine the optimal number. Furthermore, the modelling process was repeated five times, and this enabled a model to be created with the least errors, and highest precision and output predictions.

5.3.6 Sample analysis

Both the cation concentrations (Na^+ , K^+ , Mg^{2+} , Ca^{2+}) and anion concentrations (SO_4^{2-} , Cl^- , PO_4^{3-} -P, NO_3^- -N) were analysed by inductively coupled plasma mass spectrometry and ion chromatography (Thermo Fisher Scientific), respectively. NH_4^+ -N and NO_2^- -N concentrations were analysed using Spectroquant ammonia and nitrite test kit, respectively. DOC was analysed using Analytikjena Multi N/C 2000. Before the analysis, a 0.45 μm filter was used to filter each sample. The antibiotic concentrations in the urine samples were measured using LCMS-8060 (Shimadzu), equipped with a CORTECS C18+ 2.1 mm \times 75 mm, 2.7 μm and operated using an electrospray ionisation (ESI) source. The ESI's positive mode was employed for all antibiotics that were simultaneously revealed. More precisely, there were two mobile stages used for these analyses: mobile A stage was 100% methanol, while mobile B stage was MQ-water with 0.1%

formic acid. The gradient elution utilized was persistent at a flow rate of 0.4 mL min^{-1} . Mobile stage A was kept at 30% (0.01 to 0.29 min), raised to 95% (0.2 to 7 min) and kept at 30% (7 to 7.50 min). Considering the multiple reaction modes, they were selected as follows: SDZ (251.1 > 156.1, 251.1.1 > 92.1), SMX (254.1 > 156, 254.1 > 92), and SMZ (279.1 > 186, 279.1 > 92.1). Calibration curve was made for each antibiotic at various concentrations (2-1000 nM) with correlation coefficients (R^2) above 0.99.

5.4 Results and discussion

5.4.1 Influence of the volumetric flow rate

Figure 5-1 shows the breakthrough curves experiments for column antibiotic adsorption in nitrified urine. The breakthrough curves exemplify C_t/C_0 (C_t and C_0 the effluent concentration and the influent concentration at various time) versus time (hr). The graph displays how the fixed-bed antibiotics adsorption was influenced at different flow rates. Additionally, the breakthrough curve form was highly impacted by the ratio of adsorption/mass transferring from the solution to adsorption active sites within the particles of GAC. At lower flow rates, the breakthrough curves were closest to the S-shaped, indicating higher rate of adsorption at a higher hydraulic retention time. On the contrary, Table 5-3 displayed that at higher flow rates, both the time of breakthrough point, and saturation decreased for all the three antibiotics. This is due to the increased loading rate of antibiotics inside the fixed bed column at higher flow rates resulting in quicker saturation. Regarding the maximum adsorption capacity (q_t), volume treated at breakthrough (V_b), and breakthrough point ($t_{5\%}$) in table 5-4, the values were $\text{SMZ} > \text{SMX} > \text{SDZ}$, showing that SMZ has the highest affinity for GAC adsorption. In contrast, SDZ shows the least affinity towards GAC adsorption amongst the three studied antibiotics. The highest adsorption capacities calculated were 2.70, 2.78, and 2.90 mg/g at 0.06 L/hr flow rate ($EBCT$ of 0.0225 h), which reduced to 1.21, 1.67, and 2.09 mg/g at 0.18 L/hr of flow rate for SMZ, SMX and, SDZ, respectively. Although the rate of antibiotics mass ($EBCT$ of 0.0075 h) loading increased at higher flow rates, the reduction in the adsorption capacity at the higher flow rates might be explained by

inadequate residence time for antibiotics adsorption in the fixed-bed GAC column including probable hydraulic short-circuiting. Such experience has already been noted by other researchers in column experiments that involved antibiotic adsorption and was attributed to the lower residence time in the fixed bed as the flow rate increased (Sotelo et al., 2013).

Table 5-4 show efficiency and fixed bed column parameters obtained from the breakthrough curves for GAC adsorption of antibiotics in the nitrified urine. These parameters showed increasing operating times at $t_{5\%}$ and a larger V_b when lower flow rates were used. $FBU (q_b/ q_t)$, the ratio of antibiotics adsorbed at breakthrough point to that adsorbed at saturation varied from 0.010 – 0.007 at a flow rate of 0.06 L/hr, however reduced to between 0.007 – 0.002 at a flow rate of 0.18 L/hr. Other studies have found similar reduction in FBU values at higher flow rates which is likely attributed to short residence time for sufficient contact between the GAC and pharmaceuticals to allow adsorption (Tor et al., 2009). When the flow rate is increased, the U_r value also increased significantly and this is because, the high flow rates caused the fluid film surrounding the particles of GAC to become thinner, which causes a reduction in mass transfer resistance and an increase in mass transfer rate. This occurs because the U_r value rises at increased flow rate (Almuntashiri et al., 2022; Jaria et al., 2019).

Table 5-4 provides specific details about the experimental parameters of competence and mass transfer obtained from empirical breakthrough curves for pharmaceuticals adsorption by GAC on fixed-bed column. $t_{5\%}$ (time and breakthrough), V_a (volume treated at breakthrough), q_b (adsorption capacity at the breakthrough point), q_t (highest adsorption capacity at saturation), EBCT (empty bed contact time), h_{MTZ} (height of mass transfer zone) and U_r (usage rate), $t_{exp.50\%}$ (the experimental time required to reach 50% of micropollutant breakthrough).

Antibiotics	Experiments condition			V_b (L)	$t_{5\%}$ (hr)	q_b (mg/g)	q_t (mg/g)	EBCT (hr)	$t_{exp.50\%}$ (hr)	U_r (g/L)	h_{MTZ} (cm)	FBU
	Q (L/hr)	m (g)	Particle size (μm)									
SDZ		0.5		0.18	3	0.020	2.70		14	2.77	0.426	0.007
SMX	0.06		425	0.3	5	0.026	2.78	0.0225	15.8	1.66	0.425	0.009
SMZ				0.48	8	0.030	2.90		19	1.04	0.425	0.010
SDZ				0.11	1.9	0.007	2.15		10	4.54	0.428	0.003
SMX	0.06	0.5	600	0.18	3	0.016	2.38	0.0225	11.3	2.77	0.427	0.004
SMZ				0.27	4.5	0.022	2.72		13.2	1.85	0.426	0.008
SDZ				0.084	1.4	0.005	1.74		7	5.95	0.429	0.002
SMX	0.06	0.5	1000	0.102	1.7	0.007	1.95	0.0225	8.2	4.90	0.428	0.003
SMZ				0.12	2	0.011	2.24		9.8	4.16	0.427	0.005
SDZ	0.06	0.8	425	0.48	8	0.03	2.96		19.5	1.66	0.693	0.010

Antibiotics	Experiments condition			V_b (L)	$t_{5\%}$ (hr)	q_b (mg/g)	q_t (mg/g)	EBCT (hr)	$t_{\text{exp.50\%}}$ (hr)	U_r (g/L)	h_{MTZ} (cm)	FBU
	Q	m	Particle									
	(L/hr)	(g)	size (μm)									
SMX				0.96	16	0.043	3.15	0.04	24.2	0.83	0.690	0.014
SMZ				1.08	18	0.05	3.40		27.4	0.74	0.689	0.01
SDZ				2.1	35	0.05	4.01		43.5	0.71	1.284	0.012
SMX	0.06	1.5	425	2.52	42	0.07	4.13	0.073	52.3	0.59	1.277	0.017
SMZ				2.76	46	0.10	4.33		53.2	0.54	1.27	0.023
SDZ				0.06	0.5	0.006	1.47		3.1	8.33	0.428	0.004
SMX	0.12	0.5	425	0.12	1	0.012	2.10	0.011	3.8	4.16	0.427	0.005
SMZ				0.24	2	0.022	2.35		4.6	2.08	0.426	0.009
SDZ				0.032	0.18	0.003	1.21		1.9	15.62	0.429	0.002
SMX	0.18	0.5	425	0.072	0.4	0.008	1.67	0.0075	2.8	6.94	0.427	0.004
SMZ				0.09	0.5	0.016	2.09		4.3	5.55	0.426	0.007

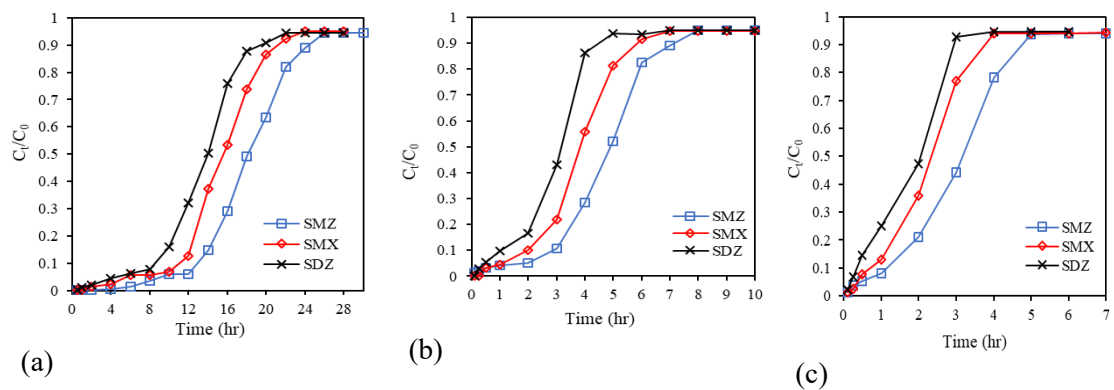


Figure 5-1 Breakthrough curves at various flow rates for antibiotics adsorption by GAC (a) 0.06; (b) 1.2 and (c) 1.8 L/hr; $m = 0.5$ g, particle size = $425 \mu\text{m}$ and $C_0 = 10 \mu\text{M}$.

5.4.2 Influence of the bed heights

The experimental columns were set at different heights, reflected by the GAC mass of 0.5 g (0.45 cm), 0.8 g (0.7 cm) and 1.5 g (1.3 cm), to assess the effect of column height on adsorption performance and the breakthrough curve, as shown in Figure 5-2. As expected, smaller adsorbent mass led to a quick breakthrough and saturation of the GAC column compared to larger adsorbent mass because of the limited adsorption sites and higher adsorption rate, consistent with findings elsewhere (Baral et al., 2009). More adsorbent mass inside a column can lead to a longer breakthrough time and higher processed urine volumes due to higher diffusion of antibiotic into the solid particles (Feizi et al., 2021).

Symmetrical and calculated parameters of the fixed bed column adsorption are presented in table 5-4. The value patterns for V_b , q_t , and $t_{5\%}$ were $\text{SMZ} > \text{SMX} > \text{SDZ}$, which very similar to those observed earlier at different flow rates. It is important to note that there was an increase in the mass adsorption capacity and FBU at a higher column height or adsorption mass. This is due to the increase in the available adsorption sites where the addition of more adsorbent mass increases the column height, which in turn increases the travel time and contact time between the adsorbent and the antibiotics. Ultimately, this causes much greater adsorption at

breakthrough and enhance the q_b , q_t and FBU (Sotelo et al., 2013).

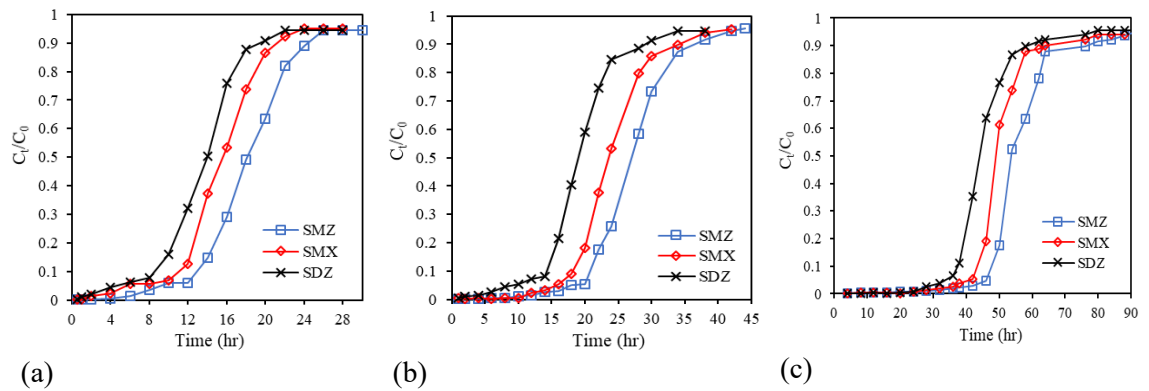


Figure 5-2 Breakthrough curves at various adsorbent mass for antibiotics adsorption by GAC (a) 0.5 (b) 0.8 and, (c) 1.5 g; particle size= 425 μm , $Q= 0.06$ L/hr, and $C_0 = 10$ μM .

5.4.3 Influence of the particles sizes

The column experiments were conducted to evaluate the effect of the GAC particle size on the adsorption performance, as presented in Figure 5-4. Both the breakthrough point and saturation time decreased for all antibiotics with larger particle size. A smaller GAC particle size led to a slower breakthrough and saturation than a bigger GAC particle size due to a shorter diffusion path for micropollutants resulting in an increase in micropollutant permeation on GAC pores, thereby, increasing adsorption (Pauletto et al., 2021). As observed, the GAC particle size of 425 μm displayed the maximum surface area (988.751 m^2/g) and pore volume (see Table 5-1), and therefore, increased active sites on surface area to capture more micropollutants. Based on the breakthrough curves, the efficiency and mass transfer parameters were acquired from for the antibiotics and nitrified urine experiments were presented in Table 5-4. The highest adsorption capacities calculated were 2.70, 2.78 and 2.90 mg/g with the smallest particle size (425 μm) which reduced to 1.74, 1.95 and 2.24 mg/g with the largest particle size (1000 μm) for SMZ, SMX and SDZ, respectively. Based on these findings from the continuous fixed-bed GAC column adsorption of antibiotics, the smallest particle size of (425 μm) was selected for all subsequent experiments.

Compared to the previous research by Sun et al. (2018) tested batch treatment using combined biochar and hydrogen peroxide (H₂O₂) processes to remove sulfonamide antibiotics (at an initial concentration of 10 µM) in hydrolysed urine. The results showed that sulfamethazine, sulfamethoxazole, and sulfadiazine were removed at rates of 74%, 49% and 39%, respectively, at 1g/L after 5 days from the adsorption process. However, the authors indicated that after H₂O₂ (1 mM) was added to biochar (1g/L) sulfamethazine, sulfamethoxazole, and sulfadiazine were degraded by approximately 60% after 1 hour. In addition, hydrophilic substances such as sulfadiazine, sulfamethoxazole, and sulfamethazine cannot be easily removed by MBR, resulting in low removal rates, around 50% (Lastre-Acosta et al., 2020). However, our results are similar with the previous study in the literature, indicating that the adsorption removal for each of sulfadiazine, sulfamethoxazole, and sulfamethazine using GAC was higher than 95% (Aslan & Şirazi, 2020; Nam et al., 2014). Given GAC's high efficiency in removing these antibiotics, its adsorption capabilities can be effectively applied to remove antibiotics from nitrified urine.

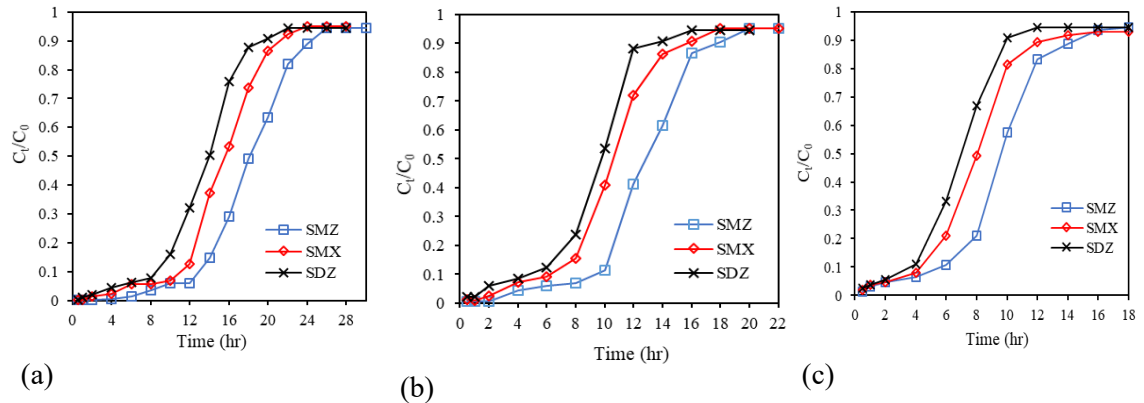


Figure 5-3 Breakthrough curves at various particle sizes for antibiotics adsorption by GAC (a) 425 µm (b) 600 µm and (c) 1,000 µm; $Q = 0.06$ L/hr, $m = 0.5$ g and $C_0 = 10$ µM.

5.4.4 Breakthrough curve modelling

An analytical modelling was used to determine the breakthrough curves and predict the efficiency and effectiveness of fixed bed column adsorption. The experimental data presented in

the breakthrough curves were described using the Yan, Thomas and Yoon-Nelson models, as shown in Figure 5-4. Meanwhile, table 5-4 shows the determination coefficients and theoretical parameters of mathematical models under various design operational conditions. In comparison to the Yan model, the Thomas model provides a better fit for antibiotics adsorption data from a GAC column experiments, particularly towards the saturation zone, as displayed in Figure 5-4. The value of k_{th} in the Thomas model increased at higher flow rates but decreased when a larger GAC mass or column bed height were employed, as shown in Table 5-5, which indicates that there was a decline in mass transfer resistance. Ultimately, this causes a decrease in pivotal dispersion and the thickness of the fluid film on the surface of particles. Huang et al. (2022) reported similar results with SMX adsorption on the modified biochar with higher k_{th} values at lower adsorbent mass. Moreover, when examining the SMX column adsorption by sugarcane bagasse, Juela et al. (2021), found that values k_{th} were higher at lower flow rates. Therefore, it can be assumed that a higher flow rate increases the mass transfer driving force in the liquid film. Furthermore, using Thomas model (equation 7), the highest capacity for the antibiotics was calculated and their projected values (shown in Table 5-5) were closely similar to those obtained from the experiments. Nonetheless, the q_0 values decreased at high flow rates, smaller adsorption bed height and bigger GAC particle size. As presented in Figure 5-4, the regression coefficient R^2 values generated through the Thomas kinetic model were 0.98, 0.96 and 0.97 for SMZ, SMX and SDZ, respectively which are in line with the experimental outcomes.

Considering Yoon-Nelson model, the projected time necessary to reach a 50% antibiotic breakthrough is assumed ($t_{pred.50\%}$). Table 5-4 shows that the model parameter, $t_{pred.50\%}$ increased when the GAC mass was increased but decreased when the flow rate increased. The projected values of $t_{pred.50\%}$ decreased from 13.7-18.6 to 1.903.0 (hr) when the flow rate increased from 0.06 to 0.18 L/hr, which was close to the computed empirical values presented in Table 5-4. On the other hand, the rate constant value K_{yn} decreased with a higher GAC mass and increased with a bigger GAC particle size and higher flow rate. Figure 5-4 depicts the Yoon-Nelson model's breakthrough curve was well fitted to experimental data, in addition to the elevated Yoon-Nelson

regression coefficients R^2 values 0.98, 0.96 and 0.97 for SMZ, SMX and SDZ, respectively. The results presented in Table 5-5 thus point out that both the Thomas and Yoon-Nelson models are effective in predicting the breakthrough curves for the antibiotics adsorption in GAC column, except the Yan model.

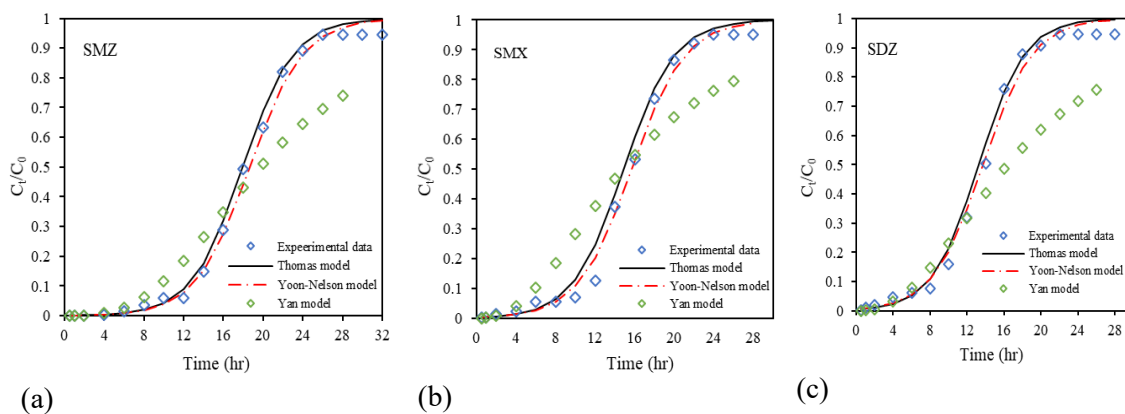


Figure 5-4 Modelling breakthrough curves for antibiotics adsorption on GAC ($Q = 0.06$ L/hr; $C_0 = 10$ μ M; particle size= 425 μ m and $m = 0.5$ g).

Table 5-5 Thomas, Yan and Yoon-Nelson models parameters acquired from breakthrough curves for antibiotics via GAC on the column.

	Experimental conditions			Thomas model			Yan model			Yoon-Nelson model		
	Flow rate (L/hr)	Mass (g)	Particle size (μm)	q_0 (mg/g)	K_{th} (L/hr/mg)	R^2	q_Y (mg/g)	α	R^2	$t_{pred.50\%}$ (hr)	K_{yn} (hr ⁻¹)	R^2
SDZ				4.45	0.038	0.97	2.04	0.014	0.86	13.70	0.38	0.97
SMX	0.06	0.5	425	4.86	0.036	0.96	1.93	0.013	0.85	15.76	0.38	0.96
SMZ				6.59	0.035	0.98	2.83	0.013	0.86	18.64	0.37	0.98
SDZ				2.75	0.044	0.97	1.26	0.010	0.79	9.33	0.45	0.97
SMX	0.06	0.5	600	3.41	0.041	0.98	3.29	0.007	0.92	10.90	0.44	0.98
SMZ				4.78	0.039	0.98	2.04	0.012	0.81	13.02	0.43	0.98
SDZ				2.25	0.062	0.93	0.75	0.013	0.94	7.70	0.67	0.93
SMX	0.06	0.5	1000	2.81	0.046	0.94	1.01	0.013	0.93	8.77	0.5	0.98
SMZ				3.68	0.045	0.96	1.34	0.012	0.90	9.18	0.49	0.96
SDZ				3.70	0.025	0.97	1.80	0.012	0.81	20.76	0.26	0.97
SMX	0.06	0.8	425	4.61	0.027	0.97	2.43	0.014	0.71	26.15	0.26	0.98

	Experimental conditions			Thomas model			Yan model			Yoon-Nelson model		
	Flow rate (L/hr)	Mass (g)	Particle size (μm)	q_0 (mg/g)	K_{th} (L/hr/mg)	R^2	q_Y (mg/g)	α	R^2	$t_{pred.50\%}$ (hr)	K_{yn} (hr ⁻¹)	R^2
Antibiotics												
SMZ				5.35	0.027	0.98	2.98	0.014	0.76	29.16	0.25	0.98
SDZ				5.53	0.014	0.93	1.17	0.028	0.90	46.70	0.16	0.93
SMX	0.06	1.5	425	5.93	0.012	0.92	2.19	0.019	0.72	52.70	0.15	0.92
SMZ				6.96	0.011	0.94	2.16	0.020	0.80	55.97	0.13	0.94
SDZ				2.20	0.098	0.94	0.18	0.019	0.88	3.30	1.09	0.94
SMX	0.12	0.5	425	2.68	0.088	0.99	0.25	0.020	0.84	3.86	1.06	0.99
SMZ				3.85	0.072	0.98	0.42	0.017	0.77	4.66	0.90	0.98
SDZ				1.92	0.14	0.94	0.078	0.027	0.91	1.90	1.63	0.94
SMX	0.18	0.5	425	2.09	0.16	0.98	0.106	0.030	0.90	2.37	1.68	0.98
SMZ				3.25	0.11	0.98	0.183	0.025	0.85	3.00	1.30	0.98

5.4.5 Antibiotics removal via ANN modelling

Figure 5-5 shows the results of the antibiotics removal predicted by ANN modelling and plotted against actual removal rates. These findings indicate that the topologies for 4-4-1, 4-17-1, and 4-15-1 indicating 4, 17, and 15 neurons in hidden layers were the best fitting for SMZ, SMX and SDZ models, correspondingly. Moreover, the coefficients for the train, validation and test data showed that the models all performed well in predicting outputs (see Figures S2-S6). In Figure 5-5, the values of R^2 for all the developed models were 0.993, 0.994 and 0.993 for SMZ, SMX and SDZ, respectively indicating the high correlation of predicted values with the actual values. Subsequently, Figure 5-6 shows the residual errors of the MAE models, the MAE values of SMZ, SMX, and SDZ were 3.039, 2.421, and 3.628 respectively, and these errors are minimal. The effectiveness of the models at removing SMZ, SMX and SDZ from nitrified urine solutions was therefore observed to be 99.3%, 99.4%, and 99.3%, respectively.

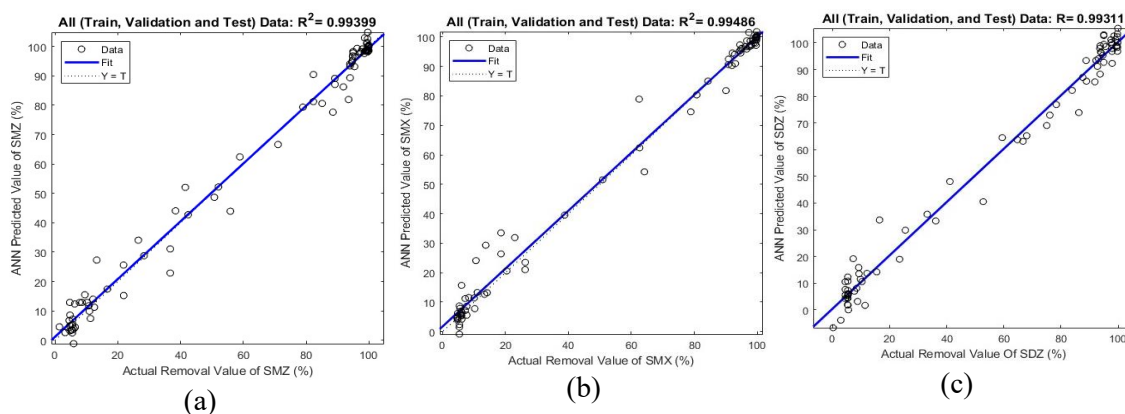


Figure 5-5 Illustration the values of ANN predicted and actual for all stages of (a) SMZ, (b) SMX and (c) SDZ removal models.

Equation -11 below is used for the prediction for all antibiotics removal via the ANN models. Tables S2-S6 displays the weights and biases values for all the three antibiotics used in this study.

ANN equation = $Purelin(W2$

$\times \tansing(W1 \times [contact\ time; particle\ size; adsorbent\ mass; flow\ rate]b1) + b2)$

As observed in Figure 5-6, the distribution of residual error was insignificant in the estimation of SMZ, SMX, and SDZ, with MAE of 3.039, 2.421, and 3.628 respectively, meaning that the developed models could mimic well with the actual data. As shown in Figure 5-7, the additional tests demonstrated considerable performance in estimation of the R^2 for SMZ, SMX and SDZ with and MAE of (0.99, 0.97, and 0.98) and (2.92, 6.65, and 5.95) respectively.

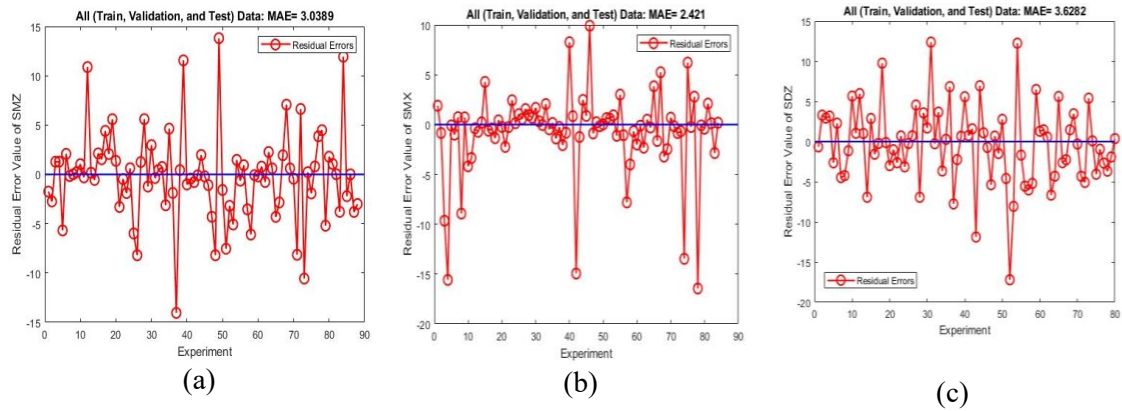


Figure 5-6 The residual errors distribution of evolved ANN models for (a) SMZ, (b) SMX and (c) SDZ.

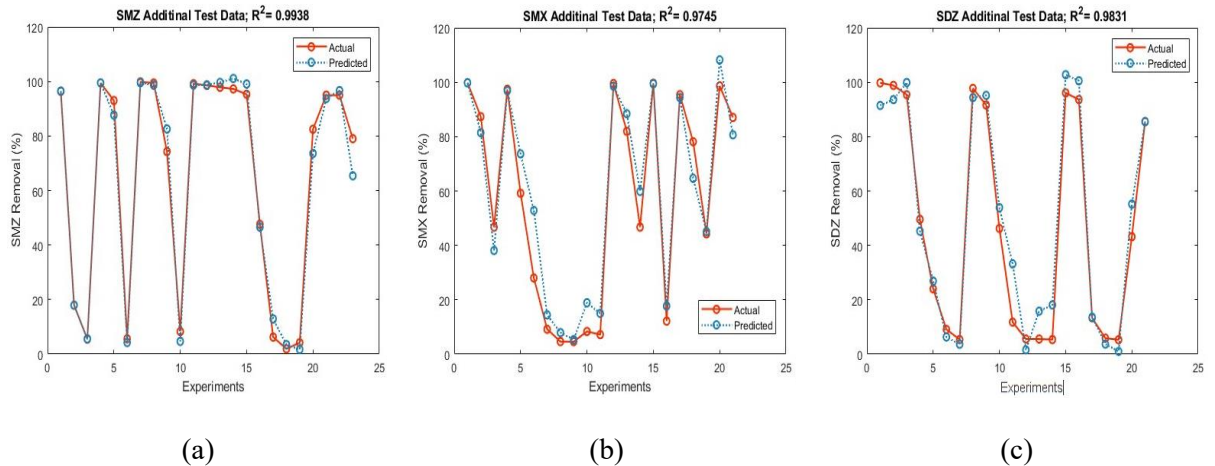


Figure 5-7 Illustration the experimental value versus predicted value of normalised removal from

developed ANN models for (a) SMZ, (b) SMX and (c) SDZ.

Our earlier studies also found that ANN models are effective and highly accurate in predicting pharmaceutical adsorption using GAC column Almuntashiri et al. (2021). For example, ANN models were able to predict the elimination of naproxen, acetaminophen, metronidazole, carbamazepine and ibuprofen from nitrified urine with the R^2 values of 99.1%, 99%, 99.1%, 99.2% and 98.4%, respectively. Pauletto et al. (2021) corroborated that the ANN models were satisfactory and highly accurate ($R^2=0.99$) in predicting experimental value versus the expected value of pharmaceuticals removal by activated carbon adsorption. Moreover, Hernández-Hernández et al. (2017) also found that ANN models were more accurate in forecasting the binary adsorption of heavy metals in bone char columns. Because of the high accuracy of ANN models, these models can be used successfully to estimate antibiotics removal.

5.4.6 Antibiotics adsorption on GAC

The characteristics of GAC such as porosity, pore size distribution, surface area and granular size are significant in identifying the adsorption affinity and adsorption capacity of various antibiotics. Most adsorption processes occur when macro-pores serve as the passages for the adsorbate to access the micropores. Therefore, surface charge of GAC's plays an essential role in determining the proportion and level of antibiotic adsorption. In our previous work, the GAC showed a point of zero charge (pH_{PZC}) at a pH value of 4.8 implying that the GAC is negatively charged in the nitrified urine (pH 6.2). Furthermore, the electrostatic and hydrophobic interactions could have a meaningful impact on antibiotics adsorption mechanism on the GAC (Nam et al., 2014; Sotelo et al., 2014).

In order to understand the electrostatic interactions, the GAC surface charge and the acid dissociation constants (pK_a) of the antibiotic are important properties to be considered. The respective pK_a values of the antibiotics reflect their charge characteristics as shown in Table S1. SMZ possessed positive charges, whereas SMX and SDZ possessed negative charges. SMX and

SDZ are negatively charged in the nitrified urine (pH 6.2) because of which electrostatic repulsion is expected with the negatively charged GAC surface however, their high removal rates suggest a lesser role played by the electrostatic interactions during the adsorption process. Thus, their adsorption affinity with the GAC surface could be due to other interaction forces such as hydrogen bonding or π - π bonding, etc. that could have resulted in their removal even though both adsorbent and adsorbate possess similar charges. Other studies have reported that π - π and hydrogen bonding interactions contributed significantly to adsorption mechanisms between SMX and SDZ with activated carbon's (Ahmed et al., 2017; Hongsawat & Prarat, 2022; Serna-Carrizales et al., 2021). On the other hand, SMZ is positively charged in the nitrified urine and is expected to exhibit electrostatic attractions which likely explains the higher adsorption capacity for SMZ compared to SMX and SDZ on the GAC surface.

Another alternative adsorption mechanism is the hydrophobicity, an essential property affecting the adsorption affinity process of antibiotics on the adsorbent, expressed in $\log K_{ow}$ (Choi et al., 2005; Jamil et al., 2019; Liu et al., 2010; Yu et al., 2008). An elevated $\log K_{ow}$ value infers a higher hydrophobicity suggesting an increased adsorption affinity of antibiotics on the GAC surface. The $\log K_{ow}$ parameters for the above three substances are SMX > SMZ > SDZ. Although the $\log K_{ow}$ the SMX was the highest however it shows a relatively lower sorption affinity for SMX compared to SMZ. Yu et al. (2008) proposed that a modified $\log K_{ow}$ parameter could be employed using equation 12 in order to comprehend the sorption affinities, regardless of their acidic or basic status.

$$\log K_{ow} = \frac{K_{ow}}{(1 + 10^{(pH-pK_a)})} \quad (12)$$

The modified $\log K_{ow}$ value of SMX was estimated to be 0.017 in the nitrified urine at pH of 6.2 using equation-12 and these pKa and K_{ow} values (see Table S1) are less than the equivalent value for SMZ of 0.60. In addition, a high molecular weight forms another variable affecting the adsorption mechanism. In this way, SMZ's higher hydrophobicity explains the increased

adsorption capacity observed in this study. Based on these observations, electrostatic and hydrophobic interactions both play a significantly role in the adsorption mechanism of antibiotics on the GAC surface depending on the properties of the antibiotics.

5.5 Conclusion

The performance of GAC column adsorption in removing three selected micropollutants from a real nitrified urine (pilot MBR permeate) was investigated in this study. Breakthrough point and saturation times were affected by the flow rate (*EBCT*), particle size, and mass of adsorbent in the GAC column studies. Surface with larger particle sizes observed a breakthrough point occurring quicker, which ultimately lead to faster adsorbent saturation. Moreover, the faster breakthrough time and saturation occurred when the operational conditions were applied using less mass of adsorbent, and a higher flow rate also resulting in reduced urine treatment. The antibiotic adsorption affinities were $SMZ > SMX > SDZ$, which suggests that SDZ is limiting of the three in the design of GAC column adsorption. The findings of this work indicate that physicochemical characteristics, $\text{Log } K_{ow}$ and the molecular weight of antibiotics impact GAC adsorption. The Thomas model best described the breakthrough curves while the Yoon Nelson model fitted well with the empirical data for described 50% of the fixed bed column saturation period. The ANN models were relatively effective in predicting the experimental and expected values of antibiotics removal from nitrified urine by GAC column adsorption. This study suggests that GAC column adsorption can be highly effective in the removal of the three most found antibiotics from the nitrified urine thereby making the urine derived fertiliser safe for growing food.

Acknowledgements

This study was supported by the Australian Research Council Industry Research Hub (IH210100001), Government of Tuvalu with GEF/UNEP (PRO20-9802), UTS Cross - faculty collaboration scheme (PRO21-12519).

CHAPTER 6 Assessing chemical regeneration of GAC saturated with pharmaceuticals

6.1 Abstract

This chapter addresses the fourth objective of our thesis, which investigates the feasibility of on-site chemical regeneration methods for granular activated carbon (GAC). The purpose is to provide a cost-effective alternative to off-site thermal regeneration for removing problematic pharmaceuticals from wastewater treatment applications. The study evaluated the effectiveness of three different regenerant solutions, namely inorganic solutions sodium hydroxide (NaOH) and hydrochloric acid (HCL), and organic solution methanol (MeOH), in desorbing five target pharmaceuticals in batch tests. Results indicated that the hydrophobicity and aqueous solubility of the pharmaceuticals were the most significant factors affecting desorption efficiency. The study found that MeOH was more efficient in desorbing the target micropollutants compared to the inorganic solutions, suggesting that MeOH has the ability to effectively desorb both hydrophilic and hydrophobic substances. The desorption efficiencies achieved with the MeOH regenerant solution ranged from approximately 40.68-75.15%, with the efficiency varying depending on the pharmaceutical.

Keyword: Desorption, Regeneration efficiency; Granular activated carbon; Pharmaceuticals; Isotherm study

6.2 Introduction

Over many years, the process of granular activated carbon (GAC) adsorption has been widely employed as a treatment method for removing the micropollutants, odour, taste and colour from different wastewater resources (Larasati et al., 2021). During adsorption process, micropollutants compounds are adsorbed within the GAC pores and surface, and with time GAC become saturation gradually. When saturation stage, or prior that if the GAC performance is inadmissible, the GAC process can no longer persist, thereby the regeneration operation is performed; this is the best option in terms of more cost-effective to length the GAC life instead of its replacement or disposal. The presence of pharmaceuticals like metronidazole, which rapidly saturate the GAC, can lead to more frequent exhaustion of the adsorbent, requiring frequent regeneration. (Almuntashiri et al., 2021; Nguyen et al., 2013).

Numerous techniques have informed for regenerating GAC such as the conventional ones: thermal (Guo & Du, 2012; Marques et al., 2017), chemical regeneration (García-Reyes et al., 2021; Larasati et al., 2020; Ying et al., 2022), microwave (Foo & Hameed, 2012) and electrochemical processes (Weng & Hsu, 2008). Thermal regeneration is one of the most used techniques for GAC regeneration. However, there are some drawbacks to using this technique, such as the fact that spent GAC must be transported to a specialised facility off-site for regeneration. Furthermore, the more repeated regeneration rises operation cost because of high GAC usage and reduced GAC service. Ordinarily 10% of GAC is lost during thermal regeneration because of excessive burn-off and attrition, necessitating the replacement of lost GAC with virgin GAC. Due to the reasons mentioned above, various the on-site regeneration studies have informed over many years ago that will be as alternates to thermal regeneration (Larasati et al., 2020). One of an effective alternate to regenerate the GAC is chemical regeneration technique that can be carried out on-site at a low energy cost via exposing the saturated GAC to chemical regenerants to desorb the micropollutants, also minimum loss of GAC, and without the requirement for particular treatment where the chemical regeneration effectiveness depends on the interaction

among GAC and micropollutants.

Nitrification is a biological oxidation process in which the ammonia/ammonium present in the hydrolysed urine is converted into nitrite via ammonia-oxidizing bacteria. The nitrite is then further converted into nitrate via nitrite-oxidizing bacteria. The urine processed through a biological nitrification in a MBR is termed as nitrified urine. The nitrification process has been recommended recently as a promising approach to remove drug contaminants from contaminated water (Volpin et al., 2020b). A MBR technique has been proposed as a recent solution for removing pharmaceuticals from industrial and wastewater. The outcomes of the studies have demonstrated the acceptability of this technique for removing pharmaceuticals like risperidone, enalapril, and atenolol, achieving a removal rate of over 95%. However, it proved to be unsuitable for hydrophilic pharmaceuticals such as naproxen, metronidazole, and carbamazepine, where the removal rate was around 40%. (Hai et al., 2011b; Tadkaew et al., 2011). A review of existing literature designates that there are limited research about regenerate the GAC after pharmaceuticals removal from nitrified urine. The study presents a comprehensive analysis of the adsorption and desorption characteristics of specific micropollutants, along with their desorption performance when subjected to different regenerant solutions. The study used nitrified urine (MBR permeate), which is intended to aid in understanding the behaviour of the studied GAC, its adsorption mechanisms, and the impact of regeneration for additional reuse. This knowledge can potentially lead to a reduction in resource consumption, environmental impact, and costs in wastewater treatment applications.

6.3 Material and Methods

6.3.1 Pharmaceuticals and adsorbent

In this work, a five pharmaceuticals compounds have been chosen based on their different physicochemical characteristics such as (molecular structure, molecular size and hydrophobicity), their happening in urine compositions, and also their excretion pathway from human urine with

high percentage around 60% -90% as presented in Table 6-1. All pharmaceuticals were purchased from Sigma Aldrich, including acetaminophen (APAP), carbamazepine (CBZ), ibuprofen (IBP), metronidazole (MTZ), and naproxen (NPX). All five pharmaceuticals were spiked in the MBR permeate urine with an initial concentration of 50 μM . The commercial GAC was utilised in this experiment that was provided by James Cumming & Sons. Beforehand GAC used, it was washed and then dried it at 100 $^{\circ}\text{C}$ for 1 day in oven. The surface area, pore volume, particle size of GAC characteristics were 878.311 m^2/g , 0.498 cm^3/g and 1000 μm , respectively.

Table 6-1 Physicochemical characteristics of the chosen pharmaceuticals.

Compounds	Molecular		Dissociation		Excretion percentage ^a	Water Solubility ^b (g/L)
	weight (g/mol)	Log K _{OW} ^a	constant (pKa) ^a			
Ibuprofen	206.28	3.50	± 4.41 ± 0.10		60 %	0.021
			0.23			
Acetaminophen	151.16	0.48	±		(60-90 %)	14
			0.21	1.72 ± 0.50		
Naproxen	230.26	2.88	± 4.84 ± 0.30		80 %	0.016
			0.24			
Carbamazepine	236.27	1.89	±		72 %	0.018
			0.59	13.94 ± 0.20		
Metronidazole	171.15	-0.14	± 2.58 ± 0.34		77 %	9.5
			0.30	14.44 ± 0.10		

^a Data from (Nguyen et al., 2012)

^b Obtained from (Almuntashiri et al., 2021)

6.3.2 Adsorption experiments

Experiments were performed to study the adsorption isotherm using varying doses of GAC (25,

50, 75, 85, and 100 mg) added to 50 mL of MBR permeate in Erlenmeyer flasks. After that, the erlenmeyer flask was placed on a mechanical shaker flat at 190 rpm until the adsorption process had achieved complete equilibrium. The adsorption experiments process was performed at 20 ± 1 °C, the concentrations of pharmaceuticals were measured using the analytical methods outlined in next section both before and after the adsorption process. The amount of adsorbed pharmaceuticals was calculated by:

$$\text{Adsorption capacity } (q_{\text{adsorption}}) = \frac{V(C_0 - C_t)}{m} \quad (1)$$

here, $q_{\text{adsorption}}$ is the amount of adsorbed pharmaceuticals ($\mu\text{mol/g}$), V is the solution volume (L), C_0 and C_t are the initial and equilibrium pharmaceuticals concentrations ($\mu\text{mol/L}$) and m is the GAC mass.

6.3.3 Desorption experiments

Three different chemical reagents - HCl, NaOH, and MeOH - were investigated to find the best eluent for desorption. After the adsorption tests were completed, the solution was decanted, and 50 mL of the selected chemical solution was added to the Erlenmeyer flasks containing the exhausted GAC. The flasks were then shaken at 190 rpm for 240 minutes to facilitate desorption of the pharmaceuticals. To calculate the pharmaceutical desorption capacity (in $\mu\text{mol/g}$) and efficiency (%), using Eqs. (2) and (3);

$$\text{Desorption capacity } (q_{\text{desorption}}) = \frac{V_i(C_i)}{m} \quad (2)$$

$$\text{Desorption efficiency } (\%) = \frac{q_{\text{desorption}}}{q_{\text{adsorption}}} \times 100 \quad (3)$$

Where, C_i is the amount of pharmaceuticals desorbed from GAC saturated ($\mu\text{mol/g}$), V_i is chemical regenerant solution (L), Desorption efficiency (%) is the amount of desorbed

pharmaceuticals ($\mu\text{mol/g}$) was measured and divided by the mass of the exhausted GAC used in the adsorption process ($\mu\text{mol/g}$).

6.3.4 Influence of contact time chemical regenerant concentrations

Kinetic research was conducted to explore the desorption behaviour of medicines using 80 mL Erlenmeyer flasks filled with 50 mL of MeOH as the chemical reagent. The flasks were put on a mechanical shaker at a constant speed of 190 rpm, and the tests were carried out across time intervals ranging from 5 to 240 minutes. Samples were collected, filtered, and examined at each time point to assess the quantity of desorbed pharmaceuticals. To obtain insight into the desorption mechanism, the resultant kinetic data were fitted to both pseudo-first order and pseudo-second-order kinetic models.

Three distinct regenerants were tried to see how varied chemical solvent concentrations affected desorption efficiency. MeOH demonstrated the maximum desorption efficiency for pharmaceuticals among them and was so chosen for further testing. To establish the appropriate MeOH concentration, solutions of 25%, 50%, 75%, and 100% were produced. Desorption experiments were subsequently carried out utilising these varied MeOH concentrations, as detailed in section 6.3.3.

6.3.5 Regeneration and reusability experiments

A batch experiment was carried out to evaluate the efficacy of the GAC in four sequential cycles of pharmaceutical adsorption and desorption. The desorption studies were carried out in 80 mL Erlenmeyer flasks containing 25 mg of GAC material, with an eluent of 50 mL of MeOH solution. The flasks were stirred for 240 minutes to enhance the pharmaceuticals desorption from GAC. Each cycle employed the same GAC, and the adsorption and desorption procedures were performed four times. This enabled us to evaluate the GAC's regenerability and reusability for removal of pharmaceuticals. The regeneration efficiency was calculated as follow:

$$\text{Regeneration efficiency (\%)} = \frac{q_{\text{adsorption (re-use)}}}{q_{\text{adsorption}}} \times 100 \quad (4)$$

Here, regeneration efficiency (%) is calculated by dividing the adsorption capacity of the regenerated GAC after a specific re-use cycle by the adsorption capacity of the fresh GAC at the start of its service life.

6.3.6 Pharmaceuticals analysis

To measure the concentration of pharmaceuticals, liquid chromatography mass spectrometry, supported by a C18+ Column, 2.7 μm , 2.1mm \times 75 mm, was used. The ESI negative mode was applied for NPPX and IBP, while the ESI positive mode was utilized for the analysis of MTZ, APAP and CBZ, where all the analytes were discovered at the same time. There are two mobile phases A and B were applied which are Milli-Q water and MeOH, respectively. During gradient elution, a steady flow rate (0.4 mL/min) was maintained, with the following pattern: mobile phase B was kept at 50% from 0.01 to 0.10 minutes, raised to 95% from 0.10 to 1.50 minutes, held at 95% from 1.50 to 3.50 minutes, and then lowered to 50% from 3.51 to 5.50 minutes. The multiple reaction mode was chosen as follows: NPX (229 > 185, ES-), MTZ (172 > 128, ES+), APAP (152 > 110, ES+), CBZ (237 > 194, ES+) and IBP (205 > 161, ES-). Individual calibration curves of pharmaceuticals were created with various concentrations of 5, 10, 20, 50, 100, and 1000 nM the determinations coefficient (R^2) were more than 0.999.

6.4 Results and discussions

6.4.1 Adsorption Isotherm

The properties of adsorption layers can be investigated with the use of adsorption isotherms. The micropollutant adsorption equilibria on GAC were determined in the current work by employing and comparing Langmuir and Freundlich models (Figure 6-1). The elevated determination coefficient parameters, i.e. R^2 , suggested that the basic parameters from the Langmuir model

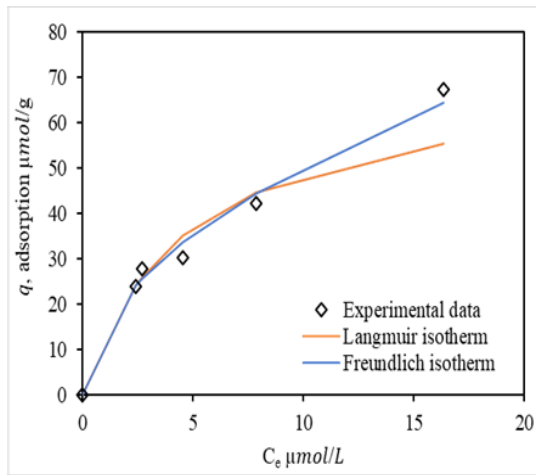
offered a superior fit. The latter was used to estimate the pharmaceutical GAC monolayer uptake capacity. The results indicated that on the GAC surface, the target compounds' respective maximum adsorption capacities (q_{max}) were dictated by their hydrophobic properties. CBZ has the highest adsorption capacity compared to the other compounds due to its considerably higher hydrophobicity. MTZ, on the other hand, which is hydrophilic, had the lowest adsorption capacity of the chemicals examined. The Freundlich model is used to explain the adsorption equilibrium of heterogeneous surfaces, and its parameters offer important information regarding the interactions between the pharmaceuticals and GAC. The data in Figure 6 1 show that the Freundlich model accurately represented the experimental outcomes.

Table 6-2 The parameters of Freundlich and Langmuir isotherm data on GAC.

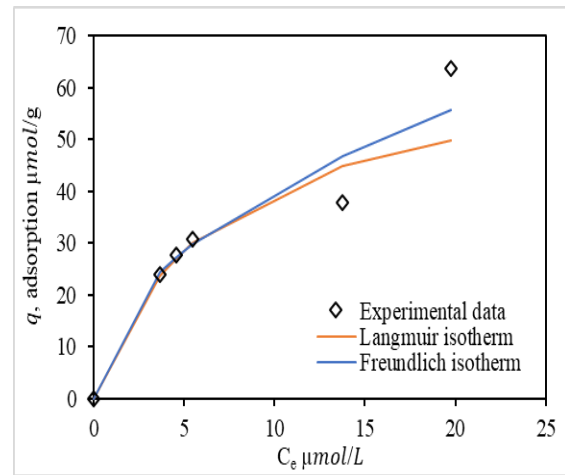
Parameters		NAP	CBZ	APAP	IBP	MTZ
Freundlich	$K_f (\mu\text{mol/g})(\text{L}/\mu\text{mol})^{1/n}$	12.75	15.33	12.18	13.46	13.46
	1/n	0.49	0.51	0.32	0.41	0.26
	R^2	0.89	0.96	0.98	0.99	0.89
Langmuir	$q_{max} (\mu\text{mol/g})$	66.67	71.42	42.01	57.14	40
	$K_L (\text{L}/\mu\text{mol})$	0.14	0.21	0.18	0.16	0.19
	R^2	0.90	0.91	0.93	0.98	0.87

The highest q_{max} (435 mg/g, CBZ) was thought to indicate the influence of its molecular configuration on the acid dissociation constant, pKa. Depending on the aqueous phase pH, ionisable substances are present as either cations or anions, and the fluctuating GAC surface charge can be either positive or negative, thus impacting electrostatic interactions (Almuntashiri et al., 2022; Calisto et al., 2015). In nitrified urine, NPX and IBP gave rise to a negative charge as their pKa parameters were less than that of the solution (6.2) which, in turn diminished NPX and IBP molecular interactions with the GAC surface negative charge. Additional van der Waals forces or hydrogen bonds may therefore impact the latter association. Electrostatic interactions

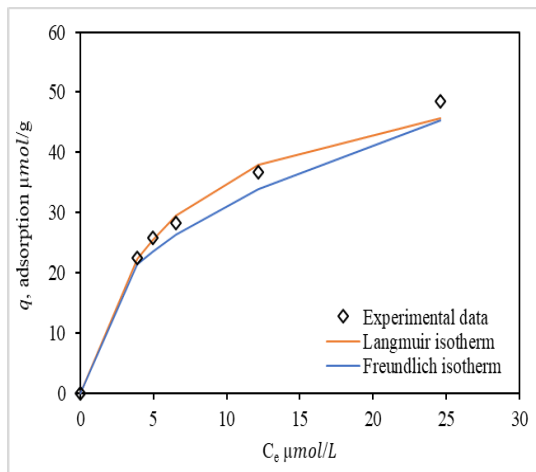
occur in relation to CBZ, MTZ and APAP in nitrified urine owing to their neutral charge (Almuntashiri et al., 2021; Solanki & Boyer, 2017). MTZ exhibited the lowest adsorption on GAC as compared to APAP. According to the outcomes, it can be concluded that the MTZ adsorption onto GAC is mostly physisorption and weakens significantly within the measured pH range. Moreover, a second investigation found that the pH range of the solution had no effect on MTZ removal (Rivera-Utrilla et al., 2009). The adsorption efficiency could therefore be ascribed to key physicochemical characteristics, such as polarisability, the partition coefficient of octanol and water, and increased molecular weight (Ahmed, 2017).



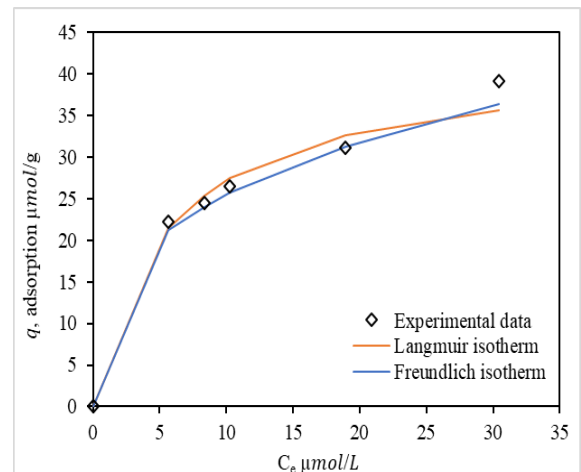
(a)



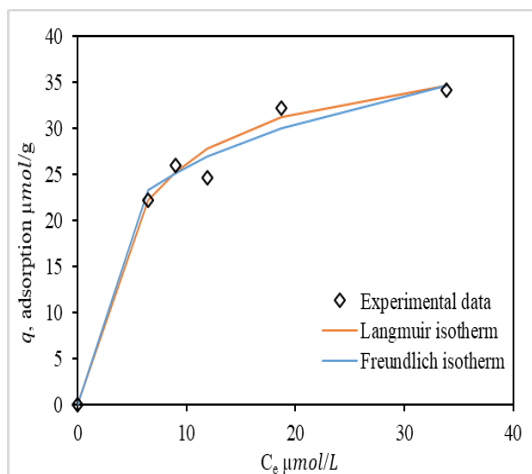
(b)



(c)



(d)



(e)

Figure 6-1 Depicts the results of empirical adsorption experiments for adsorption of CBZ (a), NAP (b), IBP (c) APAP, (d) and MTZ (e).

6.4.2 Desorption experiments

The five pharmaceuticals compounds and three alternate regenerant solvent solutions were applied to evaluate the chemical regeneration performance, and compound solubility, the effect of pH, and interactions among the pharmaceuticals, regenerant and GAC through the regeneration experiments. For this study, three solvent diluents were selected, including two inorganic options consisting of NaOH and HCL, as well as one organic solvent, MeOH.

The pH level of inorganic solutions influences the surface charge of GAC. When both the GAC surface and the pharmaceuticals carry a negative charge, there is a possibility of repulsion between them, which can enhance the desorption process, vice versa.

CBZ is known to possess a strong adsorption for GAC and mostly in its neutral form in the levels of pH (2- 14), resulting in practically negligible desorption efficiency of CBZ with HCL and NaOH solutions. For APAP, the desorption efficiency of the HCL solution was a little greater than NaOH, as shown in Table 6-3, owing to APAP having a cationic form in neutral. This behaviour indicated that the pH element could significantly influence the GAC surface characteristics. In

HCL solution, the GAC surface has a positive charge because of acid functional groups protolysis, thereby driving the desorption of neutral organic molecules, owing to repulsion between the dissociated compounds and the surface of GAC. In neutral and high pH solutions, IBP and NPX exist predominantly in a dissociated, anionic form. Consequently, an enormous desorption of IBP and NPX in NaOH solution was expected, due to the electrostatic repulsion that occurs between the negatively charged GAC surface and the dissociated compounds. However, the results showed poor desorption of these compounds, indicating that other factors beyond electrostatic repulsion play a significant role in the adsorption mechanism. Out of all the pharmaceuticals examined, MTZ exhibited the lowest affinity for GAC adsorption and did not dissociate at any pH level in aqueous solutions; consequently, neither the NaOH nor the HCL solvents significantly enhanced the desorption of MTZ. Although there are studies have used HCL and NaOH solutions to regenerate the GAC exhausted, in this study, inorganic solvents have been observed to be inefficient (Larasati et al., 2020; Leng & Pinto, 1996).

The compounds hydrophobicity, which are reported as the octanol-water partition coefficient, could play a significant role in the regeneration process, typically expressed by $\log K_{ow}$. Pharmaceuticals that have a high positive $\log K_{ow}$ values and low solubility are hydrophobic in nature, and as a result, they have a tendency to desorb and stay within the solvent particles. The desorption efficiency of pharmaceuticals was found to be higher in the organic solvent as compared to the inorganic solvents, likely due to the greater solubility of the compounds in the organic solvent as presented in Table 6-3. The values of the $\log K_{ow}$ of the all pharmaceuticals was in the following order: IBP, NAP, CBZ, APAP and MTZ. Based on this description, the outcomes by MeOH displayed that the pharmaceuticals compounds with a relatively high hydrophobicity ($\log K_{ow}$ 3.5) and low solubility, namely, NPX, > CBZ and IBP, have a high desorption efficiency, compared to MTZ and APAP that have lower hydrophobicity ($\log K_{ow}$ 0.48) as shown in Table 6-1. Furthermore, to hydrophobicity, it was estimated that the desorption efficiency utilizing MeOH was associated with the solubility of the target micropollutants in MeOH. Nevertheless, although the solubility of MTZ and APAP in the MeOH solution was higher

than in water, this did not contribute to a significant desorption efficiency, meaning that the two micropollutants favoured staying adsorbed on the GAC instead of solvate in MeOH.

Table 6-3 Desorption efficiency (%) were acquired for chemical regenerant solvent solutions.

	1 M HCL	1 M NaOH	MeOH
CBZ	6.67%	3.12%	66.31%
APAP	9.72%	2.58%	40.68%
MTZ	3.21%	1.21%	45.62%
NAP	5.01%	11.01%	70.40%
IBP	5.69%	11.72%	62.64%

6.4.3 The Influence of MeOH concentration on desorption experiments

The interactions between the GAC and pharmaceuticals can be broken down by MeOH, which facilitates liberation of the pharmaceuticals into the solution and consequent desorption of the 5 pharmaceuticals. The desorption ratio rose as MeOH concentration increased, resulting in a top rising trend that reached its maximum value at 75% MeOH concentration, as illustrated in Figure 6-2. Desorption effectiveness for pharmaceuticals decreased with MeOH content in water, as predicted. The presence of water reduced MeOH's efficiency in desorbing the pharmaceuticals due to its high solubility in water. This is due to the fact that water molecules prefer to surround MeOH, generating a hydration shell that causes it to be too big to enter the GAC pores, decreasing its capacity to efficiently desorb the pharmaceuticals. The findings are consistent with prior research, which found that adsorbate desorption efficiency increased with higher ethanol concentrations (Chen et al., 2011; Daneshvar et al., 2017; Larasati et al., 2020; Wang et al., 2021). Owing to its high hydrogen bonding interaction with micropollutants and low polarity, a 75% concentration of MeOH solution was used in the following studies.

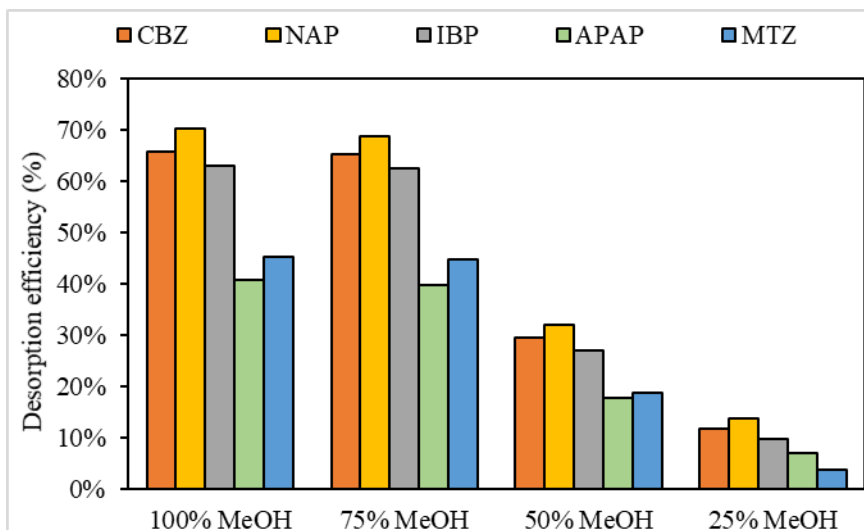


Figure 6-2 The impact of MeOH concentrations on desorption efficiency of CBZ, NAP, IBP, APAP, and MTZ.

6.4.4 Influence of contact time and kinetics models

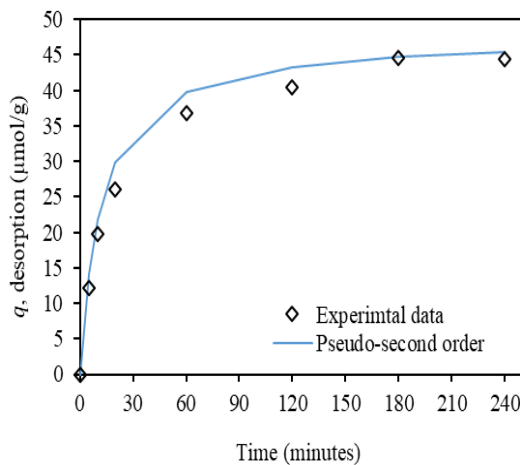
Contact time and the presence of MeOH solution both have a significant influence on the removal of pharmaceuticals from the GAC surface as well as their desorption kinetics. Figure 6-3 depicts the influence of contact time on pharmaceutical desorption at a 75% MeOH solution concentration. The data show that the desorption process happened quickly during the first 30 minutes. Following that, the rate of desorption dropped throughout the 30-120 minute period until reaching a steady level that stayed constant until the 240-minute interval. The preliminary rapid desorption process reflected the strong driving force generated by the high initial concentration in the solid phase together with the MeOH purity. Yet, as time passed, the pharmaceuticals' concentration in the solid phase declined while increasing in the liquid phase, resulting in a decrease in the pharmaceuticals' desorption rate until equilibrium was reached. Understanding desorption kinetics is critical for adsorbent design and regeneration, as well as selecting the optimal operational conditions for full-scale systems. To evaluate the desorption kinetics, a pseudo-first-order and pseudo-second-order kinetic equation was fitted to the experimental data, as published by (Chang et al., 2016; Njikam & Schiewer, 2012):

$$q_D = q_{0D}(1 - e^{-K_{P1D}t}) \quad (5)$$

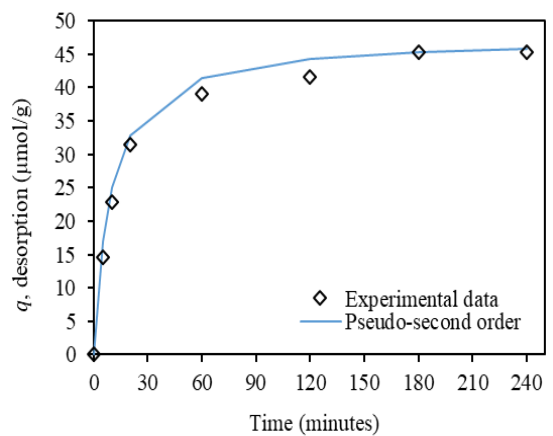
$$q_D = \frac{q_{0D}^2 \cdot K_{P2D} \cdot t}{1 + K_{P2D} \cdot q_{0D} \cdot t} \quad (6)$$

Where q_{0D} represents the amount of pharmaceuticals desorbed at desorption equilibrium ($\mu\text{mol/g}$); q_D represents the amount of desorbed ($\mu\text{mol/g}$); K_{P1D} is the reaction rate for the pseudo-first order (1/min); and K_{P2D} is the reaction rate for the pseudo-second order (g/ $\mu\text{mol} \cdot \text{min}$).

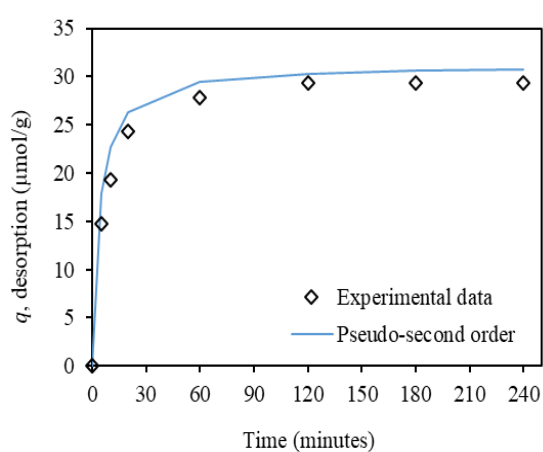
Table 6 4 displays the level of consent between the actual and model-predicted values using determination coefficients (R^2). The outcomes exhibited that the pseudo-second order equation predicted the equilibrium desorption capabilities (q_{0D}), more accurately, with estimated values closer to the empirical values than the pseudo-first order equation. The desorption process was discovered to be a pseudo-second order reaction as seen in Figure 6-3, implying that it was the rate-limiting phase. Consequently, the kinetic analysis findings indicate that the desorption process is critical in determining the overall efficiency of the system.



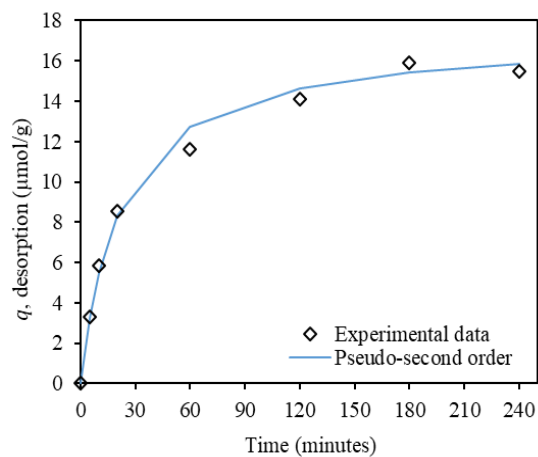
(a)



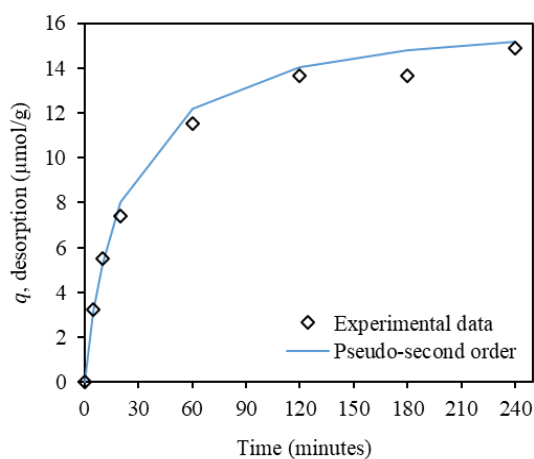
(b)



(c)



(d)



(e)

Figure 6-3 Kinetic modelling for pharmaceuticals desorption onto GAC of CBZ (a), NAP (b), IBP (c) APAP, (d) and MTZ (e).

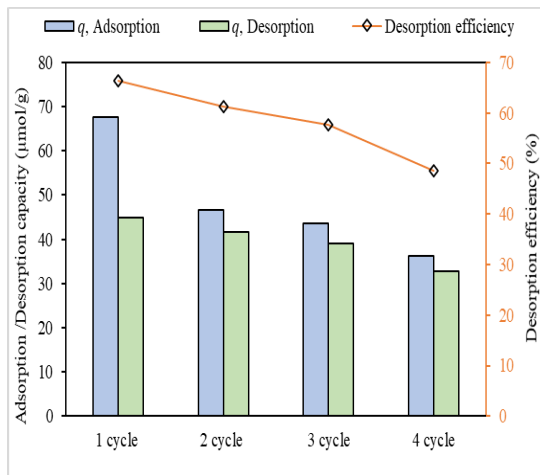
Table 6-4 Parameters of pseudo-second order for the target pharmaceutical adsorption on the studied GAC.

Model	Parameters	Pharmaceuticals				
		NAP	CBZ	IBP	APAP	MTZ
	$q, \text{Exp.}$	45.27	44.43	29.28	15.48	14.86
	($\mu\text{mol/g}$)					
	K_{P1D}	0.0023	0.0019	0.0085	0.0027	0.0028

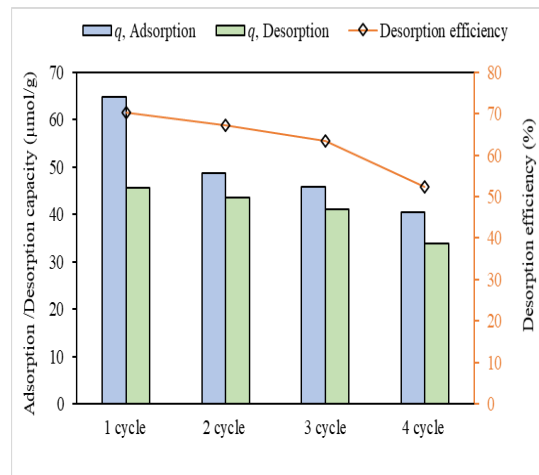
Pseudo-second-order	(1/min)					
	q_{0D}	47.61	45.45	31.25	17.24	16.66
	($\mu\text{mol/g}$)					
	R^2	0.99	0.99	0.99	0.99	0.99

6.4.5 Reusability: Adsorption and desorption

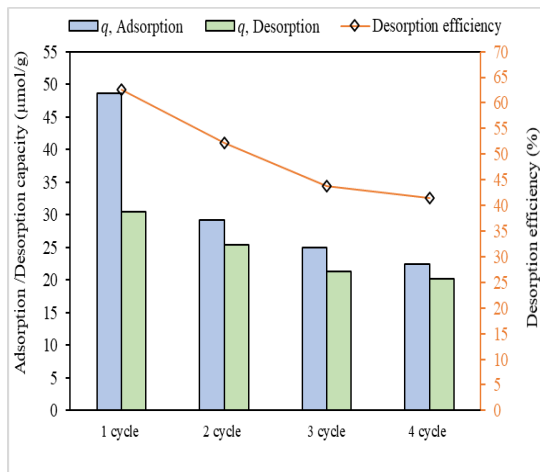
The major goal of the desorption tests is to determine the adsorbent's ability to be reused after the sorption process. This property is a key benefit for practical and cost-effective adsorbent applications. The viability of reusing the GAC was investigated in this work employing a series of 4th consecutive adsorption/desorption cycles using a MeOH solution as the eluent. These investigations were carried out in batch study to assess the adsorbent's capability for recurrent usage, as shown in Figure 6-4. Results for the five pharmaceuticals compounds can be noted, each cycle containing of the two columns, where the column represent the quantity of adsorption or desorption for adsorbate. As observed that, GAC can be able of adsorbing all pharmaceuticals after regeneration, although it is not complete removal of pharmaceuticals from GAC surface sites. It was also shown that the adsorption capacity value increased in subsequent cycles due to the emigration of adsorbed pharmaceuticals to alternate locations or deeper within the pores of the GAC. This procedure liberates surface adsorption sites, which can then be adsorbed in succeeding cycles. According to the data in Figure 6-4, it is clear that the desorption efficiency values decrease with each consecutive reuse of the GAC. After the 4th cycle, the reduction in desorption efficiency becomes more apparent.



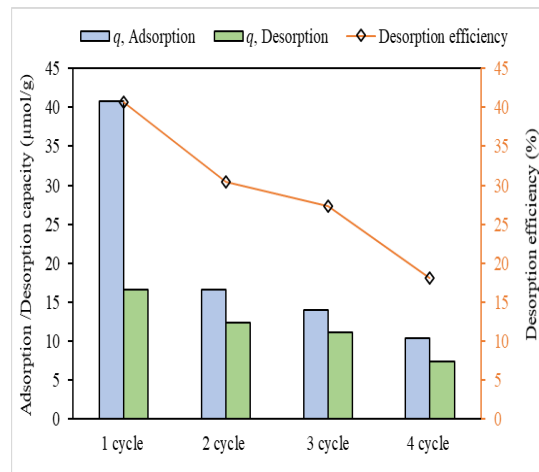
(a)



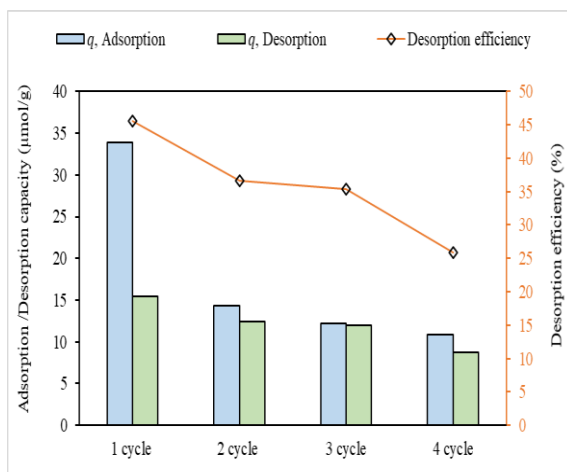
(b)



(c)



(d)



(e)

Figure 6-4 Adsorption/desorption cycles of pharmaceuticals onto/from GAC of CBZ (a), NAP

(b), IBP (c) APAP, (d) and MTZ (e).

Regeneration efficiency (RE), which provided an understanding of the adsorption capacity of the material following recycling, was computed using Eq. (4) which incorporates the relative adsorption abilities of the latter 3 cycles in comparison to the first. Table 6 5 summarises their findings. For the second cycle, regeneration efficiencies of over 75%, 68%, 59%, 42%, and 40% were reached for NAP, CBZ, IBP, MTZ, and APAP, respectively. After the fourth cycle, the efficiencies of the compounds were reduced by 62%, 53%, 46%, 32%, and 25%, respectively. This behaviour underscores the importance of solubility in the desorption of these adsorbates. This indicates that if an adsorbate is very soluble in a certain solvent, it will tend to desorb from the adsorbent and stay inside the solvent particles (Larasati et al., 2021).

Nonetheless, prior research has shed light on the effectiveness of certain regenerants. Notably, studies such as the one by Larasati et al. (2020) and Martin (1985) have demonstrated the efficacy of organic solvents as regenerants for pharmaceutical compounds. Larasati et al. achieved high regeneration efficiencies of 62.1%, 44.6%, and 67.9% for pharmaceuticals like phenol, nitrobenzene, and isoproturon using organic solvents, while inorganic solvent, sodium hydroxide, yielded lower regeneration efficiencies of 46.8%, 0.1%, and 4.2%, respectively. Martin's 1985 study revealed a regeneration efficiency of 51% for 2-chlorophenol using methanol as a solvent. Previous findings have demonstrated the effectiveness of chemical regeneration methods that involve using methanol as a solvent.

Table 6-5 Regeneration efficiency (%) acquired for consecutive cycles.

	Cycle		
	2	3	4
CBZ	68.69%	64.33%	53.46%
APAP	40.68%	34.22%	25.51%

MTZ	42.46%	36.17%	32.12%
NAP	75.15%	70.73%	62.47%
IBP	59.93%	51.34%	46.23%

6.5 Conclusion

A batch study was conducted to assess the adsorption/desorption of five medicines and three regenerant solutions to determine the practicality of in-situ chemical regeneration of GAC (laboratory grade HCL, NaOH, and MeOH). The efficacy of several regenerant solutions was investigated, and it was discovered that a MeOH solution was efficient in regenerating the GAC exhausted by NAP, CBZ, IBP, APAP, and MTZ, with regeneration efficiencies (RE) of 75%, 69%, 60%, 41%, and 42%, respectively. Desorption efficiency of pharmaceutical increased with concentration of the eluent used. During 4th consecutive adsorption/desorption cycles, the GAC mass was reusable. Nevertheless, the GAC performance was shown to be diminished in the subsequent adsorption phase, presumably due to the presence of non-desorbed medicines that remained on the GAC after regeneration. In my future studies, I intend to investigate the efficiency of using multiple regeneration cycles in fixed bed column tests, as well as the possible impact of chemical solutions on GAC properties, will be investigated in future study. The goal is to test the efficacy of chemical regeneration in extending the lifespan of the GAC fixed-bed column, reducing the requirement for complete thermal regeneration and carbon disposal. By incorporating these aspects into my future study, I aim to provide a more comprehensive and well-rounded understanding of the on-site chemical regeneration methods and their potential drawbacks and limitations.

CHAPTER 7 Conclusion and recommendations

7.1 Conclusion

The outcomes from the study indicate that the GAC adsorption process is effective for removing the selected pharmaceuticals under the studied conditions. The following conclusions have been drawn from the studies:

- (1) Experiments were carried out at the laboratory column scale to investigate the efficiency of removing target pharmaceuticals from synthetic stored and nitrified urine under various operational conditions. Both the breakthrough point, and saturation time were influenced by the mass of the adsorbent and the flow rate. Increasing the flow rate resulted in a faster breakthrough, quicker saturation, and exhaustion of the adsorbent. On the other hand, reducing the bed height led to a shorter breakthrough time and less urine volume for treatment. The investigation also illustrated that the adsorption of pharmaceuticals by GAC relies on their physicochemical characteristics, such as solubility in solution, molecular weight, and log K_{ow}. Furthermore, both Yoon-Nelson and Thomas models were effective in fitting and predicting experimental breakthrough curves for the GAC adsorption of fixed-bed columns.
- (2) Tests were carried out in batches to assess the adsorption kinetics, which explained how pharmaceuticals were eliminated from nitrified urine. The findings indicated that increasing the dose of GAC and the duration of contact time led to an improved elimination of pharmaceutical contaminants in nitrified urine. Therefore, optimizing the adsorbent dose and contact time can increase the elimination of pharmaceuticals. Although GAC adsorption eliminated a proportion of the nutrients (21% TN and 14% PO₄-P) from nitrified urine, it's important to note that GAC was more efficient in eliminating micropollutants while causing insignificant adsorption of nutrients from the nitrified urine. On the other hand, the ANN

models employed in this research exhibited a high level of accuracy in forecasting the removal of NAP, CBZ, APAP, IBP, and MTZ, with the predicted values closely aligning with the experimental values at 99.1%, 99.2%, 99.0%, 98.4%, and 99.1%, respectively.

(3) Batch experiments were conducted to assess the adsorption/desorption of five pharmaceuticals and three different regenerant solutions (HCL, NaOH, and MeOH). The effectiveness of various regenerant solutions was analysed, and it was found that MeOH was effective in regenerating the GAC that was exhausted by NAP, CBZ, IBP, APAP, and MTZ, achieving a regeneration efficiency of 75%, 69%, 60%, 41%, and 42%, respectively. The results showed that desorption efficiency of the pharmaceuticals increased with the concentration of the eluent used. The GAC mass was reusable for up to four consecutive adsorption/desorption cycles, but its performance was reduced in the subsequent adsorption process due to the presence of non-desorbed pharmaceuticals that remained on the GAC after regeneration. In addition, an isotherm study was conducted to examine the adsorption behaviour, and in most cases, the Fredulich model was observed to provide a little better fit than the Langmuir model. In contrast, the desorption behaviour was investigated using kinetic models, and the experimental data showed that the pseudo-second order model was a better fit than the pseudo-first model.

7.2 Recommendations and Future Work

(1) Human urine contains hundreds of thousands of different pharmaceutical compounds, but this study was limited to just few selected pharmaceutical compounds which does not simulate the real human urine scenario. It is important to extend the study to cover majority of all the pharmaceutical compounds to study the effectiveness of the GAC adsorption.

(2) While GAC adsorbent is effective in removing majority of the pharmaceuticals however, several others may not be removed easily. Other adsorbents including novel adsorbents could be explored for pharmaceuticals from the human urine.

(3) GAC adsorption process can be applied at any stages of the urine treatment train and this study evaluated pharmaceutical removal from hydrolysed urine (stored untreated urine) and nitrified urine (MBR effluent). Removal of pharmaceuticals from a concentrated urine should be explored as this involve significantly low volume of urine to be treated.

Appendix

Table S3.1. Synthetic hydrolysed compositions urine (Sun et al., 2018).

Compositions	Quantity
NH ₄ -Acetate	9.60 g/L
NH ₄ HCO ₃	21.4 g/L
NaH ₂ PO ₄	2.1 g /L
KCl	4.2 g /L
Na ₂ SO ₄	2.3 g/L
NaCl	3.6 g/L
NH ₄ OH (25% NH ₃)	13.0 ml

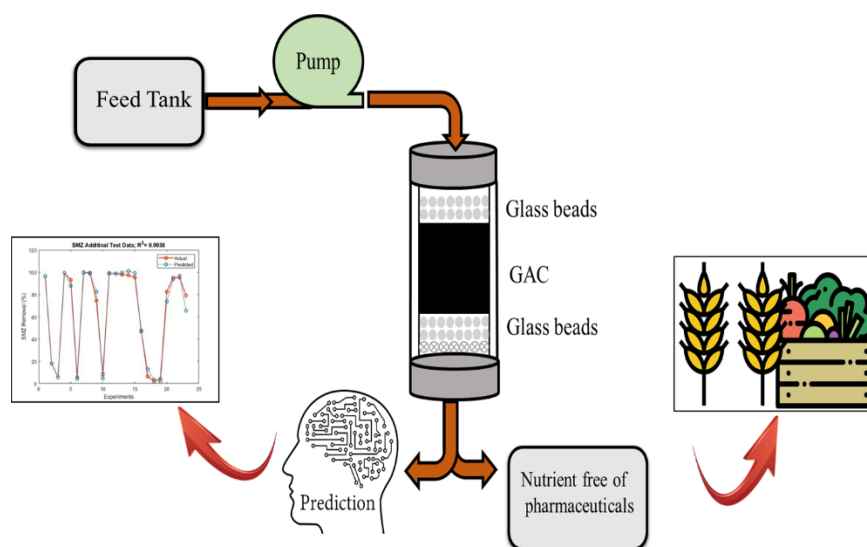


Figure S3.1. Schematic diagram of the fixed-bed column experiment.

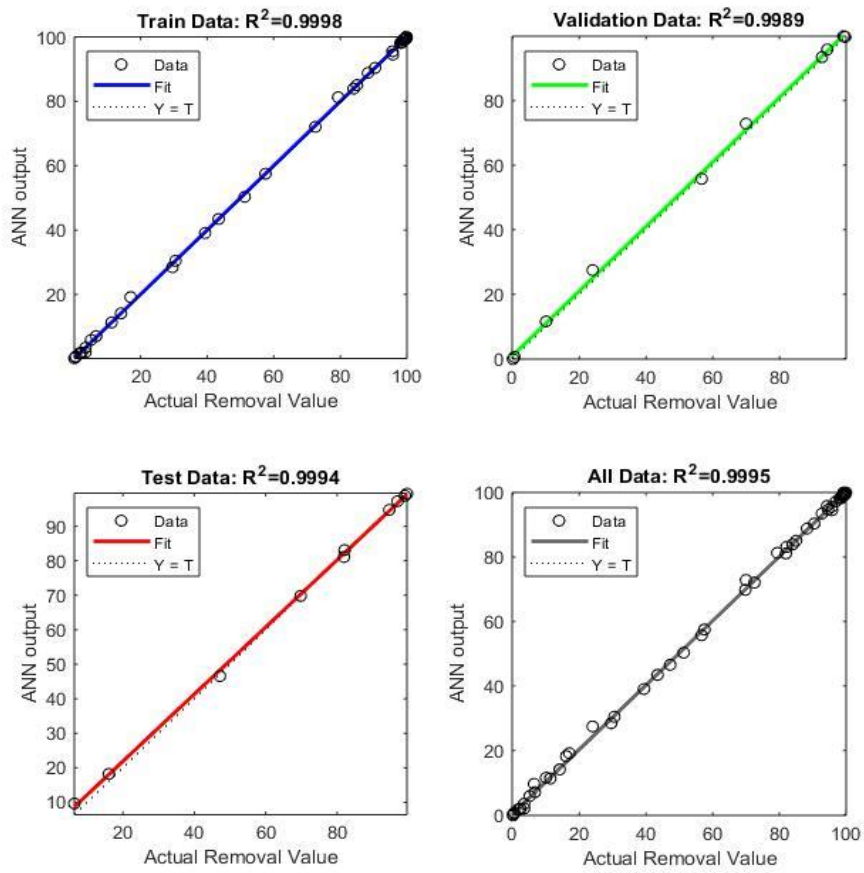


Figure S3.2. Scatter plots of values of predicated NAP versus the values of empirical data.

Table S3.2. Both weight and bias values of a trained ANN model for predicting NAP removal.

Neurons	IW					
	Adsorbent			LW	b1	b2
	Time	mass	Flow rate			
1	-3.26	-2.90	-0.50	0.78	3.01	
2	0.26	0.18	-3.82	-0.26	-2.75	
3	-5.72	5.51	-3.96	2.19	0.70	
4	3.47	-0.19	-0.72	1.25	-1.25	
5	-0.90	0.52	3.30	0.0017	1.30	
6	-3.35	2.58	-3.07	-1.33	0.12	-0.36
7	2.39	-0.81	0.78	2.72	-3.53	
8	1.34	1.12	-3.05	0.050	-0.40	
9	4.53	-1.67	-2.18	-0.990	-1.59	
10	4.31	0.16	-0.70	-0.425	-0.41	
11	1.27	-0.20	-3.59	0.301	1.90	
12	0.92	-2.86	1.70	-0.730	1.96	
13	-1.72	2.46	-2.28	0.155	-1.80	
14	-0.16	2.19	-2.87	-0.874	-2.39	
15	7.27	-0.12	-1.30	5.508	8.96	
16	11.06	-1.79	-3.30	-3.386	12.07	

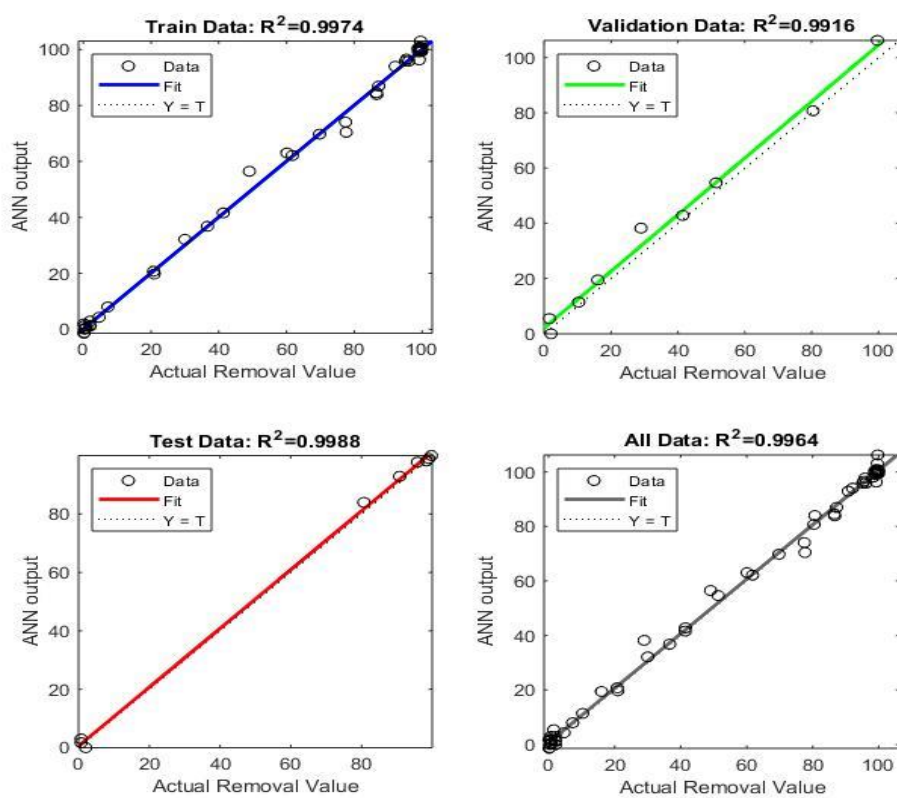


Figure S3.3. Scatter plots of values of predicated IBP versus the values of empirical data.

Table S3.3. Both weight and bias values of a trained ANN model for predicting IBP removal.

Neurons	IW					
	Adsorbent					
	Time	mass	Flow rate	LW	b1	b2
1	0.61	2.27	2.63	0.64	-3.51	
2	0.74	-2.58	-2.57	-0.58	-3.08	
3	-0.26	-2.83	2.08	-0.15	2.53	
4	12.18	-4.35	7.92	-1.95	-0.58	
5	-0.42	-1.97	-2.87	1.15	-1.92	
6	4.35	-3.28	-3.03	2.46	-0.27	0.87

7	4.85	-3.87	-3.28	-2.50	-0.11
8	2.93	2.60	-0.07	0.58	-0.35
9	4.38	-0.66	4.17	2.36	0.00
10	1.28	-1.01	-3.76	-0.15	1.19
11	1.54	-3.37	-0.69	-0.94	1.34
12	-0.49	2.92	-2.14	-0.12	1.48
13	4.91	0.22	0.92	-0.46	4.47
14	-0.97	2.73	1.23	-0.72	-3.16
15	0.81	-3.22	2.10	0.80	2.79
16	-4.86	1.03	-1.96	0.66	-3.44

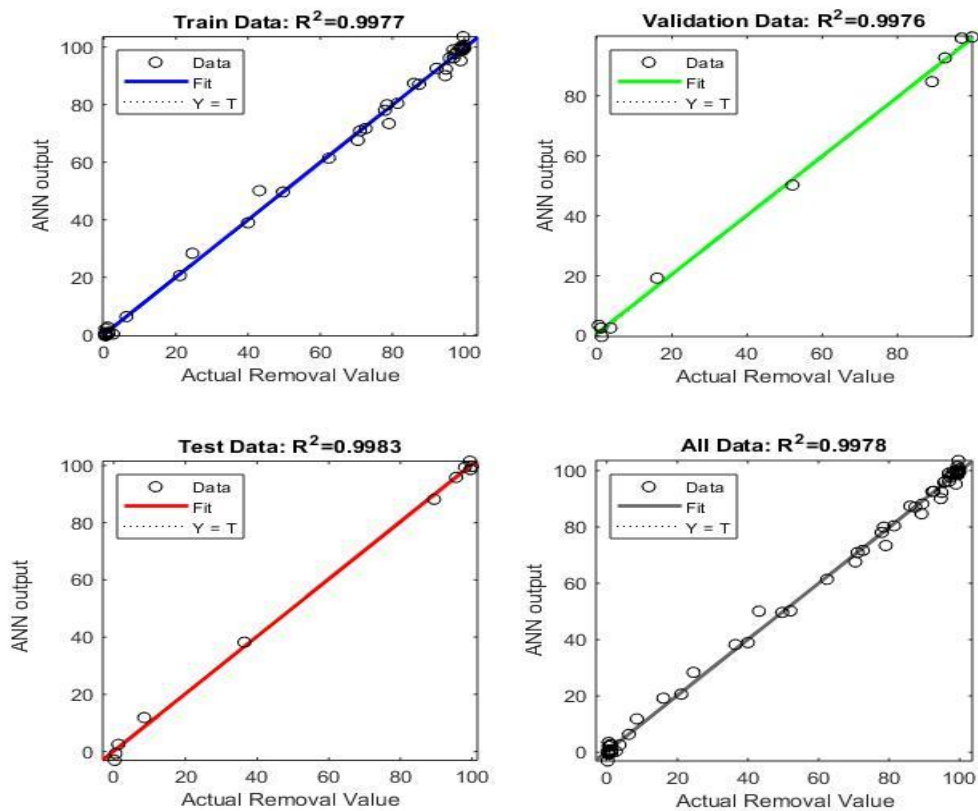


Figure S3.4. Scatter plots of values of predicated CBZ versus the values of empirical data.

Table S3.4. Both weight and bias values of a trained ANN model for predicting CBZ removal.

IW						
Neurons	Adsorbent					
	Time	mass	Flow rate	LW	b1	b2
1	2.77	0.66	-1.73	-0.71	-3.42	
2	4.95	-1.48	-3.10	-1.16	-2.05	
3	-0.90	-2.40	-1.77	-0.14	2.39	
4	2.05	-1.38	-0.71	0.46	-2.51	
5	-0.56	-0.68	2.29	-3.42	-1.14	
6	2.98	1.35	0.94	-0.90	-0.65	0.93
7	-2.49	2.43	0.44	-0.06	0.28	
8	-4.19	-1.18	-2.84	-1.64	-1.08	
9	-7.18	0.29	4.77	1.54	-5.01	
10	5.72	-1.08	-2.38	-2.74	6.53	
11	1.84	-1.60	-1.58	-1.10	4.44	
12	2.53	-1.31	-1.69	1.58	3.82	

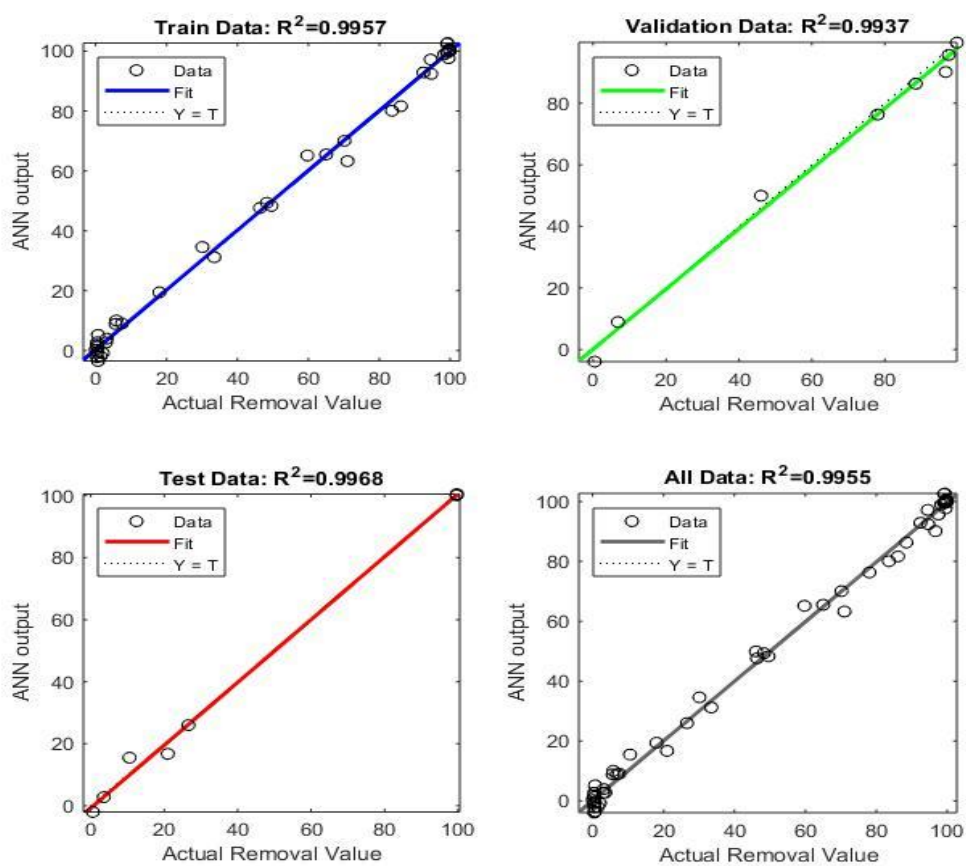


Figure S3.5. Scatter plots of values of predicated MTZ versus the values of empirical data.

Table S3.5. Both weight and bias values of a trained ANN model for predicting MTZ removal.

IW						
Neurons	Adsorbent					
	Time	mass	Flow rate	LW	b1	b2
	1	-2.12	-1.05	-2.18	0.88	3.29
2	0.85	-1.54	-2.91	1.33	2.43	
3	-1.97	-0.69	0.03	0.20	3.80	

4	4.33	0.04	0.89	-1.26	-1.85	
5	5.45	-3.44	6.40	-2.40	1.79	
6	-2.73	1.21	2.05	1.36	1.43	1.908
7	-0.56	3.16	-1.16	-0.39	-0.45	
8	-1.81	0.59	-2.40	-0.80	-0.59	
9	-3.29	0.13	-3.93	-1.68	-2.18	
10	1.68	-1.76	-2.42	1.95	2.04	
11	1.19	-2.42	-0.47	-1.95	3.80	
12	-8.29	-0.64	2.03	5.83	-11.47	

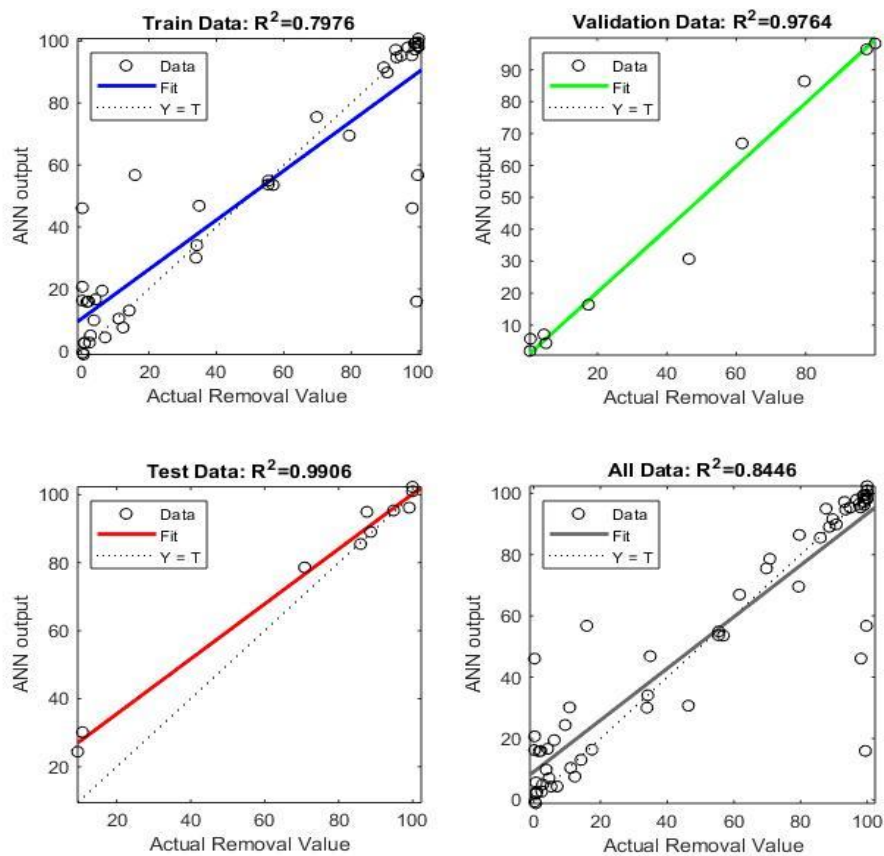
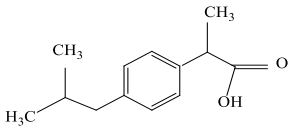
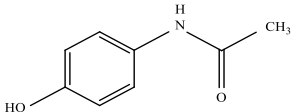
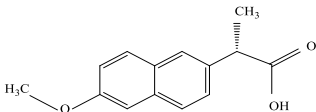
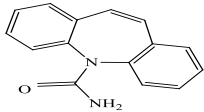


Figure S3.6. Scatter plots of values of predicated APAP versus the values of empirical data.

Table S3.6. Both weight and bias values of trained ANN for predicting the APAP removal.

IW						
Neurons						
	Adsorbent			LW	b1	b2
	Time	mass	Flow rate			
1	-1.25	-0.65	-2.24	1.15	4.37	
2	4.24	-1.27	-0.092	-0.97	0.89	
3	-9.45	-7.80	0.78	-0.04	-0.03	-1.128
4	36.93	-4.508	-13.01	0.84	10.86	
5	-25.40	-0.057	-2.10	0.88	-21.61	

Compound	CAS number	Molecular		Dissociation		Chemical structure ^a
		weight (g/mol)	Log K _{ow}	constant (pKa) ^a	Excretion percentage ^c	
Ibuprofen	15687-27-1	206.28	3.50 ± 0.23	4.41 ± 0.10	60 %	
Acetaminophen	103-90-2	151.16	0.48 ± 0.21	1.72 ± 0.50 9.86 ± 0.13	(60-90 %)	
Naproxen	22204-53-1	230.26	2.88 ± 0.24	4.84 ± 0.30	80 %	
Carbamazepine	298-46-4	236.27	1.89 ± 0.59	13.94 ± 0.20 -0.49 ± 0.20	72 %	

Metronidazole	443-48-1	171.15	-0.14 ± 0.30	14.44 ± 0.10	77 %
				2.58 ± 0.34	

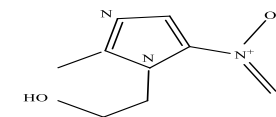


Table S4.1. Physicochemical properties of the chosen pharmaceuticals.

^a Data from (Nguyen et al., 2012)

^c Obtained from <https://www.medscape.com/>.

Table S4.2. Characteristics of GAC tested.

Specification	GAC
Iodine number (mg/(g min))	900
Ash content	5% max
Moisture content	2% max
Bulk density (kg/m ³)	250-300
Surface area (m ² /g)	950
Nominal size (m) ³	3 × 10 ⁻⁴
Type	Coal based

Table S4.3. The adsorption isotherm equations.

Model equation	Non-linear	linear
Langmuir	$q_e = \frac{q_{max}k_L C_e}{1 + k_L C_e}$	$\frac{1}{q_e} = \frac{1}{q_{max}} + \frac{1}{k_L q_{max} C_e}$
Freundlich	$q_e = K_f C_e^{\frac{1}{n}}$	$\ln q_e = \ln K_f + \frac{1}{n} \ln C_e$

where q_{max} represents the maximum adsorption capacity ($\mu\text{mol/g}$), k_L represents Langmuir constant ($\text{L}/\mu\text{mol}$), C_e represents the final concentration ($\mu\text{mol/L}$) and q_e represents the quantity adsorbed ($\mu\text{mol/g}$), K_f represents Freundlich constant ($\mu\text{mol/g}$) ($\text{L}/\mu\text{mol}$)^{1/n} and n (dimensionless) represents the intensity of adsorption.

Adsorption isotherm

Both Langmuir and Freundlich models were employed in the present study to explain the pharmaceuticals' adsorption equilibrium and their equations are summarised in Table S4. It is assumed in the Langmuir model that monolayer adsorption (when the layer of adsorbed is one molecule thick) can only take place at specific localized identical sites. Besides, the lateral interactions or steric hindrances do not occur among the adsorbed molecules, even on sites that are next to each other. This adsorption isotherm model is represented by the following (Eq. 2) (Kim et al., 2010):

$$q_e = \frac{q_{max}k_L C_e}{1 + k_L C_e} \quad (1)$$

In linear form, the Langmuir equation is presented as:

$$\frac{1}{q_e} = \frac{1}{q_{max}} + \frac{1}{k_L q_{max} C_e} \quad (2)$$

where q_{max} represents the maximum adsorption capacity ($\mu\text{mol/g}$), k_L represents Langmuir constant ($\text{L}/\mu\text{mol}$), C_e represents the final concentration ($\mu\text{mol/L}$) and q_e represents the quantity adsorbed ($\mu\text{mol/g}$). q_{max} and k_L are calculated by using the linear plot of $1/q_e$ versus $1/C_e$.

The Freundlich isotherm refers to heterogeneous surfaces. Moreover, the isotherm parameters provides important details about the interactions that take place between adsorbent and adsorbate.

The subsequent equation can be used to represent this (4) (Kim et al., 2010):

$$q_e = K_f C_e^{\frac{1}{n}} \quad (3)$$

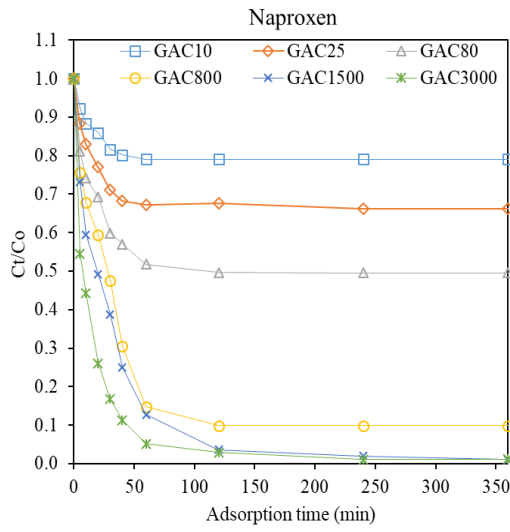
where K_f represents Freundlich constant ($\mu\text{mol/g}$) $(\text{L}/\mu\text{mol})^{1/n}$ and n (dimensionless) represents the intensity of adsorption. (Eq. 5) shows the linearisation Freundlich isotherm model as below (4):

$$\ln q_e = \ln K_f + \frac{1}{n} \ln C_e \quad (4)$$

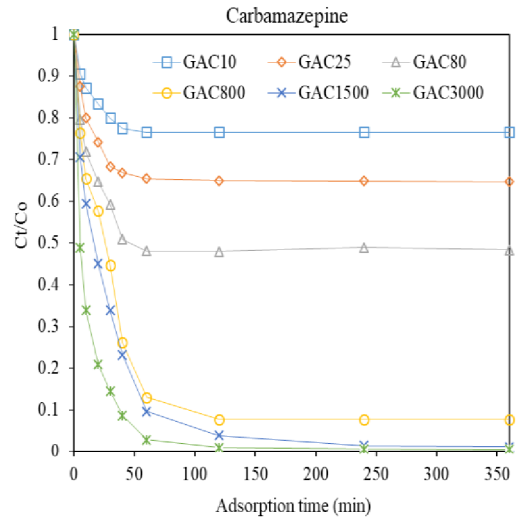
After linearly plotting the experimental data for $\ln(q_e)$ and $\ln(C_e)$, the intercept and slope may be used to estimate the values of K_f and n .

Table S4.4. The Freundlich and Langmuir isotherm parameters values on activated carbon.

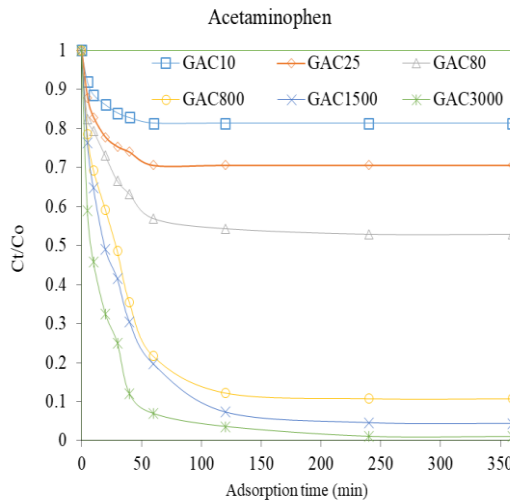
Parameters		Napro- xen	Carbama- zepine	Acetamino- phen	Ibupro- fen	Metroni- dazole
	$K_f (\mu\text{mol/g})(\text{L}/\mu\text{mol})^{1/n}$	32.97	60.1	19	19	18.45
Freundlich	1/n	0.84	0.72	0.91	0.8	0.85
	R^2	0.93	0.90	0.93	0.94	0.91
	$q_{\text{max}} (\mu\text{mol/g})$	833	909	769	833	714
Langmuir	$K_L (\text{L}/\mu\text{mol})$	0.052	0.076	0.035	0.03	0.032
	R^2	0.96	0.94	0.92	0.94	0.91



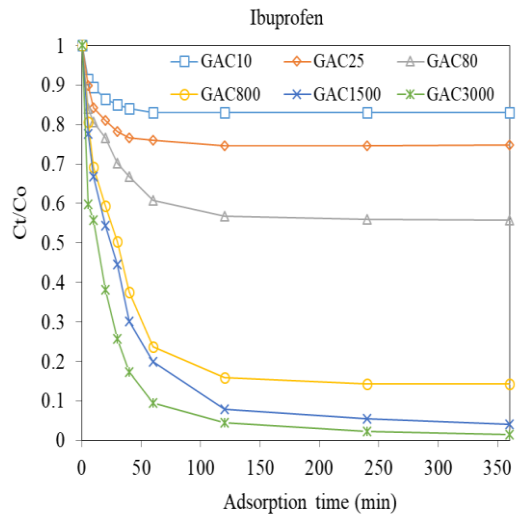
(a)



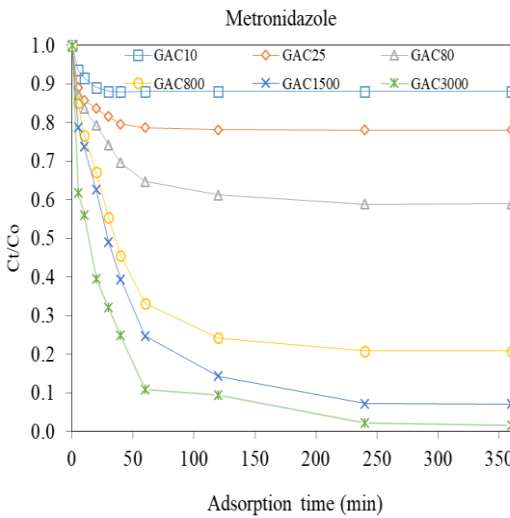
(b)



(c)

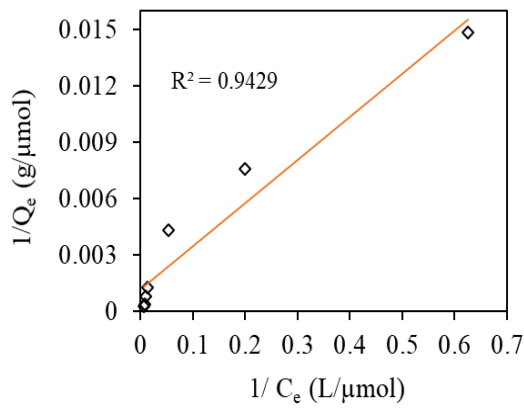


(d)

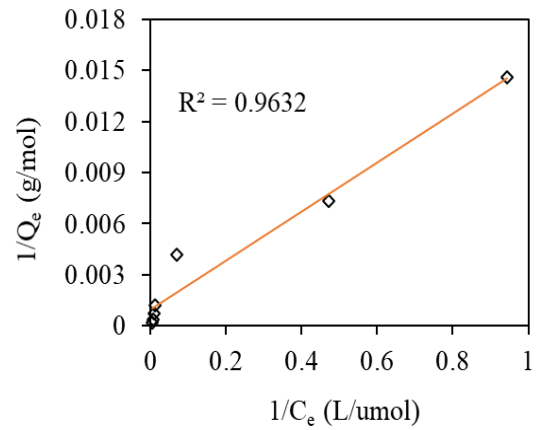


(e)

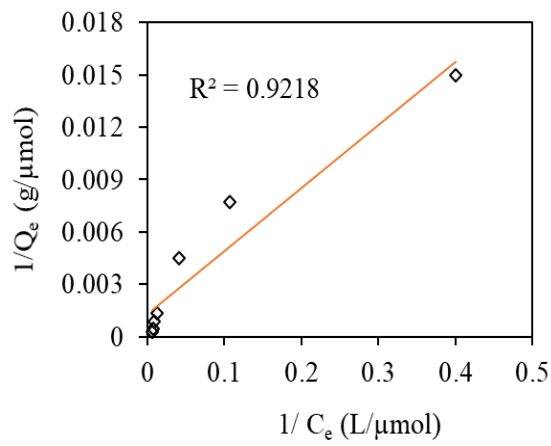
Figure S4.1. Removal of micro pollutants from nitrified urine with different GAC dosages; naproxen (a), carbamazepine (b), acetaminophen (c), ibuprofen (d), and metronidazole (e).



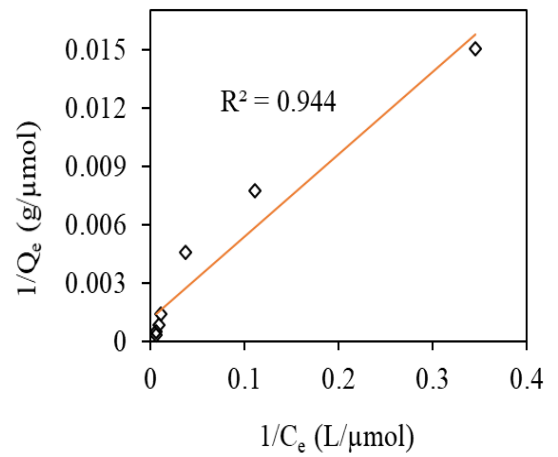
(a)



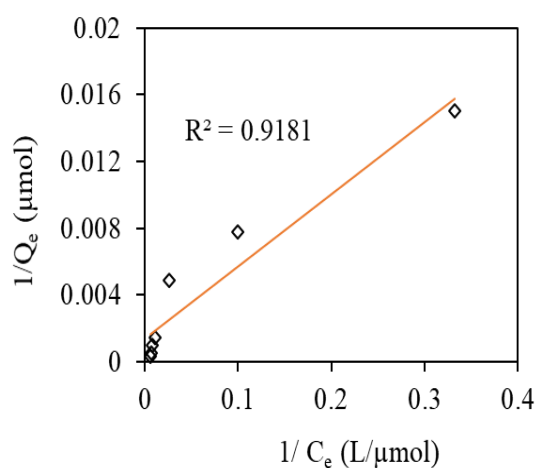
(b)



(c)



(d)



(e)

Figure S4.2. Experimental data (dots) and linear Langmuir isotherm (line) for adsorption of naproxen (a), carbamazepine (b), acetaminophen (c), ibuprofen (d), and metronidazole (e).

Table S4.5. The values of both weight and bias of trained ANN for predicting the removal of naproxen.

Neurons	IW		LW	b1	b2
	Time	Dosage			
1	2.274	-4.703	1.273	-3.911	
2	-4.454	2.055	-0.061	3.906	
3	4.762	-1.012	0.544	-3.059	
4	-4.198	-4.821	1.995	0.240	
5	2.197	4.985	1.829	-1.056	
6	-4.806	0.311	-0.047	0.375	-4.843
7	4.577	-3.694	-0.353	1.109	
8	1.029	4.019	1.004	3.174	
9	-2.016	4.211	0.138	-3.466	

10	0.273	-4.993	0.939	-2.714
11	9.213	-0.293	4.409	10.064
12	-0.932	6.120	2.949	6.120

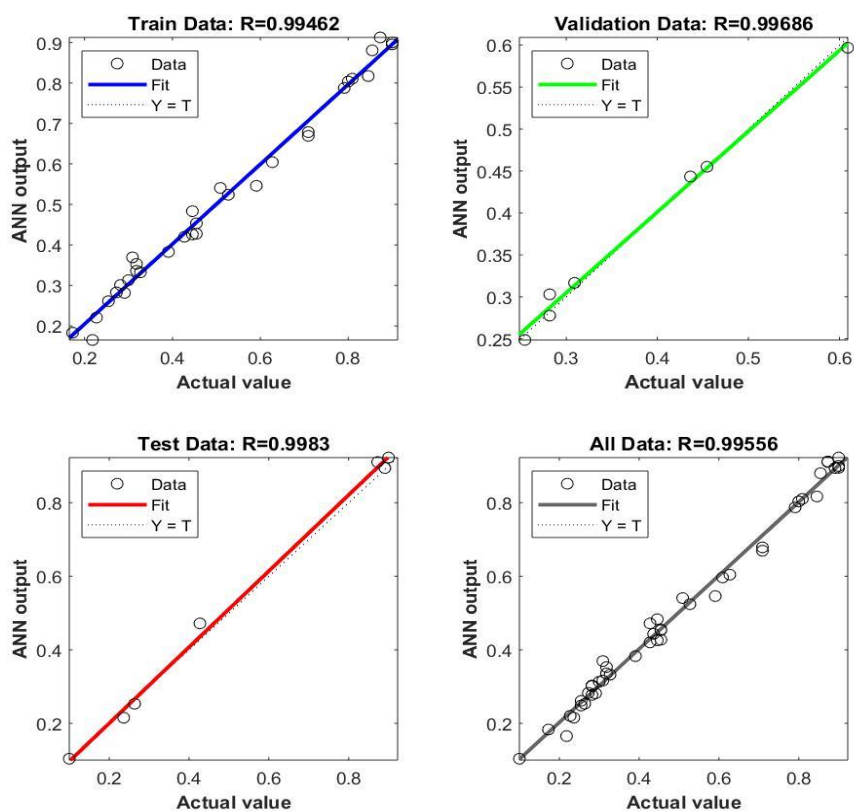


Figure S4.3. Scatter plots of predicted naproxen values versus the experimental data values.

Table S4.6. The values of weight and bias of trained ANN for predicting the carbamazepine removal.

Neurons	IW				
	Time	Dosage	LW	b1	b2
1	3.302	4.170	1.103	-5.027	
2	-2.609	-5.047	-1.062	3.710	
3	5.334	0.110	-0.471	-3.526	
4	-6.187	-7.237	2.526	1.634	
5	3.788	-2.847	1.092	-1.846	
6	-5.176	0.587	0.062	1.133	
7	0.269	-5.611	-2.681	-5.871	
8	2.020	5.120	1.947	1.436	-5.892
9	-2.594	4.291	1.048	-1.762	
10	3.256	-5.379	1.754	0.979	
11	5.875	-1.433	-0.782	4.555	
12	4.044	-2.604	1.147	5.699	
13	7.161	-0.331	5.756	7.927	
14	3.399	-4.358	-0.679	4.893	

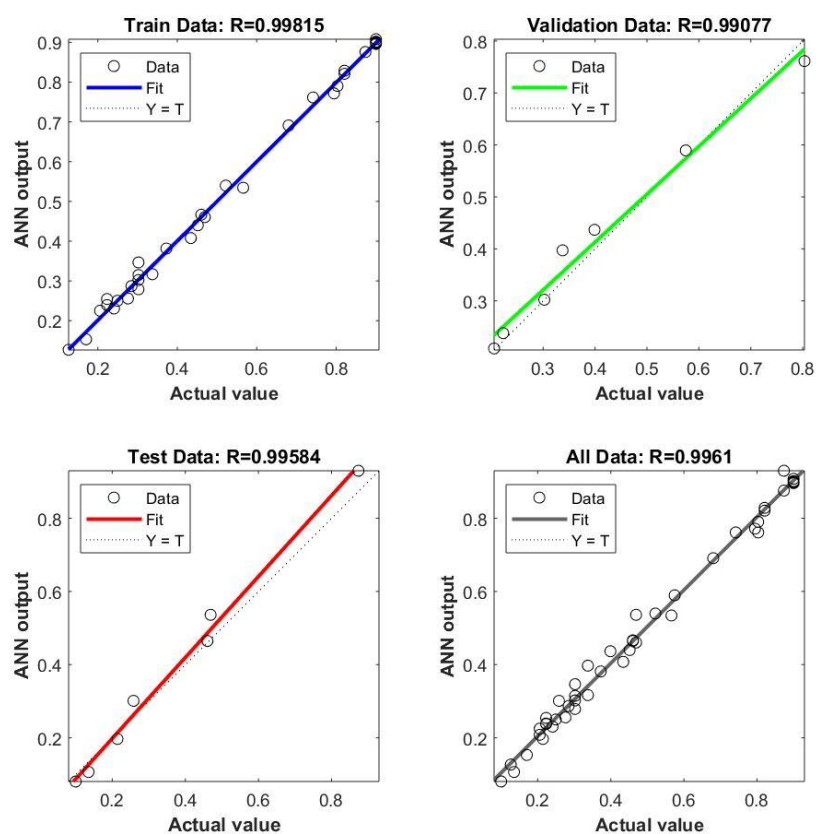


Figure S4.4. Scatter plots of predicted carbamazepine values versus the experimental data values.

Table S4.7. The values of weight and bias of trained ANN for predicting the acetaminophen removal.

Neurons	IW		LW	b1	b2
	Time	Dosage			
1	0.530	3.238	4.045	-5.271	
2	-1.135	5.225	2.906	-3.333	
3	-1.059	3.966	4.315	-2.517	
4	-1.411	1.475	-7.839	-6.999	
5	-1.668	-4.179	-5.168	2.008	
6	-0.801	1.244	5.060	-1.328	

7	-1.215	-4.506	2.447	0.941	-4.843
8	-1.269	1.798	3.946	0.248	
9	1.089	0.965	5.913	0.257	
10	0.094	-0.821	4.900	-2.647	
11	4.500	-4.751	2.011	-6.993	
12	0.197	5.628	2.005	6.163	
13	-0.504	-3.856	0.468	-6.447	
14	-4.892	-11.796	0.444	-12.667	

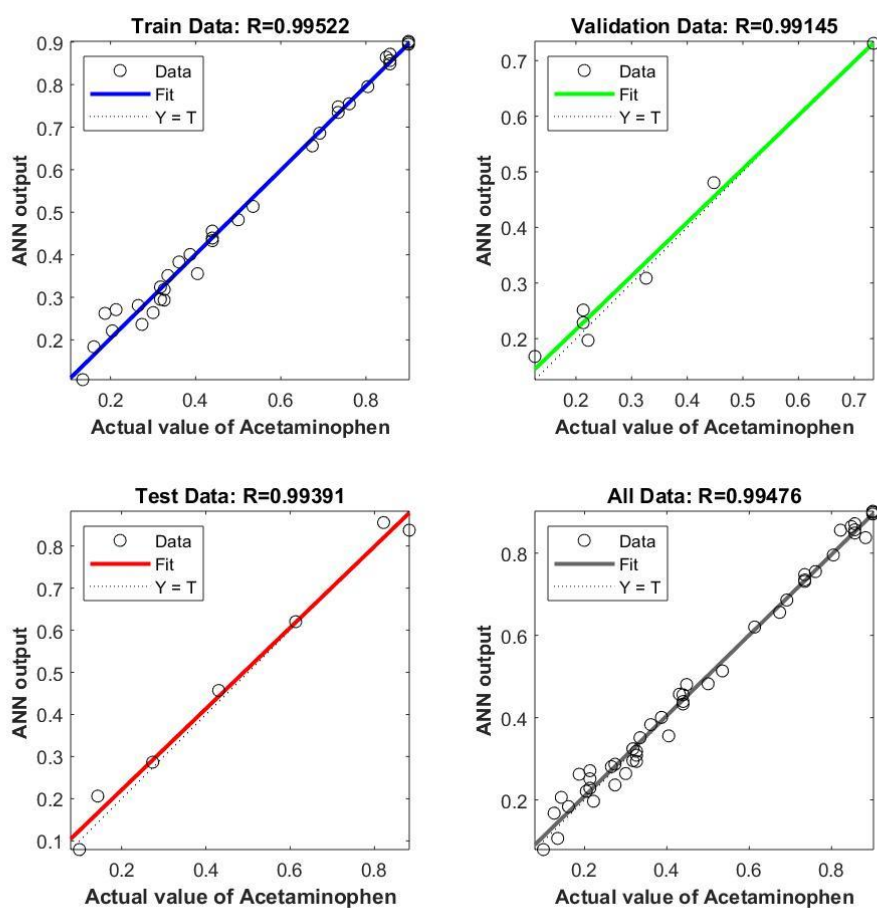


Figure S4.5. Scatter plots of predicted acetaminophen values versus the experimental data values.

Table S4.8. The values of weight and bias of trained ANN for predicting the ibuprofen removal.

IW					
Neurons	Time	Dosage	LW	b1	b2
1	-0.326	13.247	3.763	14.263	
2	3.040	0.014	1.344	-3.234	
3	-3.792	-0.431	0.544	2.209	
4	-0.323	-6.059	-0.1154	-1.461	-5.5459
5	-10.411	1.014	2.819	-11.408	
6	8.6844	9.809	0.393	13.048	
7	11.537	-0.522	5.856	12.350	

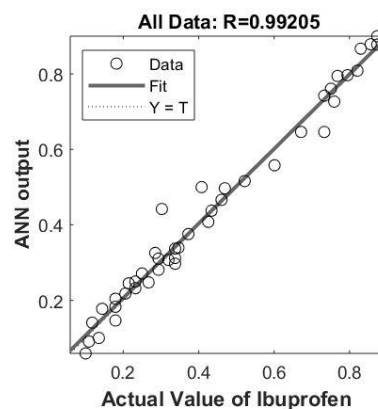
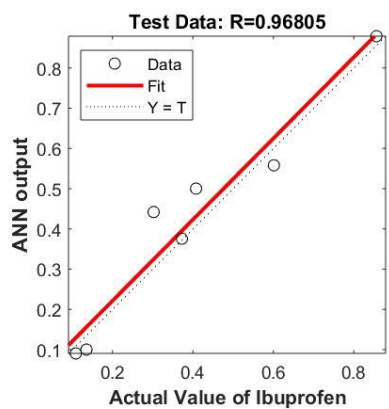
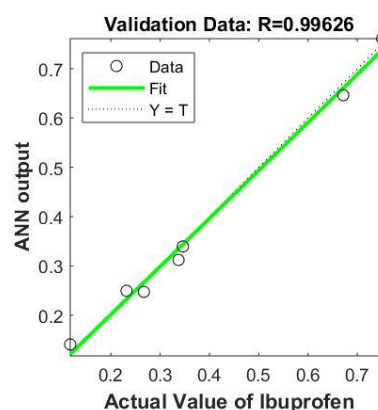
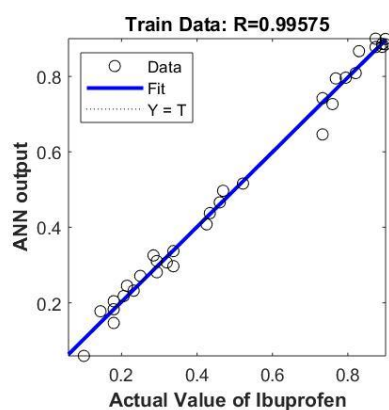


Figure S4.6. Scatter plots of predicated ibuprofen values versus the experimental data values.

Table S4.9. The values of weight and bias of trained ANN for predicting the metronidazole removal.

Neurons	IW		LW	b1	b2
	Time	Dosage			
1	-3.696	4.097	-1.058	6.016	
2	-1.312	6.253	1.153	5.635	
3	-3.332	4.576	-0.261	4.705	
4	4.174	3.904	0.663	-3.834	
5	3.521	4.482	0.473	-3.126	-2.3912
6	-5.432	1.973	0.283	2.164	
7	1.673	5.569	-0.537	-1.408	
8	5.668	1.273	-0.344	-0.606	
9	-0.581	-5.753	-0.147	-0.005	
10	0.308	5.789	0.154	0.595	
11	1.588	-5.425	0.498	1.784	
12	-5.747	-0.321	-0.097	-2.196	
13	-2.288	5.082	0.732	-3.267	
14	0.240	-5.754	-0.134	3.620	
15	-5.730	-0.198	1.172	-5.037	
16	6.375	-0.293	3.955	6.988	
17	-6.050	-1.426	-1.038	-5.803	

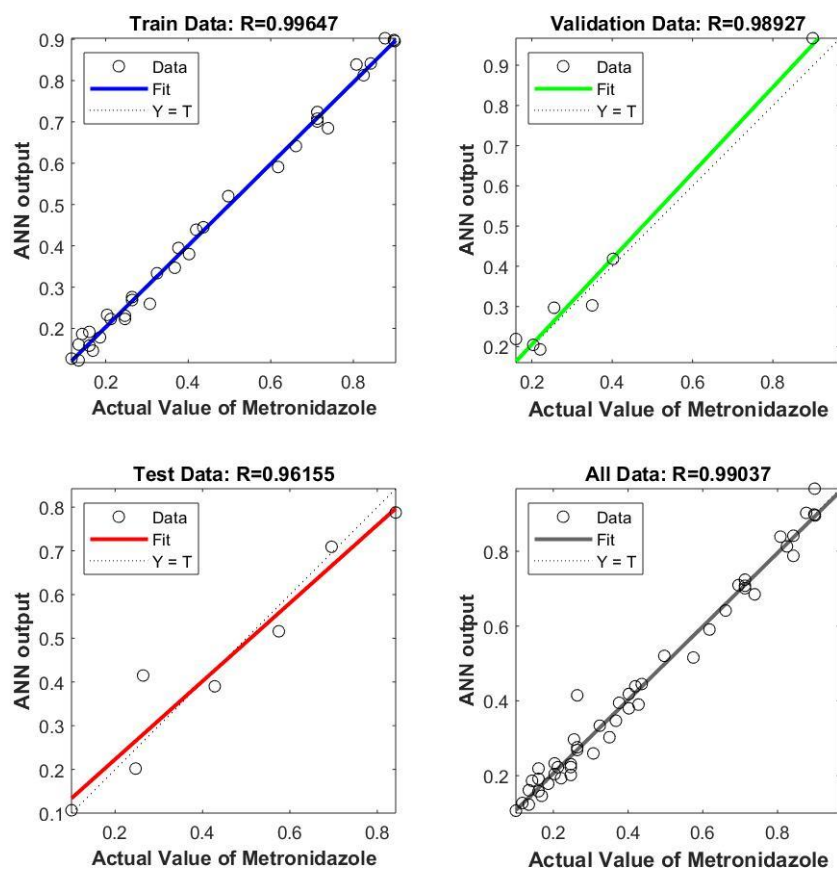


Figure S4.7. Scatter plots of predicted metronidazole values versus the experimental data values.

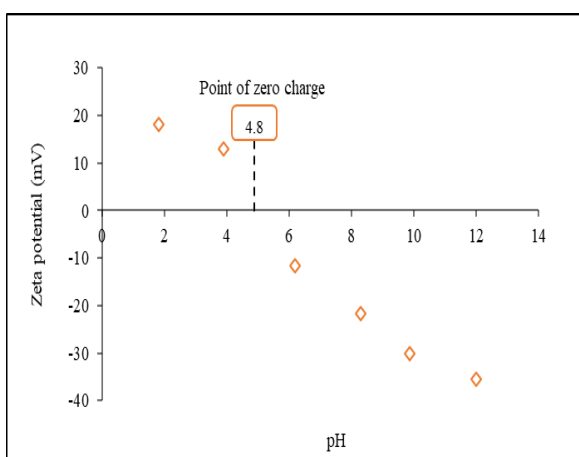


Figure S4.8. Illustrate the point of zero charge (zeta potential vs pH).

References

- Adams, C., Wang, Y., Loftin, K., Meyer, M. 2002. Removal of antibiotics from surface and distilled water in conventional water treatment processes. *Journal of environmental engineering*, **128**(3), 253-260.
- Ahmed, M.B., Zhou, J.L., Ngo, H.H., Guo, W., Johir, M.A.H., Sornalingam, K. 2017. Single and competitive sorption properties and mechanism of functionalized biochar for removing sulfonamide antibiotics from water. *Chemical Engineering Journal*, **311**, 348-358.
- Ahmed, M.J. 2017. Adsorption of non-steroidal anti-inflammatory drugs from aqueous solution using activated carbons. *Journal of environmental management*, **190**, 274-282.
- Al-Khateeb, L.A., Almotiry, S., Salam, M.A. 2014. Adsorption of pharmaceutical pollutants onto graphene nanoplatelets. *Chemical Engineering Journal*, **248**, 191-199.
- Al-Rifai, J.H., Khabbaz, H., Schäfer, A.I. 2011. Removal of pharmaceuticals and endocrine disrupting compounds in a water recycling process using reverse osmosis systems. *Separation and Purification Technology*, **77**(1), 60-67.
- Almuntashiri, A., Hosseinzadeh, A., Badeti, U., Shon, H., Freguia, S., Dorji, U., Phuntsho, S. 2022. Removal of pharmaceutical compounds from synthetic hydrolysed urine using granular activated carbon: Column study and predictive modelling. *Journal of Water Process Engineering*, **45**, 102480.
- Almuntashiri, A., Hosseinzadeh, A., Volpin, F., Ali, S.M., Dorji, U., Shon, H., Phuntsho, S. 2021. Removal of pharmaceuticals from nitrified urine. *Chemosphere*, 130870.
- Alturki, A. 2013. Removal of trace organic contaminants by integrated membrane processes for indirect potable water reuse applications.
- Alturki, A.A., Tadkaew, N., McDonald, J.A., Khan, S.J., Price, W.E., Nghiem, L.D. 2010. Combining MBR and NF/RO membrane filtration for the removal of trace organics in indirect potable water reuse applications. *Journal of Membrane Science*, **365**(1-2), 206-215.
- Aslan, S., Şirazi, M. 2020. Adsorption of sulfonamide antibiotic onto activated carbon prepared from an agro-industrial by-product as low-cost adsorbent: Equilibrium, thermodynamic, and kinetic studies. *Water, Air, & Soil Pollution*, **231**, 1-20.
- Ayawei, N., Ekubo, A.T., Wankasi, D., Dikio, E.D. 2015. Adsorption of congo red by Ni/Al-CO₃: equilibrium, thermodynamic and kinetic studies. *Oriental Journal of Chemistry*, **31**(3), 1307.
- Badeti, U., Jiang, J., Almuntashiri, A., Pathak, N., Dorji, U., Volpin, F., Freguia, S., Ang, W.L., Chanan, A., Kumarasingham, S. 2022. Impact of source-separation of urine on treatment capacity, process design, and capital expenditure of a decentralised wastewater treatment plant. *Chemosphere*, **300**, 134489.
- Badeti, U., Pathak, N.K., Volpin, F., Dorji, U., Freguia, S., Shon, H.K., Phuntsho, S. 2021. Impact of source-separation of urine on effluent quality, energy consumption and greenhouse gas emissions of a decentralized wastewater treatment plant. *Process Safety and Environmental Protection*.
- Baral, S., Das, N., Ramulu, T., Sahoo, S., Das, S., Chaudhury, G.R. 2009. Removal of Cr (VI) by thermally activated weed *Salvinia cucullata* in a fixed-bed column. *Journal of Hazardous Materials*, **161**(2-3), 1427-1435.
- Bischel, H.N., Duygan, B.D.Ö., Strande, L., Mc Ardell, C.S., Udert, K.M., Kohn, T. 2015. Pathogens and pharmaceuticals in source-separated urine in eThekweni, South Africa. *Water Research*, **85**, 57-65.
- Blagojević, N., Kukić, D., Vasić, V., Šćiban, M., Prodanović, J., Bera, O. 2019. A new approach for modelling and optimization of Cu (II) biosorption from aqueous solutions using sugar beet shreds in a fixed-bed column. *Journal of hazardous materials*, **363**, 366-375.
- Bradley, P.M., Barber, L.B., Clark, J.M., Duris, J.W., Foreman, W.T., Furlong, E.T., Givens, C.E., Hubbard, L.E., Hutchinson, K.J., Journey, C.A. 2016. Pre/post-closure assessment of groundwater pharmaceutical fate in a wastewater-facility-impacted stream reach. *Science of the Total Environment*, **568**, 916-925.

- Brown, J.N., Paxéus, N., Förlin, L., Larsson, D.J. 2007. Variations in bioconcentration of human pharmaceuticals from sewage effluents into fish blood plasma. *Environmental Toxicology and Pharmacology*, **24**(3), 267-274.
- Cabrita, I., Ruiz, B., Mestre, A.S., Fonseca, I.M., Carvalho, A.P., Ania, C.O. 2010. Removal of an analgesic using activated carbons prepared from urban and industrial residues. *Chemical Engineering Journal*, **163**(3), 249-255.
- Calisto, V., Ferreira, C.I., Oliveira, J.A., Otero, M., Esteves, V.I. 2015. Adsorptive removal of pharmaceuticals from water by commercial and waste-based carbons. *Journal of environmental management*, **152**, 83-90.
- Caluwé, M., Dobbeleers, T., D'aes, J., Miele, S., Akkermans, V., Daens, D., Geuens, L., Kiekens, F., Blust, R., Dries, J. 2017. Formation of aerobic granular sludge during the treatment of petrochemical wastewater. *Bioresource technology*, **238**, 559-567.
- Cath, T.Y., Childress, A.E., Elimelech, M. 2006. Forward osmosis: Principles, applications, and recent developments. *Journal of membrane science*, **281**(1-2), 70-87.
- Cath, T.Y., Gormly, S., Beaudry, E.G., Flynn, M.T., Adams, V.D., Childress, A.E. 2005. Membrane contactor processes for wastewater reclamation in space: Part I. Direct osmotic concentration as pretreatment for reverse osmosis. *Journal of Membrane Science*, **257**(1-2), 85-98.
- Chang, N.-B., Houmann, C., Lin, K.-S., Wanielista, M. 2016. Fate and transport with material response characterization of green sorption media for copper removal via adsorption process. *Chemosphere*, **144**, 1280-1289.
- Chen, M., Shang, T., Fang, W., Diao, G. 2011. Study on adsorption and desorption properties of the starch grafted p-tert-butyl-calix [n] arene for butyl Rhodamine B solution. *Journal of hazardous materials*, **185**(2-3), 914-921.
- Chen, Y., Liu, C., Guo, G., Zhao, Y., Qian, C., Jiang, H., Shen, B., Wu, D., Cao, F., Sun, H. 2022. Machine-learning-guided reaction kinetics prediction towards solvent identification for chemical absorption of carbonyl sulfide. *Chemical Engineering Journal*, **444**, 136662.
- Choi, K.J., Kim, S.G., Kim, C.W., Kim, S.H. 2005. Effects of activated carbon types and service life on removal of endocrine disrupting chemicals: amitrol, nonylphenol, and bisphenol-A. *Chemosphere*, **58**(11), 1535-1545.
- Cook, J.D., Strauss, K.A., Caplan, Y.H., LoDico, C.P., Bush, D.M. 2007. Urine pH: the effects of time and temperature after collection. *Journal of analytical toxicology*, **31**(8), 486-496.
- Crittenden, J.C., Sanongraj, S., Bulloch, J.L., Hand, D.W., Rogers, T.N., Speth, T.F., Ulmer, M. 1999. Correlation of aqueous-phase adsorption isotherms. *Environmental science & technology*, **33**(17), 2926-2933.
- Daneshvar, E., Vazirzadeh, A., Niazi, A., Kousha, M., Naushad, M., Bhatnagar, A. 2017. Desorption of methylene blue dye from brown macroalga: effects of operating parameters, isotherm study and kinetic modeling. *Journal of Cleaner Production*, **152**, 443-453.
- de Franco, M.A.E., de Carvalho, C.B., Bonetto, M.M., de Pelegrini Soares, R., Féris, L.A. 2018. Diclofenac removal from water by adsorption using activated carbon in batch mode and fixed-bed column: isotherms, thermodynamic study and breakthrough curves modeling. *Journal of Cleaner Production*, **181**, 145-154.
- de Franco, M.A.E., de Carvalho, C.B., Bonetto, M.M., de Pelegrini Soares, R., Féris, L.A. 2017. Removal of amoxicillin from water by adsorption onto activated carbon in batch process and fixed bed column: kinetics, isotherms, experimental design and breakthrough curves modelling. *Journal of Cleaner Production*, **161**, 947-956.
- de Wilt, A., Butkovskiy, A., Tuantet, K., Leal, L.H., Fernandes, T.V., Langenhoff, A., Zeeman, G. 2016. Micropollutant removal in an algal treatment system fed with source separated wastewater streams. *Journal of hazardous materials*, **304**, 84-92.
- Deb, C., Thawani, B., Menon, S., Gore, V., Chellappan, V., Ranjan, S., Ganesapillai, M. 2019. Design and analysis for the removal of active pharmaceutical residues from synthetic wastewater stream. *Environmental Science and Pollution Research*, **26**(18), 18739-18751.
- Del Vecchio, P., Haro, N.K., Souza, F.S., Marcílio, N.R., Féris, L.A. 2019. Ampicillin removal by

- adsorption onto activated carbon: kinetics, equilibrium and thermodynamics. *Water Science and Technology*, **79**(10), 2013-2021.
- Delgado, L.F., Charles, P., Glucina, K., Morlay, C. 2012. The removal of endocrine disrupting compounds, pharmaceutically activated compounds and cyanobacterial toxins during drinking water preparation using activated carbon—A review. *Science of the total environment*, **435**, 509-525.
- Deokar, S.K., Mandavgane, S.A. 2015. Estimation of packed-bed parameters and prediction of breakthrough curves for adsorptive removal of 2, 4-dichlorophenoxyacetic acid using rice husk ash. *Journal of environmental chemical engineering*, **3**(3), 1827-1836.
- Dodd, M.C., Zuleeg, S., Gunten, U.v., Pronk, W. 2008. Ozonation of source-separated urine for resource recovery and waste minimization: process modeling, reaction chemistry, and operational considerations. *Environmental science & technology*, **42**(24), 9329-9337.
- Duygan, B.D.Ö., Udert, K.M., Remmele, A., McArdell, C.S. 2021. Removal of pharmaceuticals from human urine during storage, aerobic biological treatment, and activated carbon adsorption to produce a safe fertilizer. *Resources, Conservation and Recycling*, **166**, 105341.
- Escher, B.I., Pronk, W., Suter, M.J.-F., Maurer, M. 2006. Monitoring the removal efficiency of pharmaceuticals and hormones in different treatment processes of source-separated urine with bioassays. *Environmental science & technology*, **40**(16), 5095-5101.
- Etter, B., Tilley, E., Khadka, R., Udert, K.M. 2011. Low-cost struvite production using source-separated urine in Nepal. *Water research*, **45**(2), 852-862.
- Etter, B., Udert, K., Gounden, T. 2014. VUNA—Scaling up nutrient recovery from urine. *to be submitted for the Tech4Dev conference (EPFL)*.
- Feizi, F., Sarmah, A.K., Rangsvik, R. 2021. Adsorption of pharmaceuticals in a fixed-bed column using tyre-based activated carbon: Experimental investigations and numerical modelling. *Journal of Hazardous Materials*, **417**, 126010.
- Figuerola, E.L., Erijman, L. 2010. Diversity of nitrifying bacteria in a full-scale petroleum refinery wastewater treatment plant experiencing unstable nitrification. *Journal of hazardous materials*, **181**(1-3), 281-288.
- Foo, K., Hameed, B. 2012. A rapid regeneration of methylene blue dye-loaded activated carbons with microwave heating. *Journal of Analytical and Applied Pyrolysis*, **98**, 123-128.
- Fumasoli, A., Etter, B., Sterkele, B., Morgenroth, E., Udert, K.M. 2016. Operating a pilot-scale nitrification/distillation plant for complete nutrient recovery from urine. *Water Science and Technology*, **73**(1), 215-222.
- García-Reyes, C.B., Salazar-Rábago, J.J., Sánchez-Polo, M., Loredó-Cancino, M., Leyva-Ramos, R. 2021. Ciprofloxacin, ranitidine, and chlorphenamine removal from aqueous solution by adsorption. Mechanistic and regeneration analysis. *Environmental Technology & Innovation*, **24**, 102060.
- Gerrity, D., Gamage, S., Holady, J.C., Mawhinney, D.B., Quiñones, O., Trenholm, R.A., Snyder, S.A. 2011. Pilot-scale evaluation of ozone and biological activated carbon for trace organic contaminant mitigation and disinfection. *Water research*, **45**(5), 2155-2165.
- Ghaedi, A.M., Karamipour, S., Vafaei, A., Baneshi, M.M., Kiarostami, V. 2019. Optimization and modeling of simultaneous ultrasound-assisted adsorption of ternary dyes using copper oxide nanoparticles immobilized on activated carbon using response surface methodology and artificial neural network. *Ultrasonics sonochemistry*, **51**, 264-280.
- Giannakis, S., Hendaoui, I., Jovic, M., Grandjean, D., De Alencastro, L.F., Girault, H., Pulgarin, C. 2017a. Solar photo-Fenton and UV/H₂O₂ processes against the antidepressant Venlafaxine in urban wastewaters and human urine. Intermediates formation and biodegradability assessment. *Chemical Engineering Journal*, **308**, 492-504.
- Giannakis, S., Jovic, M., Gasilova, N., Gelabert, M.P., Schindelholz, S., Furbringer, J.-M., Girault, H., Pulgarin, C. 2017b. Iohexol degradation in wastewater and urine by UV-based Advanced Oxidation Processes (AOPs): Process modeling and by-products identification. *Journal of Environmental Management*, **195**, 174-185.
- Gopinath, A., Retnam, B.G., Muthukkumaran, A., Aravamudan, K. 2020. Swift, versatile and a rigorous kinetic model based artificial neural network surrogate for single and

- multicomponent batch adsorption processes. *Journal of Molecular Liquids*, **297**, 111888.
- Grover, D., Zhou, J., Frickers, P., Readman, J. 2011. Improved removal of estrogenic and pharmaceutical compounds in sewage effluent by full scale granular activated carbon: impact on receiving river water. *Journal of Hazardous Materials*, **185**(2-3), 1005-1011.
- Guo, Y., Du, E. 2012. The effects of thermal regeneration conditions and inorganic compounds on the characteristics of activated carbon used in power plant. *Energy Procedia*, **17**, 444-449.
- Hai, F.I., Li, X., Price, W.E., Nghiem, L.D. 2011a. Removal of carbamazepine and sulfamethoxazole by MBR under anoxic and aerobic conditions. *Bioresource technology*, **102**(22), 10386-10390.
- Hai, F.I., Tessmer, K., Nguyen, L.N., Kang, J., Price, W.E., Nghiem, L.D. 2011b. Removal of micropollutants by membrane bioreactor under temperature variation. *Journal of membrane science*, **383**(1-2), 144-151.
- Halim, A.A., Aziz, H.A., Johari, M.A.M., Ariffin, K.S. 2010. Comparison study of ammonia and COD adsorption on zeolite, activated carbon and composite materials in landfill leachate treatment. *Desalination*, **262**(1-3), 31-35.
- Halling-Sørensen, B., Nielsen, S.N., Lanzky, P., Ingerslev, F., Lützhøft, H.H., Jørgensen, S. 1998. Occurrence, fate and effects of pharmaceutical substances in the environment-A review. *Chemosphere*, **36**(2), 357-393.
- Hammer, M., Tettenborn, F., Behrendt, J., Gulyas, H., Otterpohl, R. 2005. Pharmaceutical residues: Database assessment of occurrence in the environment and exemplary treatment processes for urine. *IWA 1st National Young Researchers Conference—Emerging Pollutants and Emerging Technologies*. pp. 27-28.
- Hellström, D., Johansson, E., Grennberg, K. 1999. Storage of human urine: acidification as a method to inhibit decomposition of urea. *Ecological Engineering*, **12**(3-4), 253-269.
- Hernández-Hernández, L., Bonilla-Petriciolet, A., Mendoza-Castillo, D., Reynel-Ávila, H. 2017. Antagonistic binary adsorption of heavy metals using stratified bone char columns. *Journal of Molecular Liquids*, **241**, 334-346.
- Hernández-Leal, L., Temmink, H., Zeeman, G., Buisman, C. 2011. Removal of micropollutants from aerobically treated grey water via ozone and activated carbon. *Water Research*, **45**(9), 2887-2896.
- Hollender, J., Zimmermann, S.G., Koepke, S., Krauss, M., McArdeell, C.S., Ort, C., Singer, H., Von Gunten, U., Siegrist, H. 2009. Elimination of organic micropollutants in a municipal wastewater treatment plant upgraded with a full-scale post-ozonation followed by sand filtration. *Environmental science & technology*, **43**(20), 7862-7869.
- Hongsawat, P., Prarat, P. 2022. Comparative adsorption performance of oxytetracycline and sulfamethoxazole antibiotic on powder activated carbon and graphene oxide. *Chemical Papers*, **76**(4), 2293-2305.
- Hosseinzadeh, A., Baziar, M., Alidadi, H., Zhou, J.L., Altaee, A., Najafpoor, A.A., Jafarpour, S. 2020a. Application of artificial neural network and multiple linear regression in modeling nutrient recovery in vermicompost under different conditions. *Bioresource Technology*, **303**, 122926.
- Hosseinzadeh, A., Najafpoor, A.A., Jafari, A.J., Jazani, R.K., Baziar, M., Bargozin, H., Piranloo, F.G. 2018. Application of response surface methodology and artificial neural network modeling to assess non-thermal plasma efficiency in simultaneous removal of BTEX from waste gases: Effect of operating parameters and prediction performance. *Process Safety and Environmental Protection*, **119**, 261-270.
- Hosseinzadeh, A., Zhou, J.L., Altaee, A., Baziar, M., Li, D. 2020b. Effective modelling of hydrogen and energy recovery in microbial electrolysis cell by artificial neural network and adaptive network-based fuzzy inference system. *Bioresource Technology*, 123967.
- Hosseinzadeh, A., Zhou, J.L., Altaee, A., Baziar, M., Li, X. 2020c. Modeling water flux in osmotic membrane bioreactor by adaptive network-based fuzzy inference system and artificial neural network. *Bioresource Technology*, **310**, 123391.
- Hosseinzadeh, A., Zhou, J.L., Altaee, A., Li, D. 2022. Machine learning modeling and analysis of biohydrogen production from wastewater by dark fermentation process. *Bioresource*

- Technology*, **343**, 126111.
- Huang, J., Zimmerman, A.R., Chen, H., Wan, Y., Zheng, Y., Yang, Y., Zhang, Y., Gao, B. 2022. Fixed bed column performance of Al-modified biochar for the removal of sulfamethoxazole and sulfapyridine antibiotics from wastewater. *Chemosphere*, **305**, 135475.
- Imwene, K., Ngumba, E., Kairigo, P. 2022. Emerging technologies for enhanced removal of residual antibiotics from source-separated urine and wastewaters: A review. *Journal of Environmental Management*, **322**, 116065.
- Jamil, S., Loganathan, P., Listowski, A., Kandasamy, J., Khourshed, C., Vigneswaran, S. 2019. Simultaneous removal of natural organic matter and micro-organic pollutants from reverse osmosis concentrate using granular activated carbon. *Water Research*, **155**, 106-114.
- Janssens, R., Cristóvão, B.M., Bronze, M.R., Crespo, J.G., Pereira, V.J., Luis, P. 2019. Photocatalysis using UV-A and UV-C light sources for advanced oxidation of anti-cancer drugs spiked in laboratory-grade water and synthetic urine. *Industrial & Engineering Chemistry Research*, **59**(2), 647-653.
- Jaria, G., Calisto, V., Silva, C.P., Gil, M.V., Otero, M., Esteves, V.I. 2019. Fixed-bed performance of a waste-derived granular activated carbon for the removal of micropollutants from municipal wastewater. *Science of The Total Environment*, **683**, 699-708.
- Juela, D., Vera, M., Cruzat, C., Alvarez, X., Vanegas, E. 2021. Mathematical modeling and numerical simulation of sulfamethoxazole adsorption onto sugarcane bagasse in a fixed-bed column. *Chemosphere*, **280**, 130687.
- Kanakaraju, D., Glass, B.D., Oelgemöller, M. 2018. Advanced oxidation process-mediated removal of pharmaceuticals from water: a review. *Journal of environmental management*, **219**, 189-207.
- Kim, S., Shon, H., Ngo, H. 2010. Adsorption characteristics of antibiotics trimethoprim on powdered and granular activated carbon. *Journal of Industrial and Engineering Chemistry*, **16**(3), 344-349.
- Kim, S.D., Cho, J., Kim, I.S., Vanderford, B.J., Snyder, S.A. 2007. Occurrence and removal of pharmaceuticals and endocrine disruptors in South Korean surface, drinking, and waste waters. *Water research*, **41**(5), 1013-1021.
- Klein, E.Y., Van Boeckel, T.P., Martinez, E.M., Pant, S., Gandra, S., Levin, S.A., Goossens, H., Laxminarayan, R. 2018. Global increase and geographic convergence in antibiotic consumption between 2000 and 2015. *Proceedings of the National Academy of Sciences*, **115**(15), E3463-E3470.
- Kolpin, D.W., Furlong, E.T., Meyer, M.T., Thurman, E.M., Zaugg, S.D., Barber, L.B., Buxton, H.T. 2002. Pharmaceuticals, hormones, and other organic wastewater contaminants in US streams, 1999– 2000: A national reconnaissance. *Environmental science & technology*, **36**(6), 1202-1211.
- Köpping, I., McArdell, C.S., Borowska, E., Böhler, M.A., Udert, K.M. 2020. Removal of pharmaceuticals from nitrified urine by adsorption on granular activated carbon. *Water research X*, **9**, 100057.
- Kovalova, L., Siegrist, H., Singer, H., Wittmer, A., McArdell, C.S. 2012. Hospital wastewater treatment by membrane bioreactor: performance and efficiency for organic micropollutant elimination. *Environmental science & technology*, **46**(3), 1536-1545.
- Kovalova, L., Siegrist, H., Von Gunten, U., Eugster, J., Hagenbuch, M., Wittmer, A., Moser, R., McArdell, C.S. 2013. Elimination of micropollutants during post-treatment of hospital wastewater with powdered activated carbon, ozone, and UV. *Environmental science & technology*, **47**(14), 7899-7908.
- Lan, Y., Coetsier, C., Causserand, C., Serrano, K.G. 2018. An experimental and modelling study of the electrochemical oxidation of pharmaceuticals using a boron-doped diamond anode. *Chemical Engineering Journal*, **333**, 486-494.
- Landry, K.A., Boyer, T.H. 2013. Diclofenac removal in urine using strong-base anion exchange polymer resins. *Water research*, **47**(17), 6432-6444.
- Larasati, A., Fowler, G.D., Graham, N.J. 2020. Chemical regeneration of granular activated

- carbon: preliminary evaluation of alternative regenerant solutions. *Environmental Science: Water Research & Technology*, **6**(8), 2043-2056.
- Larasati, A., Fowler, G.D., Graham, N.J. 2021. Insights into chemical regeneration of activated carbon for water treatment. *Journal of Environmental Chemical Engineering*, **9**(4), 105555.
- Larsen, T.A., Riechmann, M.E., Udert, K.M. 2021. State of the art of urine treatment technologies: A critical review. *Water Research X*, **13**, 100114.
- Lastre-Acosta, A.M., Palharim, P.H., Barbosa, I.M., Mierzwa, J.C., Teixeira, A.C.S.C. 2020. Removal of sulfadiazine from simulated industrial wastewater by a membrane bioreactor and ozonation. *Journal of Environmental Management*, **271**, 111040.
- Lefebvre, O., Hu, J., Ong, S.L., Ng, H.Y. 2016. Optimization of resource and water recovery from urine. *Journal of Water Reuse and Desalination*, **6**(2), 229-234.
- Leng, C.-C., Pinto, N.G. 1996. An investigation of the mechanisms of chemical regeneration of activated carbon. *Industrial & engineering chemistry research*, **35**(6), 2024-2031.
- Li, J., Zhou, Q., Campos, L.C. 2018. The application of GAC sandwich slow sand filtration to remove pharmaceutical and personal care products. *Science of the Total Environment*, **635**, 1182-1190.
- Lienert, J., Bürki, T., Escher, B.I. 2007. Reducing micropollutants with source control: substance flow analysis of 212 pharmaceuticals in faeces and urine. *Water Science and Technology*, **56**(5), 87-96.
- Lin, Y.-L., Chiou, J.-H., Lee, C.-H. 2014. Effect of silica fouling on the removal of pharmaceuticals and personal care products by nanofiltration and reverse osmosis membranes. *Journal of hazardous materials*, **277**, 102-109.
- Lind, B.-B., Ban, Z., Bydén, S. 2000. Nutrient recovery from human urine by struvite crystallization with ammonia adsorption on zeolite and wollastonite. *Bioresource technology*, **73**(2), 169-174.
- Liu, Q.-S., Zheng, T., Wang, P., Jiang, J.-P., Li, N. 2010. Adsorption isotherm, kinetic and mechanism studies of some substituted phenols on activated carbon fibers. *Chemical engineering journal*, **157**(2-3), 348-356.
- Luo, S., Wei, Z., Spinney, R., Zhang, Z., Dionysiou, D.D., Gao, L., Chai, L., Wang, D., Xiao, R. 2018. UV direct photolysis of sulfamethoxazole and ibuprofen: an experimental and modelling study. *Journal of Hazardous Materials*, **343**, 132-139.
- Madikizela, L.M., Tavengwa, N.T., Chimuka, L. 2017. Status of pharmaceuticals in African water bodies: occurrence, removal and analytical methods. *Journal of environmental management*, **193**, 211-220.
- Mailler, R., Gasperi, J., Coquet, Y., Deshayes, S., Zedek, S., Cren-Olivé, C., Cartiser, N., Eudes, V., Bressy, A., Caupos, E. 2015. Study of a large scale powdered activated carbon pilot: Removals of a wide range of emerging and priority micropollutants from wastewater treatment plant effluents. *Water Research*, **72**, 315-330.
- Marques, S.C., Marcuzzo, J.M., Baldan, M.R., Mestre, A.S., Carvalho, A.P. 2017. Pharmaceuticals removal by activated carbons: role of morphology on cyclic thermal regeneration. *Chemical Engineering Journal*, **321**, 233-244.
- Massoud, M.A., Tarhini, A., Nasr, J.A. 2009. Decentralized approaches to wastewater treatment and management: applicability in developing countries. *Journal of environmental management*, **90**(1), 652-659.
- Maurer, M., Pronk, W., Larsen, T. 2006. Treatment processes for source-separated urine. *Water research*, **40**(17), 3151-3166.
- Maurer, M., Schwegler, P., Larsen, T. 2003. Nutrients in urine: energetic aspects of removal and recovery. *Water Science and technology*, **48**(1), 37-46.
- McCleaf, P., Englund, S., Östlund, A., Lindegren, K., Wiberg, K., Ahrens, L. 2017. Removal efficiency of multiple poly-and perfluoroalkyl substances (PFASs) in drinking water using granular activated carbon (GAC) and anion exchange (AE) column tests. *Water research*, **120**, 77-87.
- Mendoza-Castillo, D., Reynel-Ávila, H., Sánchez-Ruiz, F., Trejo-Valencia, R., Jaime-Leal, J., Bonilla-Petriciolet, A. 2018. Insights and pitfalls of artificial neural network modeling of

- competitive multi-metallic adsorption data. *Journal of Molecular Liquids*, **251**, 15-27.
- Mohanty, K., Das, D., Biswas, M. 2006. Preparation and characterization of activated carbons from *Sterculia alata* nutshell by chemical activation with zinc chloride to remove phenol from wastewater. *Adsorption*, **12**(2), 119-132.
- Mojiri, A., Andasht Kazeroon, R., Gholami, A. 2019. Cross-linked magnetic chitosan/activated biochar for removal of emerging micropollutants from water: Optimization by the artificial neural network. *Water*, **11**(3), 551.
- Mojiri, A., Zhou, J., Vakili, M., Van Le, H. 2020. Removal performance and optimisation of pharmaceutical micropollutants from synthetic domestic wastewater by hybrid treatment. *Journal of contaminant hydrology*, **235**, 103736.
- Moreno-Pérez, J., Bonilla-Petriciolet, A., Mendoza-Castillo, D., Reynel-Ávila, H., Verde-Gómez, Y., Trejo-Valencia, R. 2018. Artificial neural network-based surrogate modeling of multi-component dynamic adsorption of heavy metals with a biochar. *Journal of Environmental Chemical Engineering*, **6**(4), 5389-5400.
- Naidu, G., Jeong, S., Choi, Y., Vigneswaran, S. 2017. Membrane distillation for wastewater reverse osmosis concentrate treatment with water reuse potential. *Journal of Membrane Science*, **524**, 565-575.
- Nam, S.-W., Choi, D.-J., Kim, S.-K., Her, N., Zoh, K.-D. 2014. Adsorption characteristics of selected hydrophilic and hydrophobic micropollutants in water using activated carbon. *Journal of hazardous materials*, **270**, 144-152.
- Ngumba, E., Gachanja, A., Nyirenda, J., Maldonado, J., Tuhkanen, T. 2020. Occurrence of antibiotics and antiretroviral drugs in source-separated urine, groundwater, surface water and wastewater in the peri-urban area of Chunga in Lusaka, Zambia. *Water SA*, **46**(2), 278-284.
- Nguyen, L.N., Hai, F.I., Kang, J., Price, W.E., Nghiem, L.D. 2013. Coupling granular activated carbon adsorption with membrane bioreactor treatment for trace organic contaminant removal: Breakthrough behaviour of persistent and hydrophilic compounds. *Journal of environmental management*, **119**, 173-181.
- Nguyen, L.N., Hai, F.I., Kang, J., Price, W.E., Nghiem, L.D. 2012. Removal of trace organic contaminants by a membrane bioreactor–granular activated carbon (MBR–GAC) system. *Bioresource technology*, **113**, 169-173.
- Njikam, E., Schiewer, S. 2012. Optimization and kinetic modeling of cadmium desorption from citrus peels: A process for biosorbent regeneration. *Journal of Hazardous Materials*, **213**, 242-248.
- Oaks, J.L., Gilbert, M., Virani, M.Z., Watson, R.T., Meteyer, C.U., Rideout, B.A., Shivaprasad, H., Ahmed, S., Chaudhry, M.J.I., Arshad, M. 2004. Diclofenac residues as the cause of vulture population decline in Pakistan. *Nature*, **427**(6975), 630-633.
- Paredes-Laverde, M., Silva-Agredo, J., Torres-Palma, R.A. 2018. Removal of norfloxacin in deionized, municipal water and urine using rice (*Oryza sativa*) and coffee (*Coffea arabica*) husk wastes as natural adsorbents. *Journal of environmental management*, **213**, 98-108.
- Patel, A., Mungray, A.A., Mungray, A.K. 2020. Technologies for the recovery of nutrients, water and energy from human urine: A review. *Chemosphere*, **259**, 127372.
- Pauletto, P., Gonçalves, J., Pinto, L., Dotto, G., Salau, N. 2020a. Single and competitive dye adsorption onto chitosan–based hybrid hydrogels using artificial neural network modeling. *Journal of colloid and interface science*, **560**, 722-729.
- Pauletto, P., Lütke, S., Dotto, G., Salau, N. 2021. Forecasting the multicomponent adsorption of nimesulide and paracetamol through artificial neural network. *Chemical Engineering Journal*, **412**, 127527.
- Pauletto, P.S., Dotto, G.L., Salau, N.P. 2020b. Optimal artificial neural network design for simultaneous modeling of multicomponent adsorption. *Journal of Molecular Liquids*, **320**, 114418.
- Pronk, W., Palmquist, H., Biebow, M., Boller, M. 2006. Nanofiltration for the separation of pharmaceuticals from nutrients in source-separated urine. *Water Research*, **40**(7), 1405-1412.

- Pronk, W., Zuleeg, S., Lienert, J., Escher, B., Koller, M., Berner, A., Koch, G., Boller, M. 2007. Pilot experiments with electro dialysis and ozonation for the production of a fertiliser from urine. *Water science and technology*, **56**(5), 219-227.
- Quinn, B., Gagné, F., Blaise, C. 2009. Evaluation of the acute, chronic and teratogenic effects of a mixture of eleven pharmaceuticals on the cnidarian, *Hydra attenuata*. *Science of the Total Environment*, **407**(3), 1072-1079.
- Rawat, I., Kumar, R.R., Mutanda, T., Bux, F. 2011. Dual role of microalgae: phycoremediation of domestic wastewater and biomass production for sustainable biofuels production. *Applied energy*, **88**(10), 3411-3424.
- Ren, J., Hao, D., Jiang, J., Phuntsho, S., Freguia, S., Ni, B.-J., Dai, P., Guan, J., Shon, H.K. 2021. Fertiliser recovery from source-separated urine via membrane bioreactor and heat localized solar evaporation. *Water Research*, **207**, 117810.
- Reynel-Avila, H.E., Mendoza-Castillo, D.I., Bonilla-Petriciolet, A., Silvestre-Albero, J. 2015. Assessment of naproxen adsorption on bone char in aqueous solutions using batch and fixed-bed processes. *Journal of Molecular Liquids*, **209**, 187-195.
- Rivera-Utrilla, J., Prados-Joya, G., Sánchez-Polo, M., Ferro-García, M., Bautista-Toledo, I. 2009. Removal of nitroimidazole antibiotics from aqueous solution by adsorption/bioadsorption on activated carbon. *Journal of hazardous materials*, **170**(1), 298-305.
- Ronteltap, M., Maurer, M., Gujer, W. 2007. Struvite precipitation thermodynamics in source-separated urine. *Water Research*, **41**(5), 977-984.
- Rose, C., Parker, A., Jefferson, B., Cartmell, E. 2015. The characterization of feces and urine: a review of the literature to inform advanced treatment technology. *Critical reviews in environmental science and technology*, **45**(17), 1827-1879.
- Sakthivel, S.R., Tilley, E., Udert, K.M. 2012. Wood ash as a magnesium source for phosphorus recovery from source-separated urine. *Science of the total environment*, **419**, 68-75.
- Salman, J., Njoku, V., Hameed, B. 2011. Batch and fixed-bed adsorption of 2, 4-dichlorophenoxyacetic acid onto oil palm frond activated carbon. *Chemical Engineering Journal*, **174**(1), 33-40.
- Schürmann, B., Everding, W., Montag, D., Pinnekamp, J. 2012. Fate of pharmaceuticals and bacteria in stored urine during precipitation and drying of struvite. *Water Science and Technology*, **65**(10), 1774-1780.
- Serna-Carrizales, J.C., Collins-Martínez, V.H., Flórez, E., Gomez-Duran, C.F., Palestino, G., Ocampo-Pérez, R. 2021. Adsorption of sulfamethoxazole, sulfadiazine and sulfametazine in single and ternary systems on activated carbon. Experimental and DFT computations. *Journal of Molecular Liquids*, **324**, 114740.
- Shaffer, D.L., Yip, N.Y., Gilron, J., Elimelech, M. 2012. Seawater desalination for agriculture by integrated forward and reverse osmosis: Improved product water quality for potentially less energy. *Journal of membrane science*, **415**, 1-8.
- Shanmuganathan, S., Nguyen, T.V., Jeong, S., Kandasamy, J., Vigneswaran, S. 2015. Submerged membrane-(GAC) adsorption hybrid system in reverse osmosis concentrate treatment. *Separation and Purification Technology*, **146**, 8-14.
- Siegrist, H., Laurenzi, M., Udert, K.M., Larsen, T., Udert, K., Lienert, J. 2013. Transfer into the gas phase: ammonia stripping. *Source Separation and Decentralization for Wastewater Management*, 337-350.
- Singh, A.K. 2015. *Engineered nanoparticles: structure, properties and mechanisms of toxicity*. Academic Press.
- Snyder, S.A., Adham, S., Redding, A.M., Cannon, F.S., DeCarolis, J., Oppenheimer, J., Wert, E.C., Yoon, Y. 2007. Role of membranes and activated carbon in the removal of endocrine disruptors and pharmaceuticals. *Desalination*, **202**(1-3), 156-181.
- Sohn, W., Jiang, J., Phuntsho, S., Choden, Y., Shon, H.K. 2023. Nutrients in a circular economy: Role of urine separation and treatment. *Desalination*, **560**, 116663.
- Solanki, A., Boyer, T.H. 2017. Pharmaceutical removal in synthetic human urine using biochar. *Environmental Science: Water Research & Technology*, **3**(3), 553-565.
- Solanki, A., Boyer, T.H. 2019. Physical-chemical interactions between pharmaceuticals and

- biochar in synthetic and real urine. *Chemosphere*, **218**, 818-826.
- Sotelo, J.L., Ovejero, G., Rodríguez, A., Álvarez, S., Galán, J., García, J. 2014. Competitive adsorption studies of caffeine and diclofenac aqueous solutions by activated carbon. *Chemical engineering journal*, **240**, 443-453.
- Sotelo, J.L., Ovejero, G., Rodríguez, A., Álvarez, S., García, J. 2013. Analysis and modeling of fixed bed column operations on flumequine removal onto activated carbon: pH influence and desorption studies. *Chemical engineering journal*, **228**, 102-113.
- Stefov, V., Šoptrajanov, B., Kuzmanovski, I., Lutz, H., Engelen, B. 2005. Infrared and Raman spectra of magnesium ammonium phosphate hexahydrate (struvite) and its isomorphous analogues. III. Spectra of protiated and partially deuterated magnesium ammonium phosphate hexahydrate. *Journal of Molecular Structure*, **752**(1-3), 60-67.
- Sui, Q., Huang, J., Deng, S., Yu, G., Fan, Q. 2010. Occurrence and removal of pharmaceuticals, caffeine and DEET in wastewater treatment plants of Beijing, China. *Water research*, **44**(2), 417-426.
- Sun, P., Li, Y., Meng, T., Zhang, R., Song, M., Ren, J. 2018. Removal of sulfonamide antibiotics and human metabolite by biochar and biochar/H₂O₂ in synthetic urine. *Water research*, **147**, 91-100.
- Swan, G.E., Cuthbert, R., Quevedo, M., Green, R.E., Pain, D.J., Bartels, P., Cunningham, A.A., Duncan, N., Meharg, A.A., Lindsay Oaks, J. 2006. Toxicity of diclofenac to Gyps vultures. *Biology letters*, **2**(2), 279-282.
- Tadkaew, N., Hai, F.I., McDonald, J.A., Khan, S.J., Nghiem, L.D. 2011. Removal of trace organics by MBR treatment: the role of molecular properties. *Water research*, **45**(8), 2439-2451.
- Tadkaew, N., Sivakumar, M., Khan, S.J., McDonald, J.A., Nghiem, L.D. 2010. Effect of mixed liquor pH on the removal of trace organic contaminants in a membrane bioreactor. *Bioresource technology*, **101**(5), 1494-1500.
- Ternes, T.A., Meisenheimer, M., McDowell, D., Sacher, F., Brauch, H.-J., Haist-Gulde, B., Preuss, G., Wilme, U., Zulei-Seibert, N. 2002. Removal of pharmaceuticals during drinking water treatment. *Environmental science & technology*, **36**(17), 3855-3863.
- Tian, Y., Gao, B., Morales, V.L., Chen, H., Wang, Y., Li, H. 2013. Removal of sulfamethoxazole and sulfapyridine by carbon nanotubes in fixed-bed columns. *Chemosphere*, **90**(10), 2597-2605.
- Tor, A., Danaoglu, N., Arslan, G., Cengeloglu, Y. 2009. Removal of fluoride from water by using granular red mud: batch and column studies. *Journal of hazardous materials*, **164**(1), 271-278.
- Tun, L.L., Jeong, D., Jeong, S., Cho, K., Lee, S., Bae, H. 2016. Dewatering of source-separated human urine for nitrogen recovery by membrane distillation. *Journal of Membrane Science*, **512**, 13-20.
- Udert, K., Larsen, T.A., Gujer, W. 2006. Fate of major compounds in source-separated urine. *Water Science and Technology*, **54**(11-12), 413-420.
- Udert, K.M., Larsen, T.A., Biebow, M., Gujer, W. 2003a. Urea hydrolysis and precipitation dynamics in a urine-collecting system. *Water research*, **37**(11), 2571-2582.
- Udert, K.M., Larsen, T.A., Gujer, W. 2003b. Estimating the precipitation potential in urine-collecting systems. *Water Research*, **37**(11), 2667-2677.
- Urriaga, A., Pérez, G., Ibáñez, R., Ortiz, I. 2013. Removal of pharmaceuticals from a WWTP secondary effluent by ultrafiltration/reverse osmosis followed by electrochemical oxidation of the RO concentrate. *Desalination*, **331**, 26-34.
- Vakili, M., Mojiri, A., Kindaichi, T., Cagnetta, G., Yuan, J., Wang, B., Giwa, A.S. 2019. Cross-linked chitosan/zeolite as a fixed-bed column for organic micropollutants removal from aqueous solution, optimization with RSM and artificial neural network. *Journal of environmental management*, **250**, 109434.
- Virkutyte, J., Varma, R.S., Jegatheesan, V. 2010. *Treatment of micropollutants in water and wastewater*. IWA Publishing.
- Volpin, F., Badeti, U., Wang, C., Jiang, J., Vogel, J., Freguia, S., Fam, D., Cho, J., Phuntsho, S., Shon, H.K. 2020a. Urine treatment on the international space station: current practice and novel approaches. *Membranes*, **10**(11), 327.

- Volpin, F., Chekli, L., Phuntsho, S., Cho, J., Ghaffour, N., Vrouwenvelder, J.S., Kyong Shon, H. 2018. Simultaneous phosphorous and nitrogen recovery from source-separated urine: A novel application for fertiliser drawn forward osmosis. *Chemosphere*, **203**, 482-489.
- Volpin, F., Chekli, L., Phuntsho, S., Ghaffour, N., Vrouwenvelder, J.S., Shon, H.K. 2019. Optimisation of a forward osmosis and membrane distillation hybrid system for the treatment of source-separated urine. *Separation and Purification Technology*, **212**, 368-375.
- Volpin, F., Jiang, J., El Saliby, I., Preire, M., Lim, S., Johir, M.A.H., Cho, J., Han, D.S., Phuntsho, S., Shon, H.K. 2020b. Sanitation and dewatering of human urine via membrane bioreactor and membrane distillation and its reuse for fertigation. *Journal of Cleaner Production*, 122390.
- Wang, X., Su, J., Chu, X., Zhang, X., Kan, Q., Liu, R., Fu, X. 2021. Adsorption and desorption characteristics of total flavonoids from *Acanthopanax senticosus* on macroporous adsorption resins. *Molecules*, **26**(14), 4162.
- Weng, C.-H., Hsu, M.-C. 2008. Regeneration of granular activated carbon by an electrochemical process. *Separation and Purification Technology*, **64**(2), 227-236.
- Westerhoff, P., Yoon, Y., Snyder, S., Wert, E. 2005. Fate of endocrine-disruptor, pharmaceutical, and personal care product chemicals during simulated drinking water treatment processes. *Environmental science & technology*, **39**(17), 6649-6663.
- Wilsenach, J., Schuurbiens, C., Van Loosdrecht, M. 2007. Phosphate and potassium recovery from source separated urine through struvite precipitation. *Water research*, **41**(2), 458-466.
- Wood, F. 1982. The changing face of desalination—A consulting engineer's viewpoint. *Desalination*, **42**(1), 17-25.
- Yan, G., Viraraghavan, T., Chen, M. 2001. A new model for heavy metal removal in a biosorption column. *Adsorption Science & Technology*, **19**(1), 25-43.
- Ying, X., Kim, G., Han, I., Sheng, J., Mei, Q., Kim, Y. 2022. High Efficiency Regeneration Performance of Exhausted Activated Carbon by Superheated Steam and Comparison with Conventional Chemical Regeneration Method. *KSCE Journal of Civil Engineering*, **26**(5), 2058-2067.
- Yu, Z., Peldszus, S., Huck, P.M. 2008. Adsorption characteristics of selected pharmaceuticals and an endocrine disrupting compound—Naproxen, carbamazepine and nonylphenol—on activated carbon. *Water research*, **42**(12), 2873-2882.
- Zhang, R., Li, Y., Wang, Z., Tong, Y., Sun, P. 2020. Biochar-activated peroxydisulfate as an effective process to eliminate pharmaceutical and metabolite in hydrolyzed urine. *Water research*, **177**, 115809.
- Zhang, R., Sun, P., Boyer, T.H., Zhao, L., Huang, C.-H. 2015. Degradation of pharmaceuticals and metabolite in synthetic human urine by UV, UV/H₂O₂, and UV/PDS. *Environmental science & technology*, **49**(5), 3056-3066.
- Zhang, R., Yang, Y., Huang, C.-H., Zhao, L., Sun, P. 2016. Kinetics and modeling of sulfonamide antibiotic degradation in wastewater and human urine by UV/H₂O₂ and UV/PDS. *Water research*, **103**, 283-292.
- Zhang, T., Ding, L., Ren, H. 2009. Pretreatment of ammonium removal from landfill leachate by chemical precipitation. *Journal of hazardous materials*, **166**(2-3), 911-915.
- Zhang, Y., Jin, F., Shen, Z., Wang, F., Lynch, R., Al-Tabbaa, A. 2019. Adsorption of methyl tert-butyl ether (MTBE) onto ZSM-5 zeolite: Fixed-bed column tests, breakthrough curve modelling and regeneration. *Chemosphere*, **220**, 422-431.